Spring 1-1-2015

Integrating Service-Life Modeling and Life-Cycle Assessment for Recycled-Aggregate Concrete

Todd Lee Bergman
University of Colorado at Boulder, tobe9952@colorado.edu

INTEGRATING SERVICE-LIFE MODELING AND LIFE-CYCLE ASSESSMENT FOR RECYCLED-AGGREGATE CONCRETE

by:

TODD LEE BERGMAN

B.S., University of Missouri – Saint Louis, 2013

A thesis submitted to the

Faculty of the Graduate School of the

University of Colorado in partial fulfillment

of the requirement for the degree of

Master of Science

Civil Engineering

2015

This thesis entitled:

Integrating Service-Life Modeling and Life-Cycle Assessment
for Recycled-Aggregate Concrete

written by Todd Lee Bergman

has been approved
for the Department of Civil, Environmental, and Architectural Engineering

Wil V. Srubar III

Prof. Abbie Liel

Prof. Joseph Kasprzyk

Date May 12, 2015

The final copy of this thesis has been examined by the signatories, and we find that both the content and the form meet acceptable presentation standards of scholarly work in the above mentioned discipline.

Bergman, Todd Lee (M.S., Civil Engineering)
Integrating Service-Life Modeling and Life-Cycle Assessment for Recycled-Aggregate Concrete

Thesis directed by Assistant Professor Wil V. Srubar III

The development and implementation of one-dimensional (a) analytical and (b) numerical service-life models for chloride-induced corrosion of reinforced concrete containing both recycled-aggregates and supplementary cementitious materials (SCMs) are presented in this work. Both the analytical and numerical models account for initial chloride contamination levels due to previous applications. The effects of aggregate type (e.g., virgin, recycled aggregate, recycled mortar), aggregate replacement ratio, severity of chloride contamination levels, severity of in-service chloride exposure, reinforcement cover depth, SCM type (e.g., fly ash, slag, slice fume, metakaolin), and SCM replacement ratio on the expected service life of recycled-aggregate reinforced concrete were investigated. Results illustrated trends between concrete mixes and life cycle costs, which were employed to make conclusions on the trade-offs presented by cost, sustainability, and service life.

DEDICATION

This thesis is dedicated to all of my family, friends, and faculty who have supported me throughout my entire academic career.

Without you this would not have been possible.

ACKNOWLEDGMENTS

I would like to express my gratitude to my research professor and academic advisor, Dr. Wil V. Srubar, whose expertise and guidance led me to discover aspects of structural engineering that I would otherwise not have been exposed to. In addition to the knowledge that he passed on to me, his attention to detail and stylistic preferences are something that will stay with me throughout my career. I would like to thank Dr. Abbie P. Leil for her statistical knowledge and guidance in writing this paper. I would also like to thank Dr. Joseph Kasprzyk for taking interest in my work, and offering his expertise with such short notice.

A special thanks is due to Elizibeth Houle for taking time out of her own research to help me with my own. She is brilliant and selfless and without her I would not have been able to complete this thesis. I would also like to thank all of the members of my SIMLab family including Kristen Hess, Sean Hinchcliffe, Denis Mauney, Luke Traeger, Danielle Dorr, Partick Barnhouse, Torin Mccue, Matt Rankins, JP Gevaudan, and Shane Frazier.

Lastly, I want to thank every professor, administrator, friend, and classmate I had the pleasure of interacting with at CU. Completing my masters at CU Boulder made up two of the best years of my life, and you all shaped that experience for me.

CONTENTS

CHAPTER

LIST OF TABLES

LIST OF FIGURES

CHAPTER I

INTRODUCTION

Concrete is the most heavily consumed material in the construction industry and the second most consumed material in the world after water (Mehta et al., 2003). It is no surprise that the waste produced by the production, use, and disposal of this material is also one of the greatest contributors to the industrial waste stream in the United States. While concrete recycling is common in practice, the use of recycled concrete waste as aggregates is uncommon, due to lack of confidence in the mechanical and service-life performance of recycled-aggregate concrete (Malesev et al., 2010; Berndt, 2009). In recent years, a number of studies have reported that the use of recycled aggregates reduces the environmental impact of virgin-aggregate concrete (WuPing et al., 2011; Knoeri et al., 2013; Estanqueiro; Evangelista et al.). However, most of these studies either quantify cradle-to-gate impacts, which is incomplete, or, if quantifying cradle-to-grave impacts, assume that virgin- and recycled-aggregate concrete exhibit equivalent service-life performances. As substantiated by numerous research reports, this assumption is not accurate for concrete containing recycled aggregates.

In this study, “service life” is defined as the time to corrosion-induced-cracking of the cover in reinforced concrete. In order to comprehensively quantify and compare the service life of (i) recycled-aggregate and (ii) virgin-aggregate concrete, this study aimed to calculate the service-life of the two classes of materials by developing computationally inexpensive service-life performance models. This study considers chloride-induced corrosion to be the primary mechanism of concrete deterioration. Concrete’s ability to resist chloride ingress is one of the primary factors governing the service life and life cycle costs of reinforced concrete (Riding et al., 2013). When reinforced concrete is placed in environments in which it is exposed to airborne and surface chlorides, chlorides penetrate the concrete cover and eventually reach the reinforcing steel. Due to the high alkaline environment within the pore solution of concrete, steel reinforcement forms a thin passive layer, which inhibits the oxidative reactions associated with chloride-induced corrosion. As chloride concentrations at the face of the reinforcing steel increase, the alkalinity of the concrete is reduced, which depassivates the patina layer that protects the reinforcement. When the chloride concentration at the face of the reinforcement reaches a certain level, in the presence of water and oxygen, corrosion will initiate. A consequence of the corrosion of reinforcement is that the volumes of corrosion products are much larger than that of the steel reinforcement. This volumetric expansion leads to cracking and spalling of the concrete surface, which, for the purpose of this study, is defined as the functional obsolescence (end of life) for both virgin- and recycled-aggregate reinforced concrete.

Research has shown that recycled-aggregates are less resistant to chloride ingress than virgin-aggregates due to a more porous microstructure and an inherent potential for initial chloride contamination from previous applications (Debieb et al., 2010). While extensive characterization and modeling of chloride diffusion in virgin-aggregate concrete has been conducted by numerous studies (Riding et al., 2013; Life-365, 2014; Xiao et al., 2011; Liu et al., 2014), very limited research exists on modeling the diffusion of chlorides in recycled-aggregate concrete. Based on existing studies, analytical and numerical solutions have been employed to develop models for the diffusion of chlorides through the cover of conventional reinforced concrete. The models developed for this study were based on existing one-dimension chloride diffusion models. The simple analytical solution presented in this study is based on Crank's error function solution to Fick's second law of diffusion. The numerical model developed for this study was based on models employed by the well-known Life-365 service life prediction software (Life-365, 2014), which utilize the Crank-Nicolson finite difference approach to numerically solve the Fickian diffusion equation. The Crank-Nicolson approach was developed to account for limitations of the simple error function solution, namely its inability to account for non-steady-state boundary conditions and time-dependent changes in the chloride diffusion coefficients.

Numerous strategies exist to increase the service life performance of concrete that is at risk for corrosion-induced deterioration. These approaches include increasing cover depth or using alternative reinforcement (e.g., epoxy coated rebar, stainless

steel, glass fiber-reinforced polymers), but these strategies are often impractical and expensive. Replacing portions of the cement with supplementary cementitious materials (SCMs) such as fly ash, slag, silica fume, and metakaolin (typically byproducts of other industrial processes) has been shown to (a) reduce environmental impact, (b) decrease cost, and (c) improve the performance of concrete due to pozzolanic reactions (Meyer, 2009; Siddique, 2004; Fray et al., 1989; Mehta et al., 1982; Sabir et al., 2001). Improved chloride resistance, in turn, leads to increases in service life (Riding et al., 2013). The model developed for this study included the effects of SCMs by using empirical equations developed by Riding, et al. (2013) to estimate the apparent diffusivity of the concrete based on constituents (e.g., cement, water, SCMs) and mixture proportions.

To assess whether recycled-aggregate concrete is, in fact, a more sustainable material compared to virgin-aggregate concrete, a life-cycle assessment was performed for concrete mixture whose service life performance was simulated. First, a life-cycle inventory was compiled using weights (kg) of constituents. For each mix design, a volumetric functional unit was defined as a one-square meter of concrete with a depth equal to the cover depth required to resist chloride-induced corrosion for 25 and 50 years. Using volumetric conversions based on density of materials, environmental and economic impacts were quantified for each mix design in terms of embodied energy (MJ) and cost (US Dollars). This illustrative example ultimately provides a novel framework by which designers and decision-makers are able to

quantify, elucidate, and evaluate the trade-offs between material cost, service life performance, and environmental sustainability.

1.1 Objectives

The objectives of this work were:

- to develop a better understanding of service-life modeling of virgin- and recycled-aggregate reinforced concrete;
- to formulate an analytical and numerical service-life model for reinforced concrete which includes the ability to incorporate both recycled-aggregates and SCMs (e.g., fly ash, silica fume, metakaolin);
- to propose a method for linking service life and life-cycle assessment of reinforced concrete in order to make sound comparisons between conventional and "green" concrete material technologies.

1.2 Scope

This thesis is divided into 6 chapters:

Chapter 1 provides an introduction to both service-life modeling and life-cycle assessment and outlines the specific objectives of this study.

Chapter 2 provides a summary of the current state of recycling and reuse of concrete construction and demolition waste, recycled-aggregates, supplementary cementitious materials, service-life modeling, and lifecycle assessment as they pertain to reinforced concrete.

Chapter 3 outlines the theoretical development of two (2) service-life models, namely a 1D analytical and a 1D numerical service-life model, formulated in this study. This chapter covers the formulation of both models. The two-phase (i) corrosion initiation and (ii) corrosion-induced cracking phases utilized in each model are described and formulated. The parameters and boundary conditions for the subsequent analyses using these models are presented and defined.

Chapter 4 concerns the life-cycle assessment of virgin- and recycled-aggregate concrete. In this chapter, the functional unit (for the purpose of performing a life-cycle assessment) is defined. A life-cycle inventory is assembled and customized for the purposes of this study.

In *Chapter 5* the results from the service-life models and corresponding life-cycle assessments (in terms of embodied energy and cost) are presented and discussed.

In *Chapter 6* conclusions are made from the results of this study. Recommendations for future work associated with advancements in service-life modeling of recycled-aggregate concrete, improvements to the life-cycle inventory, and optimization and location-based decision-making are also discussed.

CHAPTER II

LITERATURE REVIEW

2.1 Recycling of Concrete Construction & Demolition Waste

Concrete and cement production are among the most energy- and resource-intensive processes in the construction industry. Globally, concrete is the second most consumed material on earth after water (Mehta et al., 2003), which is equivalent to approximately 25 billion tons of concrete (Ferrari et al., 2014). The production of concrete is responsible for 5-8% of man-made CO_2 emissions in the world, which contributes to greenhouse gas emissions, global warming, and climate change (Brito et al., 2013).

The rate of concrete consumption is congruent with that of its disposal. Throughout the world, concrete is the most visible component of construction and demolition waste (C&D) due to its comparative volume in relation to other construction materials. An estimated 325 million tons of C&D waste are generated annually in the US (Ferrari et al., 2014). With growing environmental concerns, developing responsible ways to better manage this waste stream has received considerable attention. 80% of R&D waste is crushed and down-cycled for road base, compacted

fill, backfill, and drainage fill, while only 10% is crushed and recycled for structural purposes. The other 10% of C&D waste is disposed of via landfilling (Kou et al., 2006). This waste ends up in either a municipal solid waste landfill (household waste) or a landfill exclusively devoted to C&D waste materials. The main sources of concrete rubble are demolition work (46%) and rehabilitation of road/highway projects (32%) (Deal, 1997). The rest is derived from construction activity, unused concrete, and failure debris (Deal, 1997).

Usually the rubble from buildings, bridges, and pavements is composed of more than concrete and steel. Rubble can contain many components of a demolished structure, such as wood, rebar, drywall, metal, roofing, various fixtures, concrete, and other materials. The separation of these materials can add significant costs to the demolition process, but provide higher market value for the end product. This increase in cost, however, is often worth the savings of transporting concrete to a landfill and eliminated the charge (usually by weight) of disposal. In terms of the overall environment, recycling concrete greatly saves energy compared to mining, processing, and transporting new aggregates (ACPA, 2010). Diverting this waste puts less stress on landfills that may have difficulty accommodating large volumes of waste and avoids depositing additional contaminants from the waste placed in landfills into ground water (IFC Inc., 1995).

2.2 Current Understanding and Use of Recycled-aggregates

Construction aggregates make up more than 80 percent of the total aggregate market (USGS, 2000). Two billion tons of virgin-aggregate is produced each year in

the United States, and this production is expected to increase to more than 2.5 billion tons per year by the year 2020 (Malesev et al., 2010), which equates to approximately 10 tons per person per year (USACE, 2004). Creating aggregates from C&D waste to be used in new concrete applications has a great potential to reduce resource use and mining impacts of natural aggregates. With a decreasing availability of high-quality natural aggregate, there is a national and global need to develop a system for recycling C&D waste into building materials. This need is especially high in urban areas where aging buildings and infrastructure are demolished. Furthermore, recycled-aggregates have seen a growth in popularity because their sources are typically much closer to urban centers when compared with natural aggregates.

The United States generates more than 200 million tons of recycled-aggregates annually (USGS, 2000). The production of recycled-aggregates requires the separation of contaminants such as asphalt, gypsum, wood, paper, joint sealants, paint, soil, chlorides, and glass. Based on intended reuse applications, limits are suggested for various contaminants (USACE, 2004). Meeting these limits can be cost intensive but will typically increase the value of the product.

Although ample research exists on recycled-aggregates, their use is almost exclusively used for low-performance applications, such as backfill and road base. According to a FHWA study, 38 states in the United States use recycled-aggregate for road sub-base and only 11 recycle it into new concrete (USDOT, 2004). Most facilities associated with recycling concrete debris specialize specifically in

producing aggregates for low-performance applications. The limitation of recycled-aggregate is mainly due to strict standards enforced by government agencies. Some countries' standards do allow the use recycled-aggregates, but their use remains limited to less than one percent of the aggregates used in structural concrete applications (Malesev et al., 2010). These standards are indicative of the low confidence levels in mechanical performance and long-term durability of reinforced concrete produced with reclaimed aggregates.

Studies have shown that mechanical properties of virgin-aggregate concrete with up to 50% aggregate replacement by recycled aggregates exhibit comparable mechanical strength (Malesev et al., 2010; Berndt, 2009). In-service durability studies have concluded that the porosity and average pore diameter of concrete increase as recycled-aggregate content increases, causing a decrease in the chloride resistance and an increase in susceptibility to the corrosion of the reinforcement (Kou et al., 2006). The increase porosity of recycled aggregates is a result of their composition, which typically consists of more crushed mortar, which is more porous than reclaimed whole or virgin aggregate. In addition to a more porous microstructure, recycled-aggregates typically come from concrete that, depending on its application, may contain residual chlorides from seawater, wastewater systems, or de-icing salts. Chlorides present within recycled-aggregates have been shown no significant effects on porosity, permeability, or mechanical properties of the reinforced concrete, but have been shown to increase the rate of chloride diffusivity (Debieb et al., 2010; Movassaghi, 2006). Thus, both aggregate microstructure

(porosity) and previous applications influences reinforced concrete's ability to resist corrosion. For this reason, researchers have low confidence in the material technology's ability to resist chloride penetration and corrosion of the reinforcing steel (Villagran-Zaccardi, 2008).

2.3 Supplementary Cementitious Materials

Concrete is typically comprised of cement, sand, coarse aggregate, and water. Out of these constituents, cement is the most energy intensive to produce (Tuutti, 1982). In recent years, engineers and scientists have developed alternative cemenititous materials, which can achieve significant reductions in embodied energy (Tuutti, 1982). In many cases for concrete design, a proportion of cement will be replaced with these supplementary cementitious materials (SCMs). Typically, SCMs are added to improve the fresh-state and/or hardened-state properties of concrete, such as workability, durability and strength (NRMCA, 2000). These improvements allow the concrete to be designed for enhanced performance in certain applications. Some SCMs can also be used to control the color of concrete when whiter concretes are desired for architectural purposes (PCA, 2010). The most common SCMs used in construction today are fly ash, slag, silica fume, and natural pozzolans, such as metakaolin (PCA, 2010).

SCMs are generally byproducts of industrial processes or made from natural materials. Since cement production requires such a significant amount of energy, using byproducts of other industrial processes, as a replacement is appealing. Fly ash is the most commonly used SCM (PCA, 2010). Fly ash is a byproduct of coal

production used to generate electricity in power plants; silica fume is a byproduct of the reduction of high quality quartz with coal in an electric furnace in order to create silicon or ferrosilicon alloy; and slag is a byproduct separating iron ore in the steel making process (PCA, 2010).

Recent studies have characterized the effects of SCMs on the diffusivity of concrete through experimental testing of concrete samples in marine environments (Riding et al., 2013). It has been shown that fly ash, silica fume, slag and metakaolin increase the chloride resistance of concrete. These studies have also shown that the inclusion of SCMs increase concrete's resistance to other types of deterioration, such as abrasion, freeze-thaw resistance, deicer-scaling resistance, drying shrinkage, creep, alkali-aggregate reactivity, sulfate resistance, and carbonation (PCA, 2010).

2.4 Service-Life Modeling of Reinforced Concrete

2.4.1 Current State

There is ample research on modeling the service life of reinforced concrete. Although concrete is subject to many deterioration mechanisms, most existing service-life models consider only the prediction of chloride-induced corrosion of steel in reinforced concrete, since chloride-induced corrosion is the most common durability concern with reinforced concrete (Riding et al., 2013). Deterioration due to chloride-induced corrosion does not attack the integrity of the concrete itself. Chloride ions are transported through the concrete and cause corrosion of the reinforcing steel, which, due to volumetric changes, expands as it corrodes.

The mass transport of chlorides through a porous concrete matrix is made possible by a number of complex physico-chemical processes. The process most commonly used to model and predict the service-life of concrete is diffusion. The diffusion process has been characterized using an error function solution to Fick's second law of diffusion, which is commonly used to predict the service life performance of reinforced concrete. Commercial software such as Life-365 (Life-365, 2014) and STADIUM (SIMCO Tech., 2015) employ numerical models to predict chloride ingress in cementitous materials. These models utilize numerical solutions to Fick's Second Law of diffusion to predict the time-to-corrosion initiation based on chloride levels throughout the concrete depth and a corresponding chloride threshold, which is, in effect, a measure of the chloride resistance of the reinforcing steel. Such models are useful for engineers because they serve as a tool for determining benefits and tradeoffs of different materials and corrosion prevention strategies that can be employed to achieve a desired service life.

2.4.2 Limitations of Existing Service-Life Performance Models

While research has led to the development of software that is capable of determining the service life of reinforced concrete, little research has been conducted on modeling the service life of reinforced concrete structures that contain recycled-aggregates – especially recycled aggregates containing initial levels of chlorides. The assumptions made in existing service-life modeling approaches are numerous, yet oftentimes necessary. For example, many models assume the diffusivity of the material to be homogenous and completely saturated with water.

Although most concrete elements used in structures do not remain completely saturated, this assumption allows for a less computationally expensive diffusion model.

The diffusion of chlorides is the driving force in service-life modeling of reinforced concrete. However, the diffusion of chlorides is just a catalyst to the corrosion of the reinforcement steel and the eventual cracking of the concrete cover. The cracking of the concrete cover takes place after the corrosion threshold of the reinforcement has been reached. Although models exist to predict this additional time needed for corrosion to cause cracking, most service-life models either add on an estimated, constant value to account time-to-cracking or ignore it completely (Life-365, 2014).

The ability to predict service life of reinforced concrete in chloride environments is essential to determine cost-effective design alternatives with minimal environmental impacts. Considerable uncertainties associated with determining appropriate values and assumptions for service-life models exist and are being addressed by many researchers (Riding et al., 2013; Malesev et al., 2010; Kou et al., 2006; Xiao et al., 2011). While properties regarding diffusivity and chloride concentrations of recycled mortar have been characterized, current models do not possess the capabilities to include recycled-aggregates.

2.5 LCAs and EPDs for Innovative Construction Materials

Increased popularity of green building programs have encouraged the development and specification of innovative construction materials that, when compared to their conventional counterparts, can significantly reduce their ecological footprint.

Concretes which incorporate high levels of recycled content (e.g., fly ash, slag, silica fume, recycled-aggregates) are examples of innovative materials which have gained popularity due to the advocacy of using recycled materials in green building technologies. Green building certification programs, such as Green Building Council's Leadership in Energy Design (LEED®) and the Green Building Initiatives Green Globes®, are rating schemes by organizations advocating for new innovative materials that possess smaller ecological footprints.

Life-cycle Assessment (LCA) is a methodology that can be employed to quantify and compare the environmental aspects and potential impacts associated with a product, process, or service (US DOE, 2004). The data collected from LCAs is summarized and used to define Environmental Product Declarations (EPD) in accordance with international standard ISO 14025. An EPD is a document that is used to communicate transparent and comparable information about the environmental impact of a product's life cycle (EPD Int., 2015). EPDs are a tool used by designers and green building certification groups to promote the use of innovative green building materials. EPDs are part of an effort to standardize the quantification of environmental impacts and promote transparency of materials manufacturing. Figure 1 shows a typical life cycle of a construction material, which can be described by five stages. Each stage requires material and energy inputs as well as waste outputs. LCAs and EPDs are typically calculated using a cradle to gate approach, as opposed to a cradle-to-grave or, more infrequently, a cradle-to-cradle approach. Oftentimes, in an attempt to produce an LCA with a cradle-to-cradle scope, disposal

assessments will be included. When service life is included in LCAs, most studies assume the in situ performance of candidate materials to be equivalent, and, therefore, exclude the consequences of having materials of variable service-life performances. It is, however, common to define and incorporate environmental impacts for in-service maintenance and replacement into LCA comparisons between conventional and innovative material options.

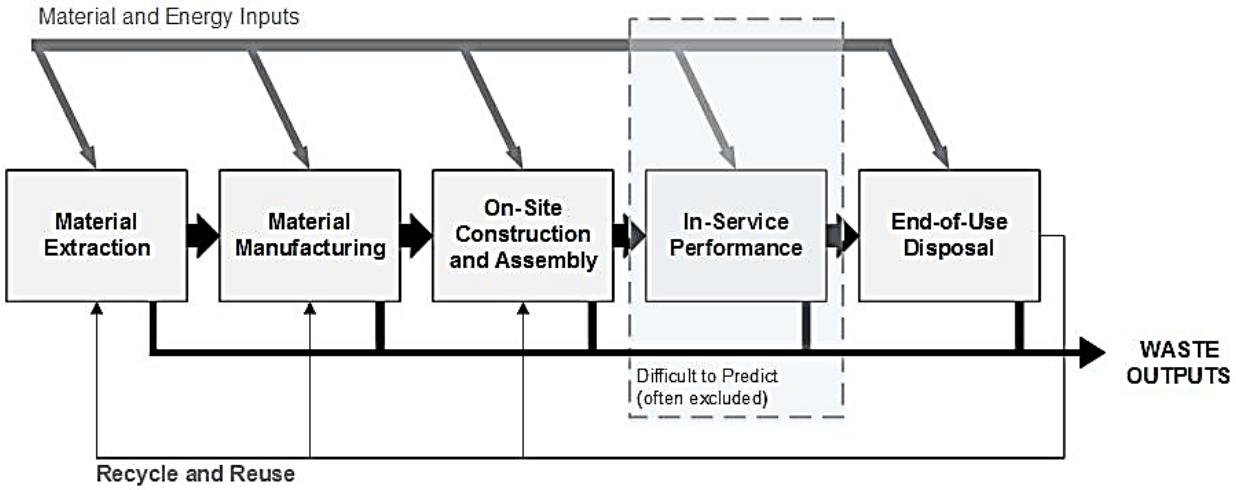

Figure 1 - Typical life cycle of a construction material, emphasizing material and energy inputs and outputs as well as the opportunities for recycling and reuse. In-service performance is often exclusded from typical life cycle-assessments

Access to recycled aggregates tends to be centered in urban areas, where construction and demolitions waste is ample. Due to restrictive accessibility and low confidence in the durability of recycled-aggregates, their practical incorporation into concrete may be limited to certain locations and application. It follows that an attempt to lower the initial environmental impact of materials (aggregates) through the use of “green” substitutes, may, in fact, negatively affect in-service performance. If estimates of in-service performance are not included in LCAs, decision makers in

the construction industry may, in turn, utilize a green material technology that, in the long term, is not more sustainable than the conventional counterpart. As demonstrated in this work, integrating accurate measures of in-service performance into LCAs can more fully elucidate the environmental tradeoffs of innovative "green" material technologies.

CHAPTER III

THEORETICAL FORMULATION

3.1 Model Development for Normal- and Recycled-aggregates

This chapter presents the formulation of (i) analytical and (ii) numerical models for predicting the service-life of virgin- and recycled-aggregate reinforced concrete. Three types of virgin- and recycled-aggregate reinforced concrete are considered herein (see Fig. 2a-c). Normal-aggregate concrete (NA-C), recycled coarse-aggregate concrete (RCA-C), and recycled mortar-aggregate concrete (RMA-C) are considered to be heterogeneous and multiphasic on a mesoscale. NA-C is considered to be a three-phase material containing normal aggregate, a surrounding interfacial transition zone (ITZ) and surrounding new mortar (Fig. 2). RCA-C is considered to be a five-phase material with the original aggregate at the center, surrounded by the old ITZ and mortar and the new ITZ and mortar (Fig. 2b). Similar to that of the NA-C, the RMA-C is also three-phase material, but has original mortar at its center rather than normal aggregate (Fig. 2c).

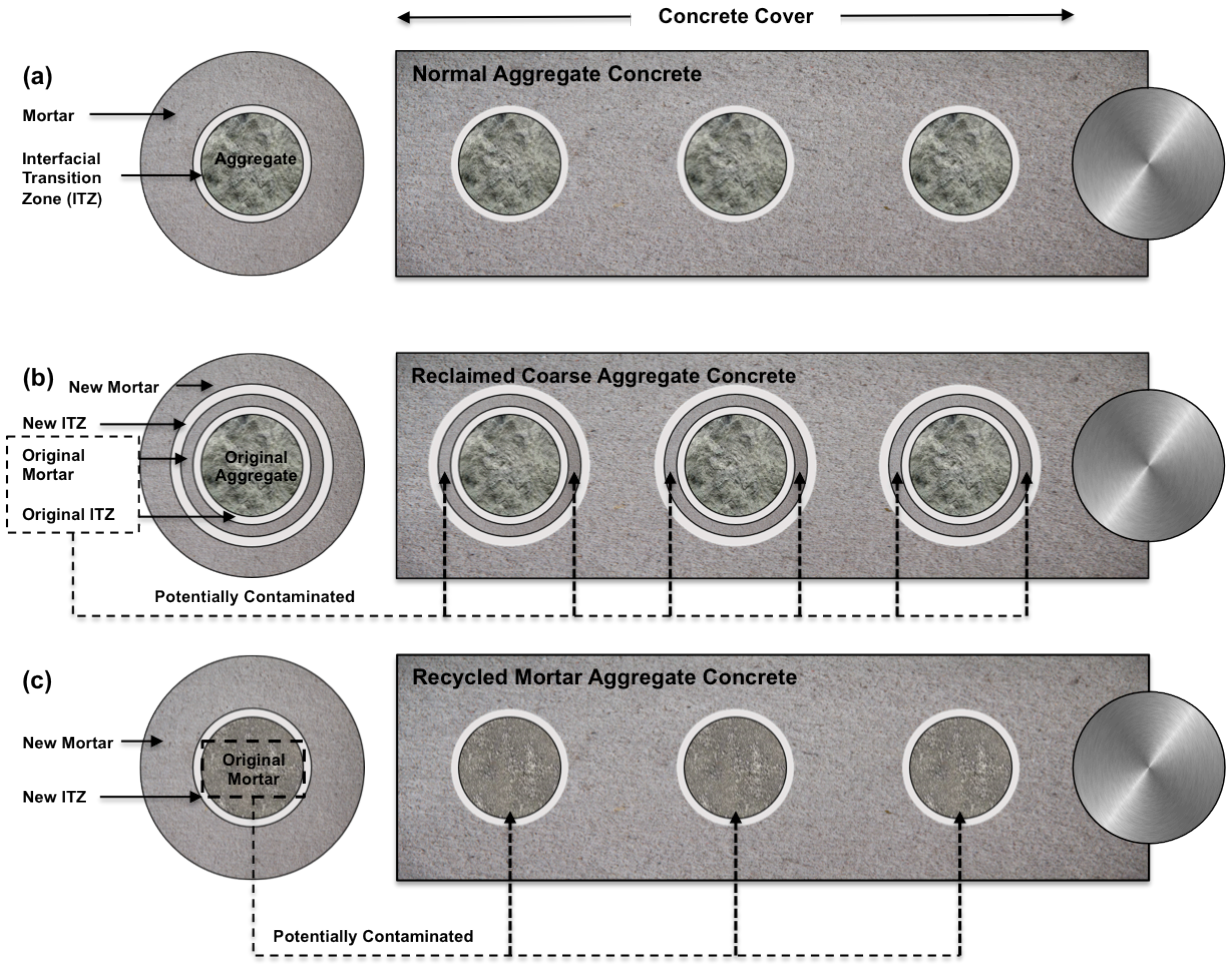

Figure 2 - Multi-phase models for NA-C, RCA-C, and RMA-C assuming an aggregate replacement ratio of 100%. Potential sources of contamination in recycled aggregates correspond to the locations of the original mortar and ITZ.

Potential locations of initial chloride contamination within each model are noted in Fig. 2. Chloride contamination is only present in the two types of recycled-aggregates. The location of these potential chloride contaminations correspond to the locations of old mortars and old ITZs. Due to their relative impermeability and limited exposure to external chlorides, the original aggregate present in NA-C and RCA-C is considered to be free of chloride contamination.

The placement of aggregates throughout the depth of the concrete is considered to be random. The location of each aggregate along a one-dimensional profile is based on the specified type of aggregate, the defined size of aggregates, the depth of concrete specimen, and the placement of reinforcement. As further discussed in the follwong sections, the placement of aggregate centers is randomly defined at the beginning of each simulation to incorporate uncertainty of aggregate placement.

3.2 Defining Service life

The first step in developing a service-life model is to determine and define "service life." For the purpose of this study, service life of reinforced concrete is defined as the time it takes for corrosion-induced cracking to occur after being placed in a chloride-rich environment, t_s. A two-phase model is adopted to describe this process, where the first phase is the time-to-corrosion initiation of the reinforcement, t_i, and the second phase is time to crack propagation, t_c. These two distinct phases are illustrated in Fig. 3 (Tuutti, 1982).

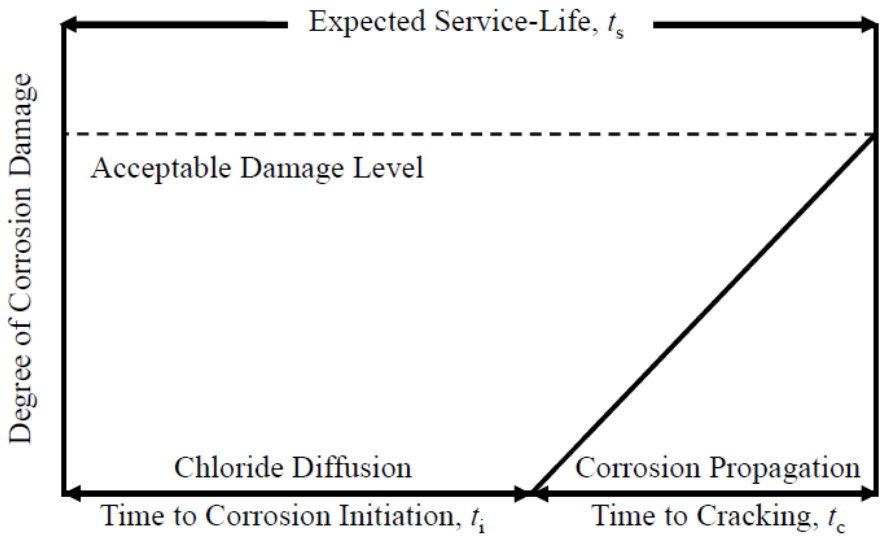

Figure 3 - A graph illustrating the chloride diffusion and corrosion propagation phases of concrete service life. The total service life is dependent upon these two phases and a prescribed acceptable damage level (Tuutti, 1982).

3.3 Corrosion Initiation Phase

The corrosion initiation period is defined herein as the time that it takes for chlorides from the surrounding environment to penetrate the concrete cover and accumulate to a sufficient concentration (chloride threshold) at the surface of the reinforcement. Chloride concentrations above the threshold locally reduce the pH near the reinforcement and results in depassivation of the protective oxide layer and corrosion initiation. It is assumed that no damage occurs during this period. The corrosion initiation period is a function of material properties of the concrete, geometry, the boundary conditions that exist within a given environment, and the required concentration of chlorides to initiate the corrosion of the reinforcing steel.

Chloride transport can take place due to a number of mechanisms including (a) diffusion under the influence of a concentration gradient, (b) absorption due to capillary action, (c) migration in an electrical field, and (d) pressure-induced flow

and wick action when water absorption and water vapor diffusion are combined (Hooton et al., 2002). Diffusion is the process by which matter is transported from one part of a system to another as a result of random molecular motions (Crank, 1975). While molecular movement is random and without preference to direction, molecules move from regions of higher concentration to regions of lower concentration (Crank, 1975). Ionic diffusion of chloride molecules is the primary mechanism of chloride transport and is considered the sole mechanism for both models discussed in this study. It has been shown that the relationship between the chloride concentrations, diffusion coefficients, and time in the random molecular motions of chloride ions in concrete can be described using Fick's Second Law (Liu et al., 2014). Fick's second law of diffusion is the governing differential equation and is used to characterize the diffusion process:

$$\frac{dC}{dt} = D \cdot \frac{d^2C}{dx^2} \tag{1}$$

Where:

C = the chloride concentration,

D = the apparent diffusion coefficient,

x = the depth from the exposed surface, and

t = time.

This study considers two approaches to Eq. 1 that allow for the inclusion of recycled aggregates. The first is a analytical error-function solution, and the second is a numerical finite difference solution.

3.3.1 Modified Error Function (Analytical Solution)

The error function is a special function of sigmoid shape that occurs in probability, statistics, and partial differential equations that has been applied as an analytical solution to Fick's second law of diffusion (Crank, 1975). The following error function solution to the diffusion equation (Eq. 2) has been used extensively to model the corrosion initiation phase due to chloride ingress.

$$C(x,t) = C_0\left(1 - erf\left(\frac{x}{2\sqrt{D_c t}}\right)\right) \quad (2)$$

Where:

$C(x,t)$ = the chloride content (kg/m^3) at distance, x, from the surface at time, t,

C_0 = the boundary chloride condition (kg/m^3) at the surface of the concrete,

D_c = the diffusion coefficient (m^2/s) with an assume 0.4 w/c ratio,

x = the depth from the exposed surface (m), and

t = time (s).

While Eq. 2 has been used in modeling chloride diffusion in conventional, NA-C, it does not account for the presence of recycled-aggregates and their initial level of chloride pre-contamination (if any is present). To account for the existence of recycled aggregates and/or the existence of initial chloride contamination levels throughout a one-dimensional profile, the following analytical solution to the diffusion equation was formulated for the purpose of this study:

$$C(x,t) = C_a\left(exp\left(\frac{-(x-x_i)^2}{4D_c t+2\sigma^2}\right) - exp\left(\frac{-(x+x_i)^2}{4D_c t+2\sigma^2}\right)\right) + C_0\left(1 - erf\left(\frac{x}{2\sqrt{D_c t}}\right)\right) \quad (3)$$

Where:

$C(x, t)$ = the chloride content (kg/m^3) at a distance, x (m) , from the surface at time, t (s),

C_a = the initial chloride concentration (kg/m^3) where old mortar is present,

C_0 = the boundary chloride condition (kg/m^3) at the surface of the concrete,

D_c = the apparent diffusion coefficient (m^2/s) with an assume 0.4 w/c ratio,

σ = the thickness of existing mortar (m),

x_i = the depth from the exposed surface (i = 1… n),

x = the depth from the exposed surface (m), and

t = time (s).

This proposed equation is based on principles of ion implantation and dopant diffusion, where a substrate is doped with a concentration of another material, which diffuses, over time, into the substrate (Srubar, 2015). While the diffusivity of the phases shown in Fig. 2 vary throughout a one-dimensional path from the surface of the concrete to the face of the reinforcement, bulk, apparent diffusion coefficients are used for both virgin- and recycled-aggregates to capture the effects of two-dimensional diffusion in a one-dimensional model.

3.3.1.1 Modeling Parameters

The corrosion threshold was determined through data collected from various experiments (Vu et al., 2000; Kirkpatrick et al., 2002; Zhang et al., 2006; Lounis, 2005; McDonald et al., 1998). The cover thickness was evaluated within a reasonable range to study its effect on service life. All other parameters used in service life simulations are modeled as independent variables and are defined by a

mean and standard deviation assuming normal distributions and lognormal distributions (when appropriate). These modeling parameters, which are based on empirical data collected from existing studies on NA-C, RCA-C and RMA-C, are shown in Table 1.

Table 1 - Modeling parameters for modified error function solution. Parametric values are displayed as a mean and standard deviation, assuming normal distribution

Modeling Parameters for the Error Function Solution

Corrosion Initiation Model					
Service-life modeling parameter	Normal aggregate concrete (NA-C)	Recycled coarse aggregate concrete (RCA-C)	Recycled mortar aggregate concrete (RMA-C)	Units	Refs.
Boundary condition (mild), c_0	1.0 ± 0.2	1.0 ± 0.2	1.0 ± 0.2	kg/m^2	(Tanaka et al., 2006; Kirkpatrick et al., 2002; Liu et al., 2012)
Boundary condition (moderate), c_0	2.0 ± 0.2	2.0 ± 0.2	2.0 ± 0.2	kg/m^2	(Tanaka et al., 2006; Vu et al., 2000; Liu et al., 2012)
Boundary condition (severe), c_0	3.0 ± 0.2	3.0 ± 0.2	3.0 ± 0.2	kg/m^2	(Tanaka et al., 2006; Vu et al., 2000; Liu et al., 2012)
Initial aggregate chloride content (mild), c_a	–	1.0 ± 0.2	1.0 ± 0.2	kg/m^2	(Tanaka et al., 2006; Vu et al., 2000; Liu et al., 2012)
Initial aggregate chloride content (severe), c_a	–	3.0 ± 0.2	3.0 ± 0.2	kg/m^2	(Tanaka et al., 2006; Vu et al., 2000; Liu et al., 2012)
Diffusion coefficient, D_c	4.5 ± 1.0	8.5 ± 1.5	12.5 ± 2.0	10^{12} m^2/s	(Xiao et al., 2013; Zhang et al., 2006; Riding et al., 2013)
Coarse aggregate diameter, d_a	10	10	10	mm	
Chloride threshold, c_c *(lognormal distribution)*	0.7 ± 0.05	0.7 ± 0.05	0.7 ± 0.05	kg/m^2	(Kirkpatrick et al., 2002; Vu et al., 2000; Mehta et al., 2003; Lounis, 2005; McDonald et al., 1998)

3.3.1.2 Simulation Procedure for Analytical Model

Errors are made in the actual production of reinforced concrete. Variables such as the concrete cover or the diffusion coefficient may be slightly different from case to case. The model developed for this study presents certain variables as distributions to account for this uncertainty. A Monte Carlo simulation process, which utilizes random sampling to obtain a distribution of results (e.g., service life), was used in this study. Variable inputs with assumed statistical distributions were used in the simulations (see Table 1). In order to determine an approximate statistical distribution of the resulting data, the Anderson-Darling goodness of fit test was employed to evaluate whether a lognormal distribution was a good model for predictions of service life.

Before running a simulation, the material scenario needs to be defined. Fig. 4 shows a flow chart of how scenarios were chosen. Each scenario was defined by aggregate type, replacement ratio, the chloride boundary condition (mild, moderate, severe) and the initial chloride content (mild, severe) for simulations including RCA-C and RMA-C. For each simulation the concrete cover, the chloride boundary condition, and the corrosion threshold of steel reinforcement are randomly generated. If the defined scenario includes a replacement ratio for RCA-C or RMA-C greater than zero, the recycled aggregate placement and corresponding contamination levels were then randomly generated. Using Eq. 3 the chloride content is calculated at the cover depth (depth to reinforcement), at each time step. Corrosion is initiated when the concentration reaches or exceeds the chloride threshold of the reinforcing steel.

The corresponding time step to corrosion initiation is then recorded as the corrosion invitation period, t_i.

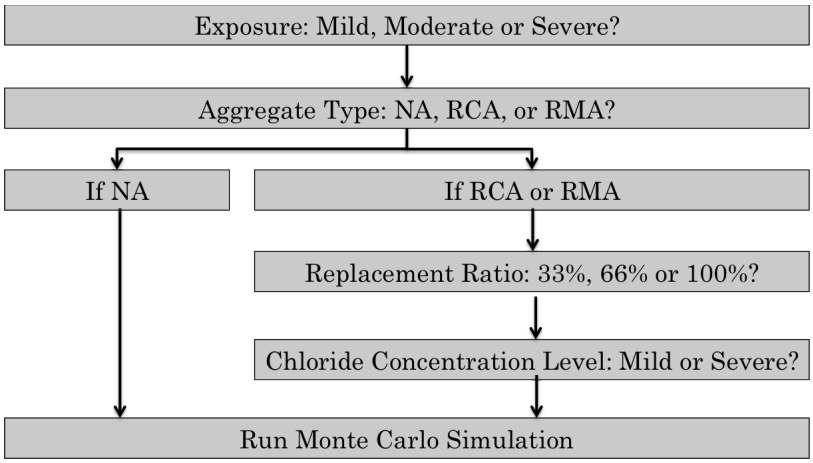

Figure 4 - A flow diagram representing the way in which scenarios are chosen for the modified error function solution before running simulations. A total of 50,000 Monte Carlo simulations were run for each modeling scenario.

3.3.2 Crank-Nicolson Finite Difference Method (Numerical Solution)

The first model presented in Section 3.3.1 employed an analytical error function solution to solve the partial differential equation of Fick's 2nd Law of diffusion (Eq. 1). The first model was computationally inexpensive, but was not capable of accounting for non-steady-state conditions such as temperature- and time-dependence. The model formulated in this portion of the study employs a one-dimensional Crank-Nicolson finite-difference approach (Eq. 4) to numerically solve the diffusion equation. This approach divides the depth of the concrete into slices, allowing for temperature- and time-dependent variables to change in each slice at a given time step. The chloride levels at a given slice i and time step t +1 are then determined by the following advection-dispersion equation:

$$-ru_{i+1}^{t+1} + (1+2r)u_i^{t+1} - ru_{i-1}^{t+1} = ru_{i+1}^{t} + (1-2r)ru_i^{t} + ru_{i-1}^{t}, \quad (4)$$

Where:

r = $D_t \frac{(dt)}{2(dx)^2}$, is the dimensionless Courant-Friedrichs-Lewy (CFL) number,

D_t = the diffusion coefficient at time t (m^2/s),

d_t = the time step, (s),

d_x = the length increment of each slice (depth divided by number of slices),

u_i^t = Chloride level at slice i and time t (% weight of concrete),

i = $i…n$, corresponding slice of concrete,

t = time step in the corrosion initiation period.

The left side of Eq. 4 represents unknown concentrations at a future time step, where the right side of the equation represents known values at the current time step. The surface chloride concentration and the time-dependent material properties (i.e., diffusion coefficient) of the reinforced concrete are calculated at the beginning (and held constant) during each time step. The diffusion constant (CFL number) is considered uniform throughout the depth of the element, which is a necessary assumption for employing the Crank-Nicolson finite difference method (Life-365, 2014). Eq. 4 is then rearranged in to matrix form to solve for future chloride levels:

$$AU^{t+1} = BU^t, \quad (5)$$

Where:

$$A = \{a_i^{t+1}\} = \begin{bmatrix} 1 & 0 & 0 & 0 & 0 \\ -r & 1+2r & -r & 0 & 0 \\ \cdots & \cdots & \cdots & \cdots & \cdots \\ 0 & 0 & -r & 1+2r & -r \\ 0 & 0 & 0 & 0 & 1 \end{bmatrix}, \quad (6)$$

$$U^{t+1} = \{u_i^{t+1}\} = \begin{bmatrix} u_1^{t+1} \\ \vdots \\ u_i^{t+1} \\ \vdots \\ u_n^{t+1} \end{bmatrix}, \quad (7)$$

$$B = \{b_i^{t+1}\} = \begin{bmatrix} 1 & 0 & 0 & 0 & 0 \\ r & 1-2r & r & 0 & 0 \\ \cdots & \cdots & \cdots & \cdots & \cdots \\ 0 & 0 & r & 1-2r & r \\ 0 & 0 & 0 & 0 & 1 \end{bmatrix}, \text{ and} \quad (8)$$

$$U^t = \{u_i^t\} = \begin{bmatrix} u_1^t \\ \vdots \\ u_i^t \\ \vdots \\ u_n^t \end{bmatrix} \quad (9)$$

Where A and B are dimensionless matrices corresponding the dimensionless CFL number, and the U matrices define chloride levels at the present and the future time steps. Using matrix inversion, Eq. 3 can be rearranged to solve for chloride levels at individual slices:

$$U^{t+1} = A^{-1}BU^t \quad (10)$$

Since this Crank-Nicolson finite difference approach accounts for both space and time, it is possible to included non-steady state conditions, which are a function of both space and time. Such conditions include the apparent chloride diffusion coefficient (which can change space [e.g., mortar, aggregate] and with time [e.g.,

densification of cement paste]) and the exposure (e.g., fluctuating chloride boundary conditions), which can vary throughout the corrosion initiation period.

Using this matrix, finite difference approach, recycled-aggregates can be modeled throughout the depth of the concrete specimen. As previously mentioned, recycled-aggregates can contain initial chloride levels and are inherently more porous than normal aggregates. Correspondingly, different levels of initial chloride concentration and different diffusion coefficients can be assigned to the slices that correspond to aggregate placement along the one-dimensional profile.

The diffusion of chlorides is a three dimensional process. In order to create diffusion models that are not computationally expensive, this three-dimensional process was represented in one dimension. Both analytical and numerical models developed for this study were one-dimensional. The analytical model proposed in this study was based on an error function solution to diffusion and required a single, bulk (apparent) diffusion coefficient. The bulk diffusion coefficients were taken from empirical data and held constant throughout the simulations. The numerical model does not require a single bulk diffusion coefficient, but rather calculates a bulk diffusion coefficient for each slice throughout the depth of the concrete at each given time step. The bulk diffusion coefficient in each slice of the concrete is dependent on the material that occupies that slice (e.g., new mortar, recycled aggregate). The second model employs a set of equations to develop a base-case bulk diffusion coefficient for each slice, which can be modified based on non-steady-state conditions (time and temperature). This base-case diffusion coefficient used

represents NA-C, and can be employed without replacing diffusion coefficients throughout the one-dimensional profile with the actual diffusion coefficient of the virgin aggregates. Since this second model does not have a single bulk diffusion coefficient and is still a one-dimensional model, it is not capable of modeling RCA-C given the near impermeability of natural aggregates.

3.3.2.1 Modeling Parameters

The modeling parameters were obtained through empirical modeling of the apparent chloride diffusion coefficient in relation to (a) mixture proportions, (b) the inclusion of SCMs, (c) time, and (d) temperature (Riding et al., 2013). In this study, these empirical models are used to account for non-steady state conditions that affect the corrosion initiation period for reinforced concrete. To account for the contamination and change in pore structure due to the incorporation of RCA and RMA, the initial chloride levels and diffusion coefficients, which are inserted into the matrix, are based on the same empirical values listed in Table 1. The threshold for corrosion initiation in this model was determined using a widely accepted 0.05% chloride by weight of concrete (Life-365, 2014; Broomfield, 2006) [45]. The following sections outline the modeling methodology to account for the effect of water-to-cement ratio, SCMs, time, and temperature on the apparent diffusion coefficient.

3.3.2.1.1 Effect of Water to Cement Ratio on the Diffusion Coefficient

Riding et al. developed this relationship between the w/c ratio and the chloride diffusivity of early age concrete by generating a "best fit" equation of data collected from various studies (Riding et al., 2013). For the numerical service-life model

developed herein, this equation was used to define a "base-case" diffusion coefficient for the corrosion initiation period of reinforced concrete:

$$D_{28} = 2.17\times10^{-12}e^{(w/cm)/0.279} \quad (11)$$

where w/cm is the w/c ratio defined for a given concrete mix design.

3.3.2.1.2 Effect of SCMs on the Diffusion Coefficient

SCMs are used to modify the properties of reinforced concrete, including its chloride resistance. Using collected data from various literature, equations were developed to characterize SCMs effect on the chloride diffusion coefficient (Riding et al., 2013). Equations 12-14 are used modify the "base-case" diffusion coefficient for the purpose of incorporating the effects of SCMS into the corrosion initiation period of this service-life model.

$$D_{SF} = D_{28} \cdot (0.206 + 0.794e^{(-SF/2.51)}) \quad (12)$$

$$D_{UFFA} = D_{28} \cdot (0.170 + 0.829e^{(-UFFA/6.07)}) \quad (13)$$

$$D_{MK} = D_{28} \cdot (0.191 + 0.809e^{(-MK/6.12)}) \quad (14)$$

D_{28} is the "base-case" diffusion coefficient as calculated in Equation 11. D_{SF}, D_{UFFA} and D_{MK} are the modified diffusion coefficients due to Silica Fume, Ultra Fine Fly Ash and Metakaolin, respectively, and *SF*, *UFFA* and *MK* are the percent replacement of cement with SCMs (in total %). It is important to find an optimum replacement when using SCMs, because an overdose can be harmful to the integrity of the concrete, such as early hardening and strength gain (PCA, 2010). These percentages are honored in this study (Table 2). The service-life model is limited to the inclusion of one SCM per simulation.

Table 2 - A table of maximum replacements of cement by SCMs type incorporated into the numerical model.

Allowable Ranges for SCMs		
SCM	Max Replacement	Source
Fly Ash	25%	(Obla, 2008)
Slag	50%	(Obla, 2008)
Silica Fume	10%	(Obla, 2008)
Metakaolin	20%	(Ismael et al., 2014)

3.3.2.1.3 Time-dependent Diffusion Coefficient

The chloride diffusion coefficient is a time-dependent parameter, and decreases over time. This decrease is due to continued hydration of concrete beyond 28 days, which reduces the porosity of the concrete. Over time, chloride levels become uniform throughout the surface and diffusion slows due to a concentration-dependence of the diffusion process. Chloride diffusion also decreases over time due to carbonation, which results in a less porous microstructure. Many researchers have demonstrated the relationship between time and diffusivity to be best described by a power law, where the exponent is the hydration effect factor (or decay factor), m (Riding et al., 2013; Liu et al., 2014). This study describes this relationship using the following equation:

$$D_t = D_{28} \cdot \left(\frac{t_{28}}{t}\right)^m \quad (15)$$

D_t is the time-dependent diffusion coefficient. D_{28} is the early-age chloride diffusion coefficient (calculated using Equation 11), t_{28} is set equal to 28 days, and t is the current time step, and m is the hydration effect factor. The hydration effect factor was previously proposed as a function of the w/c ratio, but further studies have

shown it to be primarily influenced by the inclusion of fly ash and slag (Movassaghi, 2006; Riding et al., 2013). Thus, Eq. 16 is used to determine the hydration effect factor.

$$m = 0.26 + 0.4\left(\frac{FA}{30} + \frac{SG}{50}\right) \tag{16}$$

Riding et al suggests that an indefinitely decreasing diffusion coefficient is unrealistic, and proposed that an ultimate limiting value be incorporated into the time-dependent diffusivity equation. Eq. 17 describes this ultimate limiting value based on a 100-year value used in this study:

$$D_{ult} = D_{28}\left(\frac{28}{36{,}500}\right)^{m} \tag{17}$$

Where D_{28} is the early-age chloride diffusion coefficient and m is the hydration effect factor (Riding et al., 2013). The incorporation of the ultimate limiting value is shown in Eq. 18, where Eq. 17 is added to Eq. 15 (Riding et al., 2013).

$$D_t = D_{28} \cdot \left(\frac{t_{28}}{t}\right)^{m} + D_{ult}\left(1 - \left(\frac{t_{28}}{t}\right)^{m}\right) \tag{18}$$

3.3.2.1.4 Temperature Dependent Diffusion Coefficient

As temperature increases, so does the random movement of molecules. This means that the rate at which chloride ions move in a diffusion process can be directly linked to temperature. By using temperature profiles, as shown in Fig. 5 (US Climate Data, 2015), of certain locations, a service-life simulation can be made location specific.

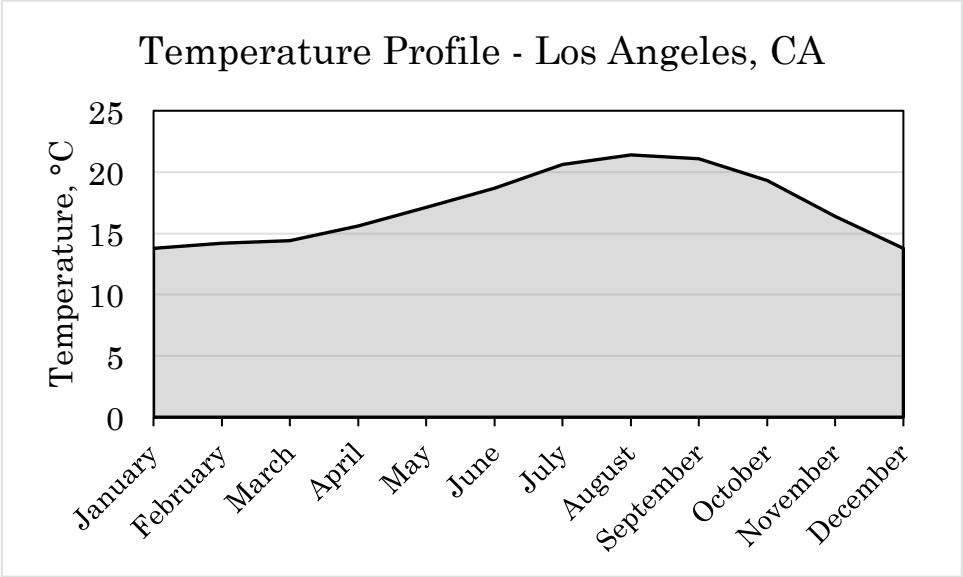

Figure 5 - Average monthly temperature data for Los Angeles, CA. These profiles are used to develop the location- and time-dependent relationships between temperature and chloride diffusion coefficients.

This model incorporates temperature dependency by using an Arrhenius relationship to modify the time-dependent diffusion coefficient. Eq. 18 describes the adjustments made to the diffusion coefficient based on a temperature profile. Using yearly temperature profiles for a specific location, this equation can be used to determine the fluctuation in the diffusion coefficient for specific locations.

$$D_T(t,T) = D_t(t) \cdot \exp\left[\frac{U}{R} \cdot \left(\frac{1}{T_{ref}} - \frac{1}{T}\right)\right] \tag{19}$$

Where D_T (m^2/s) is the diffusion coefficient at time, t (s), and temperature T (K). T_{ref} is the reference temperature; U is the activation energy (J/mol/K); and R is the universal gas constant (8.3144 J/mol/K).

3.3.2.1.5 Development of Exposure Conditions

Unlike the modified error function solution, the boundary condition of the concrete specimen is not explicitly defined within the Crank-Nicolson approach. In this

model, the exposure conditions are modeled by controlling the concentration of the slice defined at the exposed surface of the concrete specimen. Exposure levels will fluctuate based on the time of year. Some authors suggest that this exposure causes the surface chloride concentration to change with time. This model assumes a linear increase of surface chloride concentration until a prescribed maximum is attained, after which the surface chloride concentration remains constant. This ramp-up exposure condition simulates the effect of chloride build-up due to wetting and drying cycles at the concrete surface (Riding et al., 2013). This effect was developed from measurements of surface chloride levels of core samples taken over time (Phurkhao et al., 2005). Life 365 (Life-365, 2014) adopts a similar approach in modeling a linear increase of surface chloride concentration and determining a max concentration based on geographical location, structure type, and exposure field data. The maximum concentration and ramp-up time are calculated using the unit weight of concrete. This model utilizes data from Life 365 to apply the same approach in modeling chloride boundary conditions.

Los Angeles, California served as the location of interest for this study. The maximum surface chloride concentration was based on the distance from the coast, up to a certain distance (1.5km), and then was based on the type of structure (parking structure, urban bridge, rural bridge, interior element). Table 3 illustrates these values as a function of % weight of concrete.

Table 3 -Values used to determine the ramp-up duration and maximum value of surface chloride concentration given in percent weight of concrete. These values are used to characterize the chloride exposure (boundary condition) at the concrete surface.

Maximum Surface Concentration and Ramp-up Rates (Life-365, 2014)		
	Ramp-up (%/year)	Maximum (%)
Marine Spray Zone	0.1	1
Within 800 m of Coastline	0.04	0.6
Within 1.5 km of Coastline	0.02	0.6
Parking Structure	0.015	0.8
Urban Bridges	0.01275	0.85
Rural Bridges	0.0105	0.7

3.3.2.2 Simulation Procedure for Numerical Model

All modeling simulations were coded and run using MATLAB software. At the start of each simulation, an application and its location (and associated monthly temperature profile) were first defined. Then, the w/c ratio, SCM type and content, specimen cover depth, location of reinforcement, type of aggregate (normal, recycled aggregate, recycled mortar), aggregate size, aggregate replacement ratio, and level of aggregate contamination for that particular concrete specimen were defined. A flow chart illustrating the way in which these scenarios were chosen is shown in Fig. 6. From these definitions the diffusion coefficient, boundary conditions, and geometries of aggregate replacements with corresponding initial contamination and diffusion coefficients are calculated. These parameters were used to define the initial values in Eq. 4 and to calculate the chloride levels throughout the depth of the specimen at the next time step. The resulting values are placed back into Eq. 4 as the initial (known) values at the start of the next time step. This process

continues until the corrosion initiation threshold is reached (or exceeded), and the corresponding time step was recorded as the time-to-corrosion initiation, t_i.

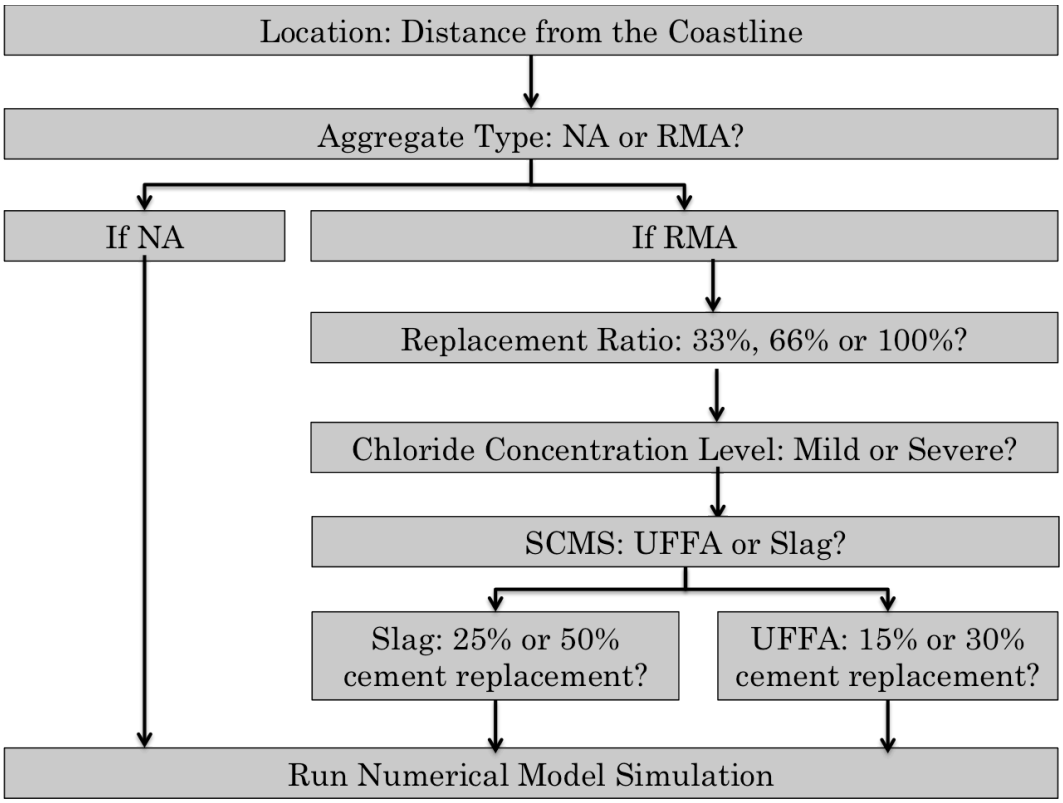

Figure 6 - A flow diagram representing the way in which scenarios are chosen for the finite difference solution before running simulations

3.4 Crack Propagation Phase

3.4.1 Model Development

Time to cracking due to chloride-induced corrosion is a crucial time period in determining the service life of recycled-aggregate concrete, but many existing service-life models (Phurkhao et al., 2005) consider this period to be a fixed value of 3 to 5 years without any calculations. Generally, this is acceptable, but for the sake of completeness, an analytical model is used in this study to determine time-to-cracking. Both service-life models discussed in this study used an analytical corrosion-induced cracking model proposed by Lui and Weyers to determine the crack propagation phase (Lui et al., 1998). This model was proposed by Liu and Weyers as an improvement upon Bazant's original model (Bazant, 1979) by including the time period in which the corrosion products fill the porous region surrounding the rebar before inducing pressure on the surround concrete.

Modeling corrosion propagation requires many simplifications and assumptions. Corrosion in concrete takes place as pitting corrosion, where corrosion production is non-uniform around the surface of the reinforcement. This model assumes a simplified uniformity in the production of rust. This assumption is accepted because, while pitting corrosion production is never uniform, as it progresses, it appears to become more uniform over time. It also assumed that only one type of corrosion product is present, when, in reality, this is not accurate. However, the corrosion products with the highest relative volume were selected, and are considered to be a conservative and acceptable assumption.

The time-to-cracking model consists of three phases:

(1) *Free Expansion ($W_t \leq W_p$).* A porous region surrounding the steel reinforcement exists due to air voids present in the transition from cement to steel (Lui et al., 1998). This corrosion phase represents the time where the total amount of corrosion products, W_t, present is less than that required to fill the porous region, W_p. This phase is illustrated in Fig. 7a.

(2) *Stress Initiation ($W_t \geq W_p$).* The total amount of corrosion products eventually exceeds the capacity of the porous region. The corrosion products begin to produce expansive pressure on the surrounding concrete, which increases with corrosion product generation. This phase is illustrated in Fig. 7b.

(3) *Cracking ($W_t = W_{crit}$).* There is a limit to the amount of internal pressure that the concrete can withstand. This limit can be quantified by a critical amount of corrosion products, W_{crit}, that are necessary to cause a sufficient amount of internal pressure. When the total amount of corrosion products exceeds this critical amount, cracking is induced. This phase is illustrated in Fig. 7c.

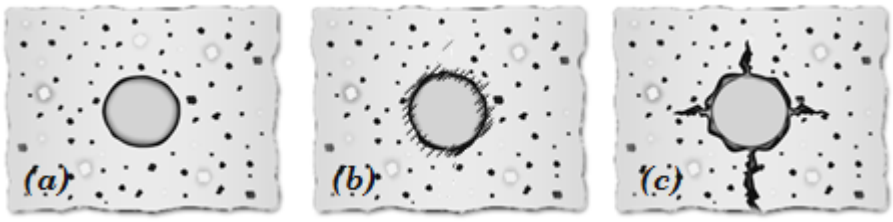

Figure 7 - This image (BP Composites LTD., 2015) represents the three stages of the corrosion-induced cracking phase that was employed for both the analytical and numerical service-life models developed and implemented in this study. (a) Corrosion products fill the porous void around the steel reinforcement. (b) The surrounding concrete is exposed to expansive pressure. (c) Critical amount of pressure is reached and the concrete cover cracks or spalls (end of service life).

The model is based on a hypothetical cylinder exposed to internal pressures caused by the generation of corrosion products. The time-to-corrosion-induced cracking, tc, was determined for both models in this study using the following equation (Lui et al., 1998):

$$t_c = \frac{W_{crit}^2}{2k_p} \tag{20}$$

Where:

W_{crit} = the amount of corrosion products required to induce cracking, and

k_p = the rate of rust production.

3.4.2 Modeling Parameters

This model of the time-to-corrosion induced cracking is a function of the corrosion rate, cover depth, bar spacing, and certain mechanical properties of concrete, such as tensile strength, modulus of elasticity, Poisson's ratio and creep coefficient (Lui et al., 1998). Eq. (21) was used to determine the critical amount of corrosion products required to induce cracking.

$$W_{crit} = \rho_r \left(\pi \left[\frac{Cf'_c}{E_{eff}} \left(\frac{a^2+b^2}{b^2-a^2} + \upsilon \right) + t_p \right] d_b + \frac{W_{st}}{\rho_{st}} \right) \tag{21}$$

Where:

$$E_{eff} = \frac{E}{(1+\varphi)} \tag{22}$$

$$a = \frac{d_b+2t_p}{2} \tag{23}$$

$$b = C + a \tag{24}$$

$$W_{st} = \alpha W_{crit} \tag{25}$$

ρ_r = the density of rust products (kg/m^3),

C = the cover depth (mm),

f'_c = the tensile strength of concrete (MPa),

E_{eff} = the effective modulus of elasticity (GPa),

t_p = the thickness of the porous zone surrounding the reinforcement (mm),

d_b = the diameter of the reinforcement (mm),

υ = poison's ratio,

W_{st} = the amount of corrosion products (kg/m^2),

ρ_{st} = the density of reinforcing steel (kg/m^3),

a = the inner diameter of the hypothetical cylinder (mm), and

b = the outer diameter of the hypothetical cylinder (mm).

E = the modulus of elasticity (GPa),

α = the creep coefficient of concrete, and

φ = the molecular weight of steel divided by the molecular weight of rust.

The rate of corrosion product production is defined by the following equation for k_p:

$$k_p = \alpha^{-1}\pi d_b i_{corr} \quad (26)$$

Where:

i_{corr} = the annual mean corrosion rate (A/m^2).

The deterministic values for these parameters are shown in Table 4, along with their appropriate citations. For both proposed models, some parameters in this table were taken as normally distributed values to account for uncertainties

associated with the tensile strength and modulus of elasticity of concrete, air voids and corrosion rates.

Table 4 - Modeling parameters for corrosion-induced cracking model. Values are presented as a mean and standard deviation and are assumed to have a normal distribution.

Corrosion-Induced Cracking Model					
Service-Life Modeling Parameter	Normal Aggregate Concrete (NA-C)	Recycled Coarse Aggregate Concrete (RCA-C)	Recycled Mortar Aggregate Concrete (RMA-C)	Units	Refs.
Tensile strength, f_t	4.0 ± 0.5	3.75 ± 0.5	3.75 ± 0.5	MPa	(Kou et al., 2006)
Modulus of elasticity, E	35 ± 2.0	30 ± 3.0	30 ± 3.0	GPa	(Kou et al., 2006)
Phi (creep coefficient), ϕ	2	2	2	–	(Lui et al., 1998)
Poisson's ratio, v	0.18	0.18	0.18	–	(Lui et al., 1998; Li, 2003)
Density of rust, ρ_r	3600	3600	3600	kg/m^3	(Lui et al., 1998; Qing, 2004)
Density of steel, ρ_s	7850	7850	7850	kg/m^3	(Lui et al., 1998; Qing, 2004)
Thickness of porous region, t_p	12.5 ± 0.5	12.5 ± 0.5	12.5 ± 0.5	mm	(Lui et al., 1998; Care et al., 2008)
Corrosion rate, i_{corr}	2.5 ± 0.5	2.5 ± 0.5	2.5 ± 0.5	A/cm^2	(Lui et al., 1998; Qing, 2004)
Alpha, α	0.523–0.622	0.523–0.622	0.523–0.622	–	(Lui et al., 1998)
Mild steel rebar diameter, d_b	16	16	16	mm	

3.5 INTEGRATING SERVICE LIFE AND LIFE-CYCLE-ASSESSMENT

The LCA methodology used in this study was developed to support decision making regarding concrete alternatives by elucidating tradeoffs in terms of service-life performance, cost (COST), and embodied energy (EE). It is important when developing an LCA of a product that results, data, methods, assumptions and limitations are transparent. The measurements of COST (US Dollar) and EE (MJ/kg) are derived from a functional unit (Fig. 8). The volumetric size of this

function unit is a 1m by 1m by a defined cover depth. Cover depths can be determined by following design guidelines set forth by the International Building Code (IBC). This study held the cover depth constant at 0.07m, which according to IBC would be an appropriate cover depth for most structural applications. No cost and energy metrics were calculated for the production, construction or transportation of the constituents included in the *original* construction. The *only* metrics calculated in this study are COST and EE.

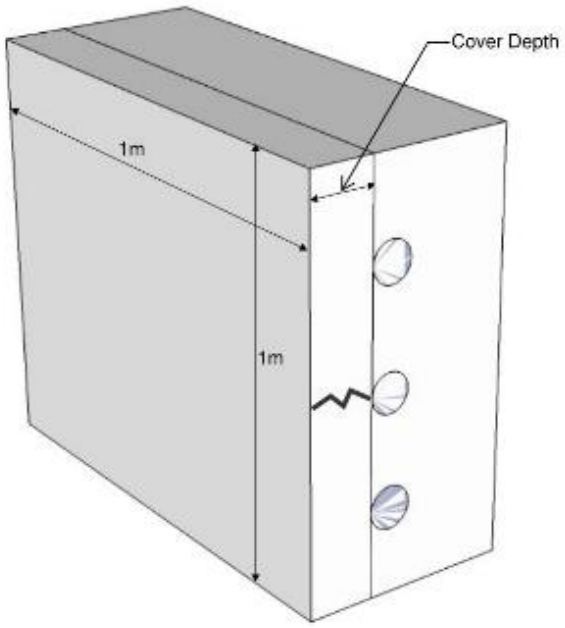

Figure 8 - A schematic drawing for the functional unit used in this study. This was considered to be the replacement of the concrete cover after cracking with an assumed area of 1mx1m and a defined cover depth.

The inventory used for EE was the Inventory of Carbon & Energy (ICE) 2.0 created by the Sustainable Energy Research Team (SERT) at the University of Bath (Hammond et al., 2011). This inventory includes EE values for various virgin and

recycled materials. The embodied energy comes from the consumption of coal, liquid petroleum gas, oil, natural gas, electricity and other energy sources required to produce and deliver the material to the site. Transportation is included in this value, but is a generalization and remains the same for all scenarios. The outputs of this inventory are in MJ/kg. ICE 2.0 life-cycle inventory laid out the embodied energy of concrete based on the percent replacement of SCMs and the concrete compressive strength (Table 5 and Table 6).

Table 5 - ICE 2.0 inventory's material profile for concrete in relation to cement replacement of fly ash and concrete strength.

Material Profile: Concrete			
Material	Embodied Energy - MJ/kg		
	FLY ASH		
% Cement Replacement:	0%	15%	30%
Recycled Concrete (25 MPa)	0.86	0.81	0.73
Recycled Concrete (30 MPa)	0.91	0.85	0.77
Recycled Concrete (35 MPa)	0.95	0.90	0.82
Recycled Concrete (40 MPa)	1.03	0.97	0.89
Recycled Concrete (50 MPa)	1.17	1.10	0.99

Table 6 - ICE 2.0 inventory's material profile for concrete in relation to cement replacement of slag and concrete strength. This table is an extension of Table 5.

GROUND GRANULATED BLAST FURNACE SLAG			
% Cement Replacement	0%	25%	50%
Recycled Concrete (25 MPa)	0.86	0.74	0.62
Recycled Concrete (30 MPa)	0.91	0.78	0.65
Recycled Concrete (35 MPa)	0.95	0.83	0.69
Recycled Concrete (40 MPa)	1.03	0.91	0.78
Recycled Concrete (50 MPa)	1.17	1.03	0.87

In order to develop an equation that relates embodied energy (MJ/kg), SCM content (%) and compressive strength (MPa), a linear least squares curve fitting routine (based on Eq.27) was employed on the data in Tables 5 and 6:

$$y = m_1 x_1 + m_2 x_2 + \cdots + b \tag{27}$$

$$EE_{kg}(MJ/Kg) = -0.0049 \cdot FA - 0.0052 \cdot SG + 0.00008 \cdot f_c + 0.0623 + .0052 \tag{28}$$

Since this equation requires the compressive strength of concrete, Popovich's model (Eq. 29) was used to determine the compressive strength based on the w/c ratio, cement content (kg) and air content (%). Weights of each constituent (e.g. cement, aggregate, water, SCMs) were developed using the Absolute Volume Methodology (ACI 211.1-91) for the functional unit.

$$f_c = \frac{51290}{23.66^{[(w/c)+.000878 \cdot C_{cem}+0.0279*air]}} \tag{29}$$

Tables 5 and 6 did not include the use of recycled-aggregates with SCMs, but Table 7 shows how recycled aggregates were included in the inventory.

Table 7 - ICE inventory's material profile for aggregates. These values were used to include the difference in embodied energy between normal aggregates and recycled-aggregates. This table also includes the embodied energy due to transportation of aggregates.

Material Profile: Aggregate			
Embodied Energy (EE) ICE-Database Statistics - MJ/Kg			
Main Material	No. Records	Average EE	Standard Deviation
Aggregate, General	37	0.11	0.12
Predominantly Recycled	3	0.25	0.21
Unspecified	17	0.11	0.07
Virgin	17	0.10	0.15
Selected Embodied Energy & Carbon Coefficients and Associated Data			
Material	Embodied Energy - MJ/Kg	Embodied Carbon - Kg CO2e/Kg	Boundaries
Transport - General Aggregate	0.083	0.0052	Cradle to Gate

The suggested penalty for including recycled aggregates was incorporated into embodied energy based on the aggregate replacement ratio, and the weight of coarse aggregate. Using the volume of the functional unit and the density of concrete, a final equation for total EE (MJ) was determined (Eq. 30).

$$EE(MJ) = EE_{kg} \cdot \rho_{conc} \cdot vol + (0.140 \cdot ARR \cdot C_{agg}) \quad (30)$$

The inventory for developing the COST was based on current US industry standards for constituents of the functional unit of concrete (USGS, 2015; ACAA, 2014; Davis et al., 2015; US EPA, 2009). Transportation costs are based on a point-to-point distance, not an actual driving distance, and are, therefore, approximations. The cost of aggregates is based on the cost from a recycling plant and does not

represent the cost from an on-site crusher. Table 8 illustrates the values used to calculate COST using Eq. 31.

Table 8 – Unit costs for constituent materials.

Unit Cost for Constituent Materials			
Material	Unit Cost	Unit	Source
Cement	0.0985	$/kg	(USGS, 2015)
Fly Ash	0.03	$/kg	(USGS, 2015)
Slag	0.017	$/kg	(USGS, 2015)(ACAA, 2014)
Virgin Aggregate	0.012	$/kg	(Davis et al., 2015)
Recycled Aggregate	0.01	$/kg	(Davis et al., 2015)
Transport	0.00055	$/kg/mile	(Davis et al., 2015)
Water	0.541	$/m3	(US EPA, 2009)

$$COST = W_{material} \cdot Unit\ Cost \tag{31}$$

Where:

$W_{material}$ = the weight (kg) or volume of the given material (m^3), and

Unit Cost = the unit cost (US dollars) taken from table 8.

The aim of this study was to develop a link between the service life performance and LCA of reinforced concrete for both virgin and recycled aggregates for the sake of comparison. The incorporation of service-life into life-cycle cost can serve as a valuable tool in making comparative decisions regarding material durability, sustainability, and cost.

CHAPTER V

RESULTS

4.1 Results from Analytical Model (Error Function Solution)

In this section, results are presented from service-life predictions of NA-C, RCA-C, and RMA-C using the error function solution to the diffusion equation. In the first set of presented results, the concrete materials were not initially doped with any initial contaminants and chloride initiation was determined with a constant bulk diffusion coefficient. As discussed, normal and lognormal distributions of variables were assumed based on empirical values shown in Table 1. The distribution of results appeared to yield a lognormal distribution of service life. The figures in this analysis were created from a lognormal mean and standard deviation, which was taken from the sample data of each Monte Carlo simulation (50,000 simulations). All results presented in this portion of the study were based the mean and standard deviation. The lognormal distribution was confirmed using the Anderson Darling goodness-of-fit test. In simplified terms, the test determines the difference between the sample data and a lognormal distribution created using a mean and standard

deviation of this sample data. If this difference falls within a certain significance level, the distribution is confirmed. Fig. 9 shows the sample data plotted next to the distributions created for the case of moderate chloride boundary conditions, severe chloride contamination levels (3.0 ± 0.2 kg/m^3), and a 100% replacement ratio. Sample data is only plotted over the lognormal distributions for the RCA-C and RMA-C is because the sample data was nearly identical and would not have been visible on this graph for NA-C.

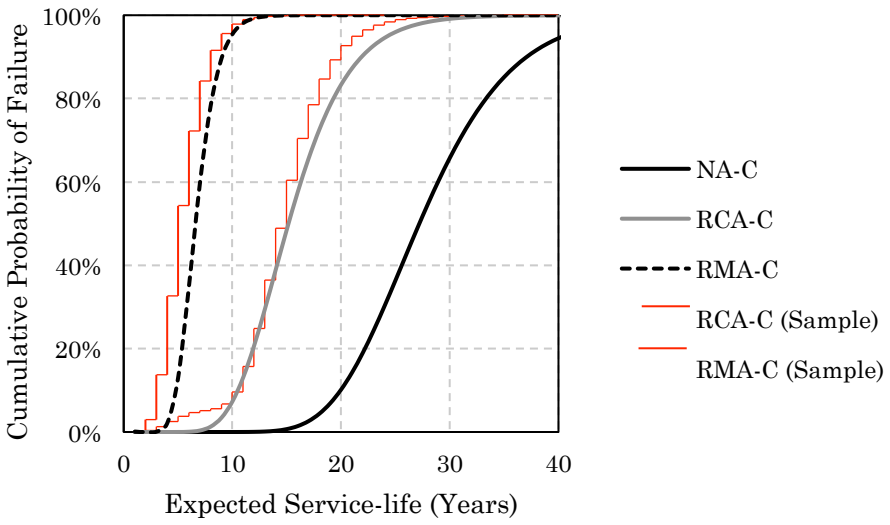

Figure 9 - Graph showing the sample data plotted next to the lognormal distribution produced using the lognormal mean and standard deviation of the sample data. The Anderson Darling test used these plots to validate the lognormal distribution of the data.

4.1.1 Cumulative Probability of Failure

Cumulative probability-of-failure distributions for mild (1 ± 0.2 kg/m^3), moderate (2 ± 0.2 kg/m^3), and severe (3 ± 0.2 kg/m^3) chloride environmental boundary conditions are shown in Figures 10, 11, and 12, respectively. These results correspond to

virgin- and recycled-aggregate concrete that contain no contaminants. All results presented in this section were determined using a constant 0.07m cover depth.

As expected, the probability of failure is shown to increase with recycled aggregate content. For example, in Fig. 10 at 50 years, NA-C has a 10% probability of failure, while RCA-C has a 30% probability of failure. However, due to the empirical values used for chloride levels, the degree to which NA-C and RCA-C differ may be exaggerated.

RMA-C contains more mortar, which has a more porous microstructure than RCA-C This high porosity is why RMA-C has the highest probability of failure of the three aggregates. Having a less porous microstructure, RCA-C has a lower probability of failure when compared to RMA-C, but a higher probability of failure when compared with NA-C. These trends remain similar for mild, moderate, and severe environments.

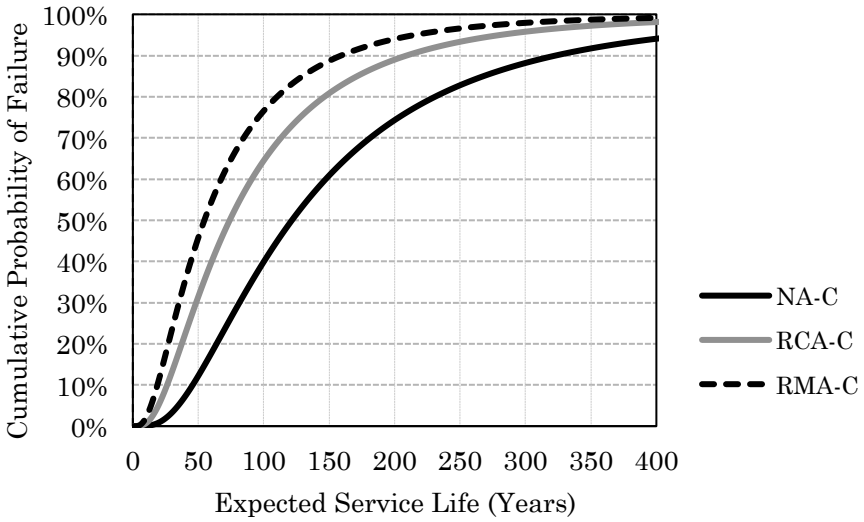

Figure 10 – A cumulative probability of failure distribution for a service-life simulation with 100% replacement ratios and no chloride contamination levels placed in a mild chloride environment for NA-C, RCA-C and RMA-C.

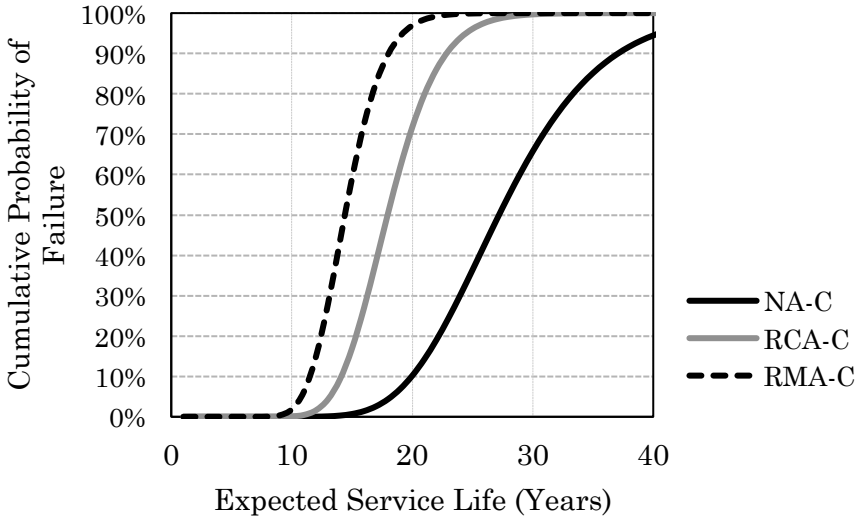

Figure 11 – A cumulative probability of failure distribution representing a service-life simulation with 100% replacement ratios and no chloride contamination levels placed in a moderate chloride environment for NA-C, RCA-C and RMA-C.

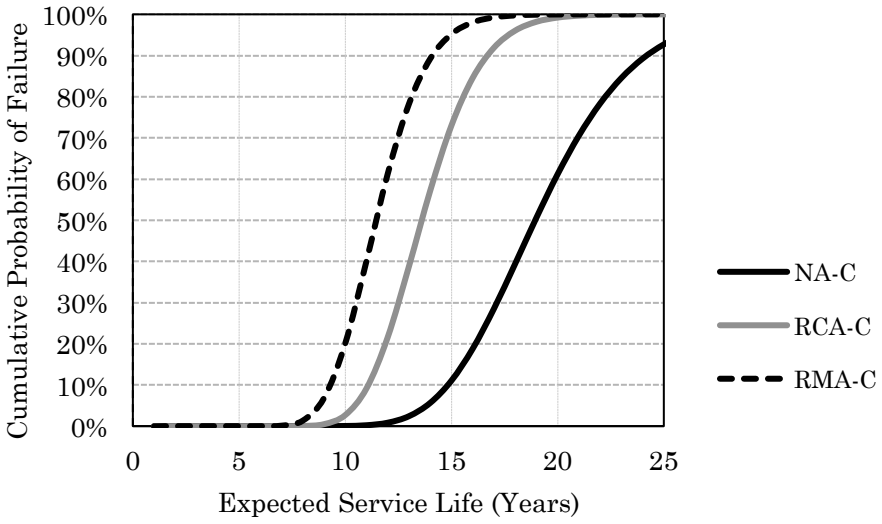

Figure 12 – A cumulative probability of failure distribution representing a service-life simulation with 100% replacement ratios and no chloride contamination levels placed in a severe chloride environment for NA-C, RCA-C and RMA-C

4.1.2 Performance of Aggregate Types in Various Environments

With outputs from simulations of various scenarios, service life comparisons can be made between "green" recycled-aggregate and virgin-aggregate alternatives. Graphs of these comparisons for each scenario simulated in this study were evaluated at a 0.07 m cover depth. All of the figures in this section represent side-by-side comparisons of median service-life values for NA-C, RCA-C and RMA-C in mild (1 ± 0.2 kg/m^3 Cl), moderate (2 ± 0.2 kg/m^3 Cl), and severe (3 ± 0.2 kg/m^3 Cl) chloride environments. The differences between each figure are the aggregate replacement ratios (33%, 66%, 100%) and the severity (mild: 1 kg/m^3, severe: 3 kg/m^3) of chloride contamination levels. Fig. 13 and 14 represent comparisons at 33% replacement ratios with mild and severe chloride contamination, respectively; Figures 15 and 16 represent comparisons at 66% replacement ratios with mild and severe chloride

contamination levels, respectively; and Figures 17 and 18 represent comparisons at 100% replacement ratios with mild and severe chloride contamination levels, respectively. Figures 13-18 show that NA-C achieves the longest service life, RCA-C achieves the second longest service life and RMA-C exhibits the shortest service life, as expected. Also as expected, service life decreases for all types of concrete as the chloride environment increases in severity. The environment in which the specimen is placed appears to have a much larger effect on service life than amount of recycled content. This can be seen when comparing any of Figures 13-18 to Fig. 19 which makes a comparison of service life for NA-C, RCA-C and RMA-C, where environment is held constant at mild and the aggregate replacement ratios are varied.

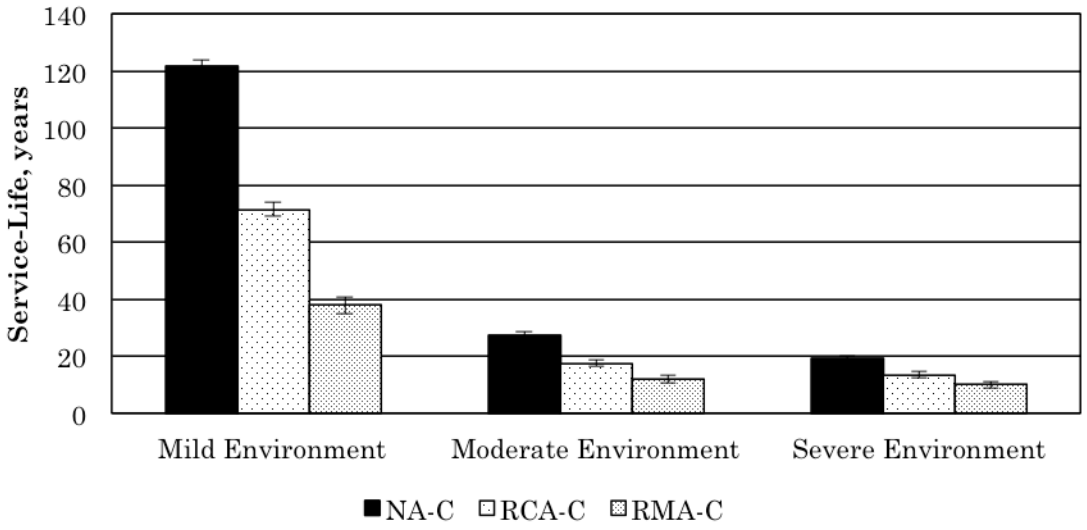

Figure 13 – Comparison of median service-life predictions for NA-C, RCA-C, and RMA-C in mild, moderate and severe chloride environments. For this graph RCA-C and RMA-C contains a 33% replacement of virgin-aggregates with mild chloride contamination levels.

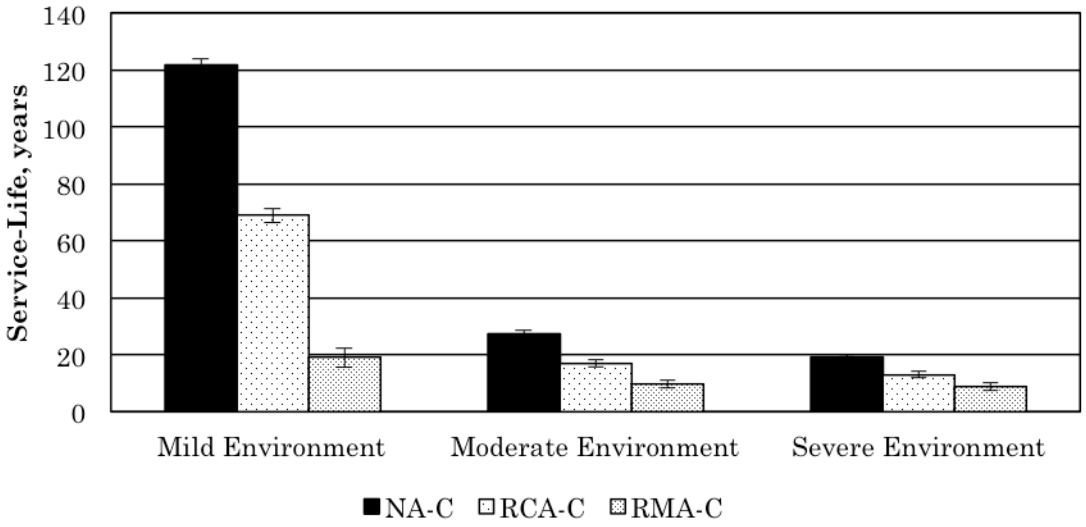

Figure 14 – Comparison of median service-life predictions for NA-C, RCA-C, and RMA-C in mild, moderate and severe chloride environments. For this graph RCA-C and RMA-C contains a 33% replacement of virgin-aggregates with severe chloride contamination levels.

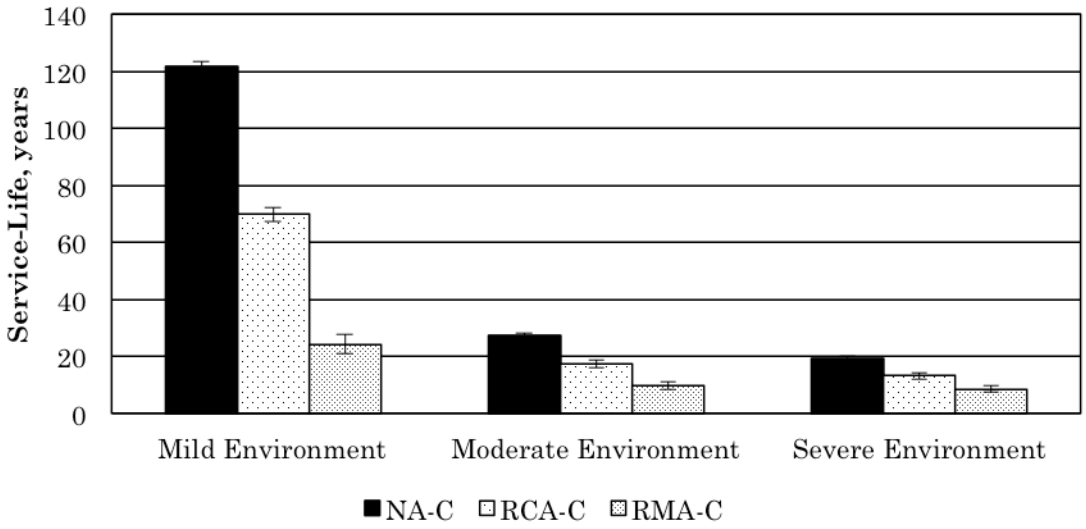

Figure 15 – Comparison of median service-life predictions for NA-C, RCA-C, and RMA-C in mild, moderate and severe chloride environments. For this graph RCA-C and RMA-C contains a 66% replacement of virgin-aggregates with mild chloride contamination levels.

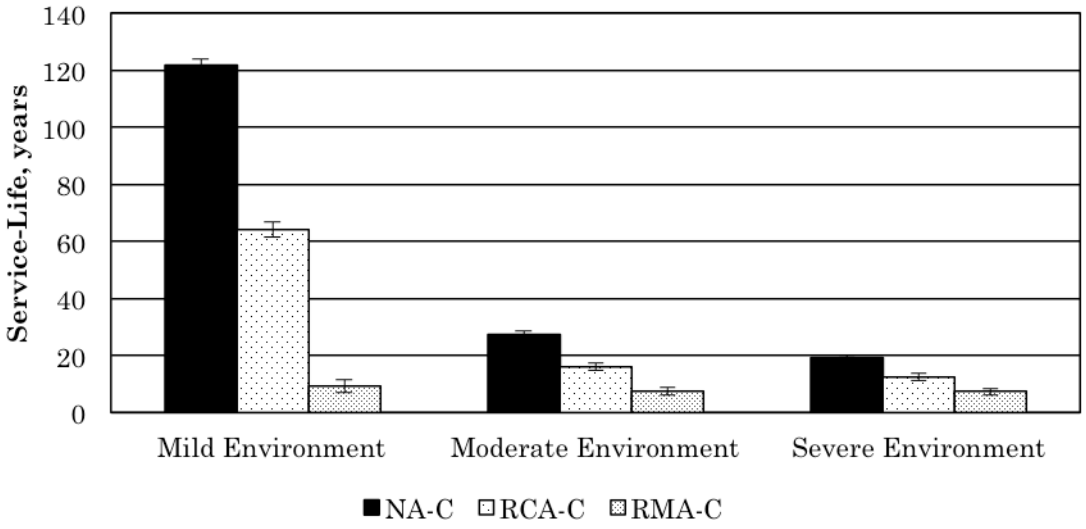

Figure 16 – Comparison of median service-life predictions for NA-C, RCA-C, and RMA-C in mild, moderate and severe chloride environments. For this graph RCA-C and RMA-C contains a 66% replacement of virgin-aggregates with severe chloride contamination levels.

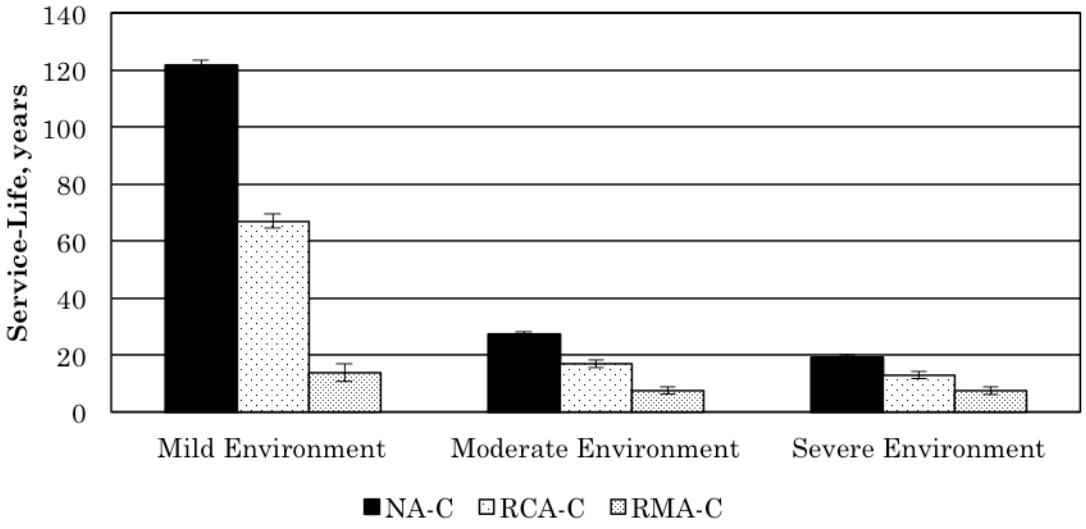

Figure 17 – Comparison of median service-life predictions for NA-C, RCA-C, and RMA-C in mild, moderate and severe chloride environments. For this graph RCA-C and RMA-C contains a 100% replacement of virgin-aggregates with mild chloride contamination levels.

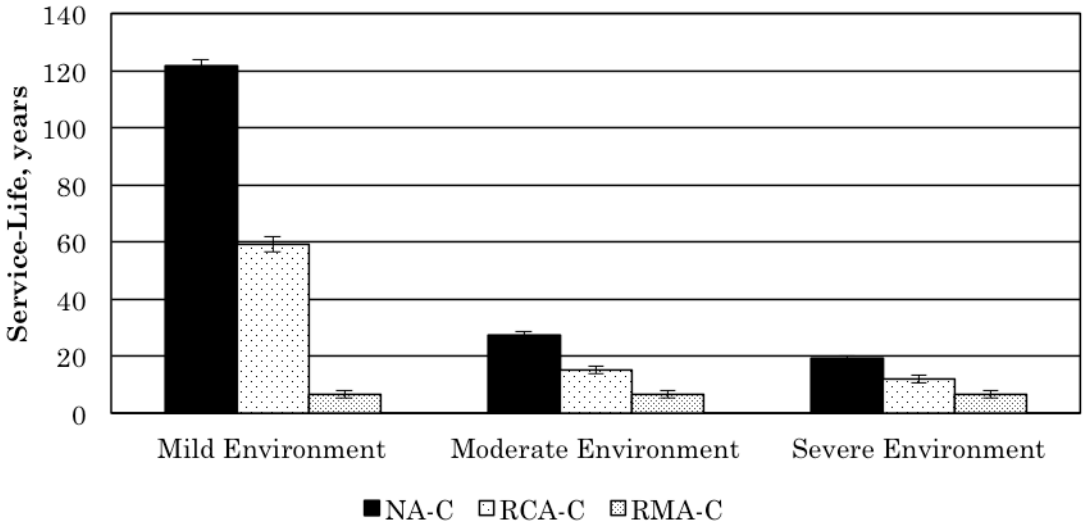

Figure 18 – Comparison of median service-life predictions for NA-C, RCA-C, and RMA-C in mild, moderate and severe chloride environments. For this graph RCA-C and RMA-C contains a 100% replacement of virgin-aggregates with severe chloride contamination levels.

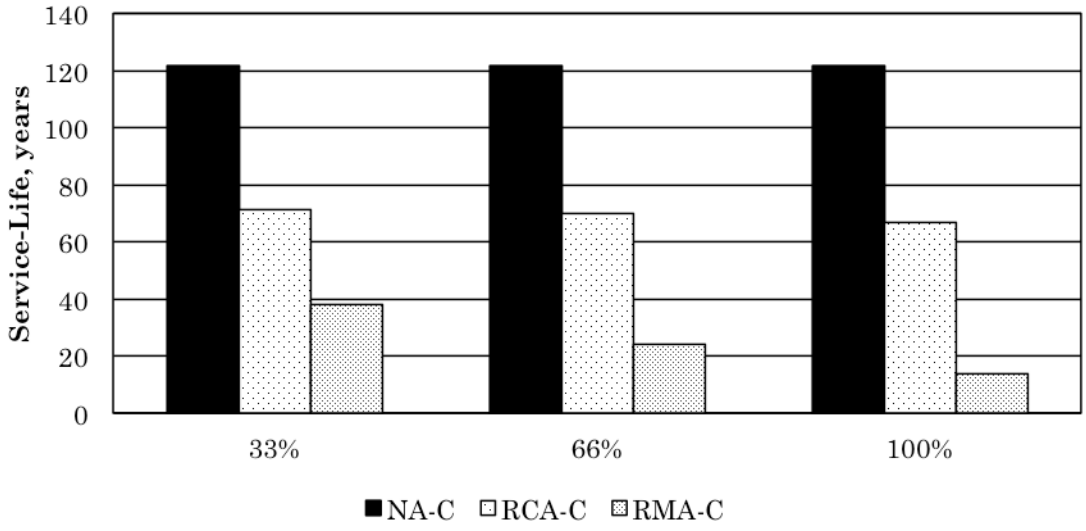

Figure 19 - Side-by-side comparison of median service-life for NA-C, RCA-C and RMA-C containing mild chloride contamination levels in a mild chloride environment at replacement ratios of 33%, 66% and 100%.

4.1.3 Manipulating Cover Depth

Given that both RCA-C and RMA-C exhibit shorter service lives than NA-C, the service-life modeling approach was used to evaluate the feasibility of increasing cover depth of RCA-C and RMA-C to achieve similar service lives to NA-C. For example, Figure 20 shows that in order to make RCA-C with a 33% replacement ratio, the cover would need to be increased by .015m. This result suggests that increasing the cover depth could prove to be an effective way to make the performance of RCA-C with mild chloride contamination levels more competitive to NA-C in mild chloride environments.

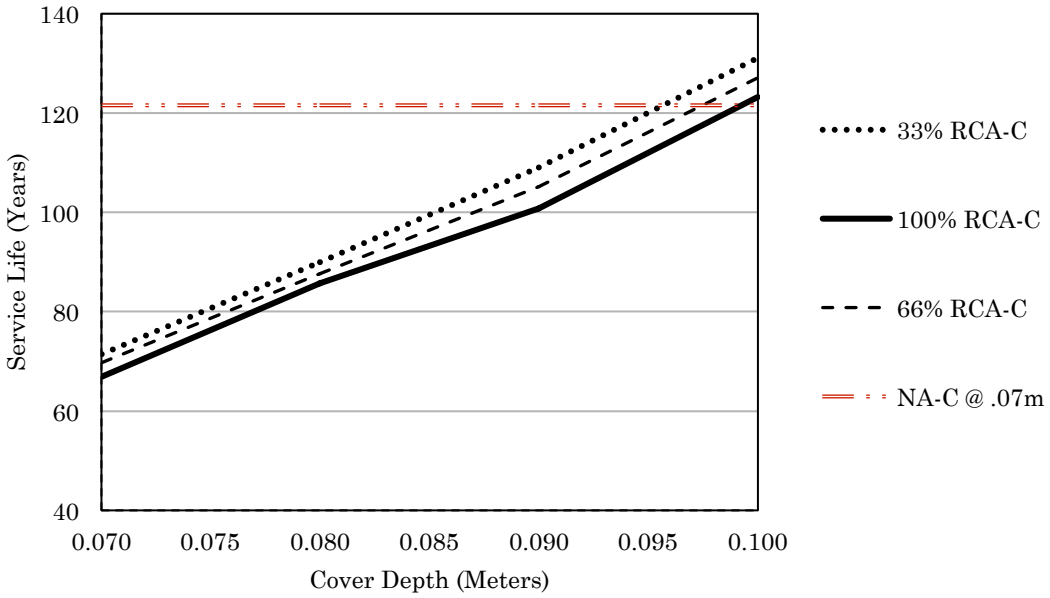

Figure 20 – A graphical representation of the cover depth (in meters) that is needed for RCA-C to achieve a service life (in years), which is equivalent to that of NA-C. The required cover depth is shown for aggregates containing mild chloride contamination levels and replacement ratios of 33%, 66% and 100% placed in a mild chloride environment.

Figure 21 shows that the strategy for increasing the cover for RMA-C to increase its competitiveness with NA-C will not work as well as it may for RCA-C. Even at low replacement ratios, increasing the cover is not that effective. For example, when the cover is increased to .120m for RMA-C with a 33% replacement ratio, it still exhibits a shorter service life than NA-C with a 0.07m cover. These results suggest that increasing the cover depth in order to achieve a longer service life is more effective with RCA-C than with RMA-C.

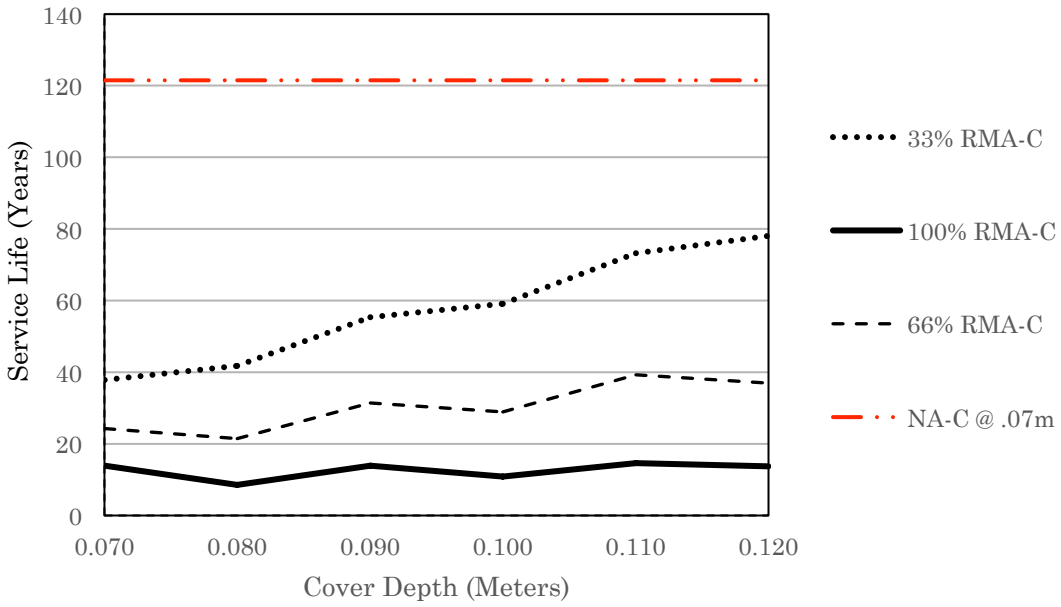

Figure 21 - A graphical representation of the cover depth (in meters) that is needed for RMA-C to achieve a service life (in years), which is equivalent to that of NA-C. The required cover depth is shown for aggregates containing mild chloride contaminant levels and replacement ratios of 33%, 66% and 100% placed in a mild chloride environment.

4.2 Results from Numerical Model (Finite Difference Solution)

The numerical model uses time and temperature dependent variables with allow for location-specific simulations. The location for all simulations presented in this study

was Los Angeles, CA where the monthly temperature profile presented in Fig. 4 was used to model the temperature-dependence of the diffusion coefficient. The parking structure exposure conditions were based on this location. The remaining boundary conditions were based on distances from the coastline. Since these diffusion coefficients and exposures were based on real data for a specific location, comparisons cannot be made between the first and the second service-life models developed in this study. As previously mentioned, the one-dimensional finite difference approach to service-life modeling is not capable of analyzing RCA-C. Thus, values in this part of the study represent those taken from simulations of NA-C and RMA-C only.

SCMs were included in this part of the study. Due to lack of life-cycle energy and cost data, silica fume and metakaolin were excluded. However, the numerical model is capable of including silica fume and metakaolin. The effect of incorporating ultra fine fly ash was assessed using cement replacement ratios of 15% and 30% (by volume). Similarly, the effect of incorporating slag was assessed at replacement ratios of 25% and 30% (by volume).

4.2.1 Model Validation

As discussed, the model developed in this study was based on the computer program Life-365 (Life-365, 2014), which calculates the service life of reinforced concrete using a numerical solution to Fick's second law of diffusion. The current commercial version of this modeling software does not include the effects of recycled aggregates. To validate the model developed in this study, an analysis with identical

parameters was performed using both models. These parameters are shown in Table 9.

Table 9 - Parameters for validation simulation.

Validation Scenario		
One-Dimensional		
Location	Los Angeles	
Exposure	Parking Garage	
Thickness	500	mm
Cover Depth	70	mm
Diffusion Coefficient, D_{28}	8.8718	$10^{-12}m^2/s$

The outputs for chloride concentration versus time at the cover depth of the specimen are represented in the line graph shown in Fig. 22a. The LIFE365 data in the line graph shown in Fig. 22a was the output from this studies numerical model, and it matched the LIFE-365 program exactly (see Fig. 22b). The NEW data shown in the line graph in Fig. 22a represents the model run with the same parameters but with an updated diffusion coefficient. The only difference between these two models is the diffusion coefficient and the decay constant. The model presented in this study uses an ultimate limiting factor to the time dependent reduction in the diffusion coefficient, and Life-365 does not include such a factor. The decay factor used for the NEW simulation was taken from Eq. 16, where Life-365 uses a value of m = 0.20. The results of this simulation show the updated model developed for this study is conservative (i.e., results in shorter service life predictions) in comparison to Life-365. The bar graph in Fig. 22b shows the same data from the line graph, but most importantly illustrates a direct comparison of the outputs from the Life365

program and the validation simulation ran using the finite difference model developed for this study.

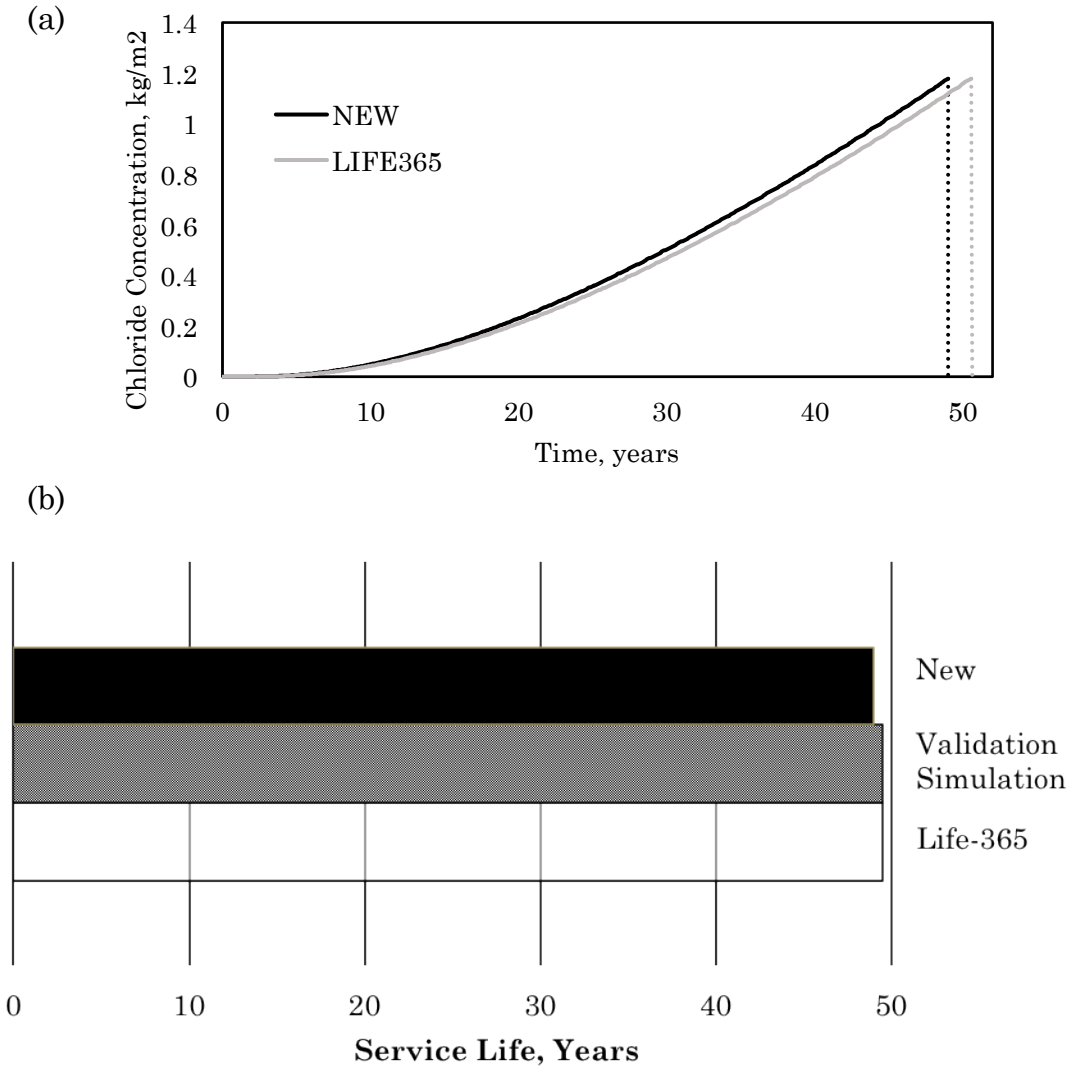

Figure 22 - A comparison of chloride concentration at the steel reinforcement vs. time for the numerical model developed for this study and Life-365 model of which it was based on.

4.2.2 Time-Dependent Solution

Figures 23, 24, and 25 shows the time-dependent chloride concentration throughout the cover depth of concrete as predicted by the finite difference approach for NA-C,

RMA-C (100% replacement, mild contamination, mild chloride environment), and RMA-C (100% replacement, severe contamination, severe chloride environment). The concentration profiles at ***Time 2*** in the figures represent the time at failure. In Fig. 23, 24, and 25, ***Time 2*** is equal to 54 ± 1 years, 44 ± 6 years, and 5 ± 3 years, respectively. ***Time 0*** in Fig. 23 (NA-C) shows that there are no initial contaminants. However, in Fig. 24 and 25 are for RMA-C, ***Time 0*** shows initial spikes of mild and severe chloride levels, respectively, that correspond to the location of original, contaminated recycled mortar aggregates. Together, these figures illustrate how chloride levels at the cover depth are exacerbated by the presences of initial chlorides from recycled-aggregates.

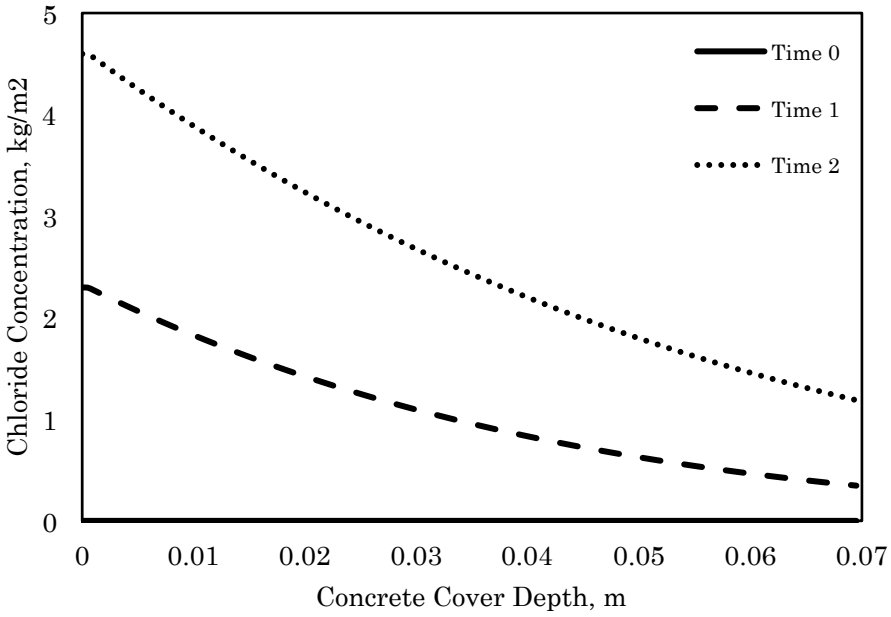

Figure 23 – a graphical representation of the time-dependent chloride concentration throughout the cover depth of the reinforced concrete specimen for NA-C used in a parking structure (>1.5km) from the coast. Note no initial chloride contamination associated with the virgin aggregates at Time 0 for NA-C.

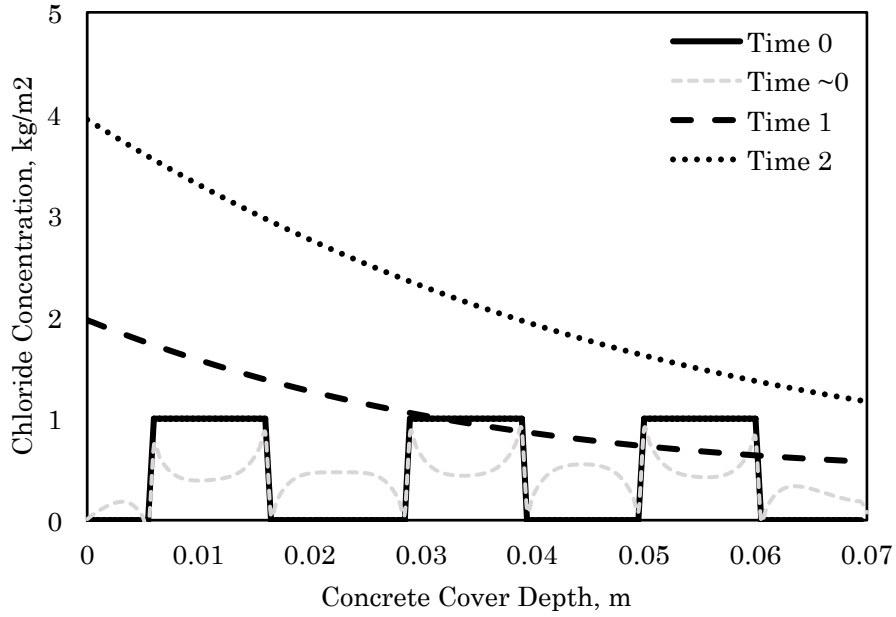

Figure 24 – A graphical representation of the time-dependent chloride concentration throughout the cover depth of the reinforced concrete specimen for RMA-C used in a parking structure (>1.5km) from the coast. This graph represents RMA-C with a 100% replacement ratio containing mild chloride contamination levels.

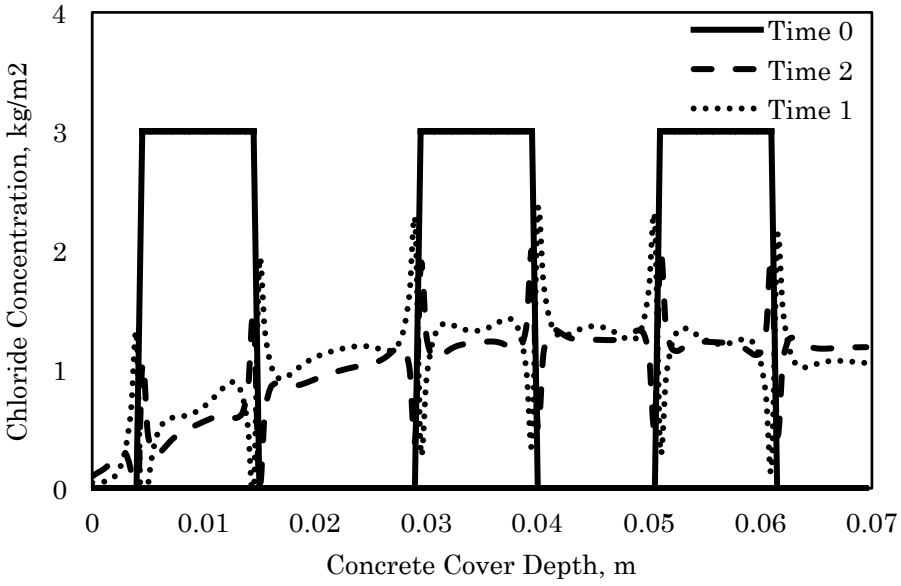

Figure 25 - A graphical representation of the time-dependent chloride concentration throughout the cover depth of the reinforced concrete specimen for RMA-C used in a parking structure (>1.5km) from the coast. This graph represents RMA-C with a 100% replacement ratio containing severe chloride contamination levels.

4.2.3 Performance of Aggregate Type in Various Environments

Comparisons between median service-life predictions for NA-C and RMA-C are illustrated in Figures 26-31. These Figures represent predictions of service life for reinforced concrete placed in various chloride environments defined by the locations presented in Table 3. As expected, as the severity of chloride exposure conditions decreases, service life increases. With a 33% replacement ratio and both mild and severe initial chloride contamination levels, RMA-C displays a comparable service-life performance to that of NA-C with an 11% difference between the two, respectively. This is show in Figures 26 and 27. Even with 66% and 100% replacement ratios and mild initial chloride contamination levels, RMA-C continues to perform relatively well next to NA-C with a 30% difference between the two. However, with a 66% replacement ratio and severe initial chloride contamination levels, the service-life performance of RMA-C decreases. This result is especially evident in Fig. 30, with a 100% replacement ratio and severe initial chloride contamination levels. In this case the corrosion initial is immediate, and the service life is due to the time it takes to crack the concrete surface. Together, the data presented in these figures suggest that the exposure conditions (rather than initial level of aggregate contamination) have the greatest effect on service life, while, at higher replacement ratios, severity of contaminants has a greater effect on expected service life.

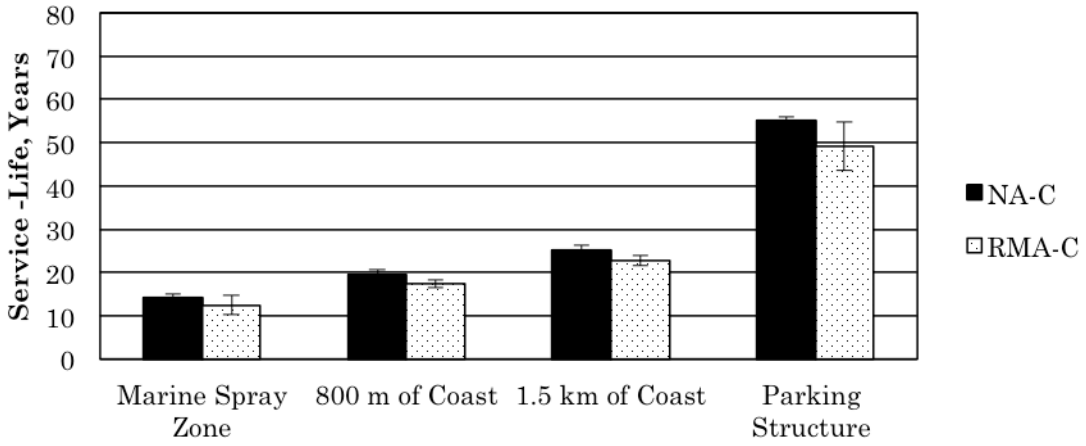

Figure 26 – A side-by-side comparison of NA-C and RMA-C with a 33% replacement ratio in various environments. In this graph, RMA-C contains mild chloride contamination levels.

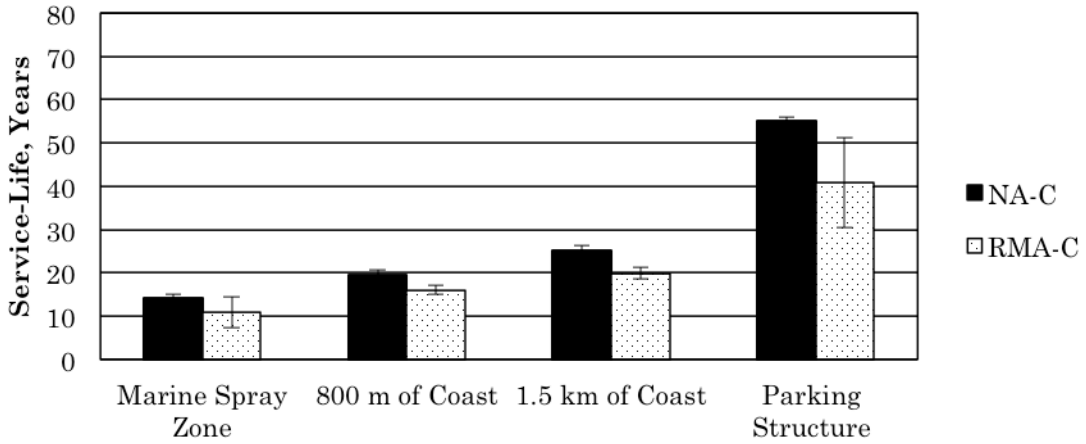

Figure 27 – A side-by-side comparison of NA-C and RMA-C with a 33% replacement ratio in various environments. In this graph, RMA-C contains severe chloride contamination levels.

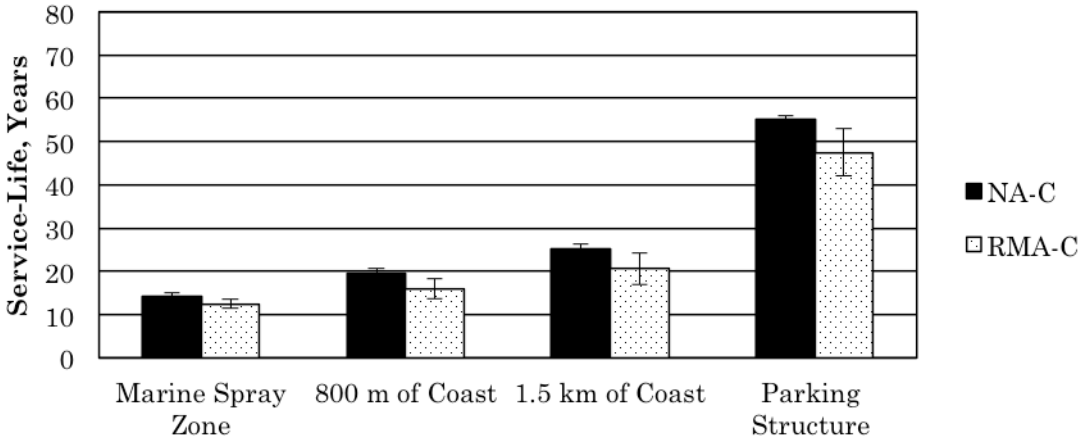

Figure 28 – A side-by-side comparison of NA-C and RMA-C with a 66% replacement ratio in various environments. In this graph, RMA-C contains mild chloride contamination levels.

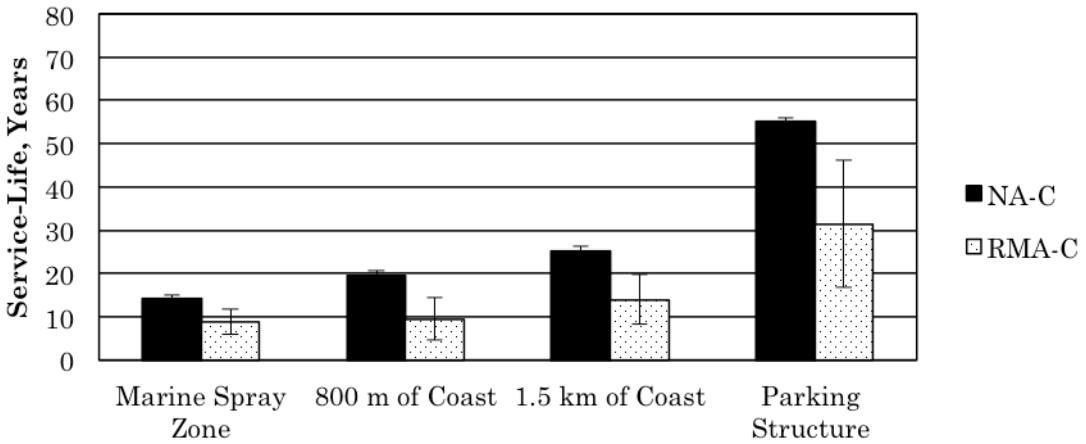

Figure 29 – A side-by-side comparison of NA-C and RMA-C with a 66% replacement ratio in various environments. In this graph, RMA-C contains severe chloride contamination levels.

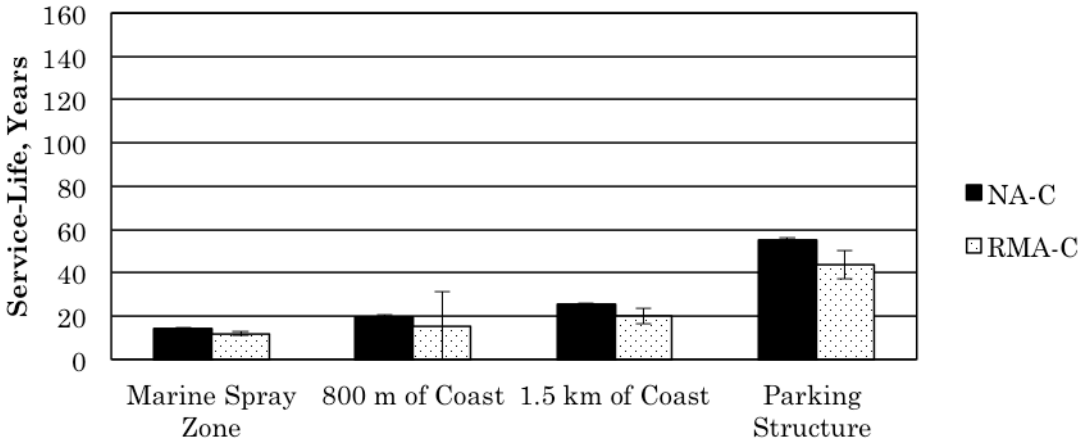

Figure 30 – A side-by-side comparison of NA-C and RMA-C with a 100% replacement ratio in various environments. In this graph, RMA-C contains mild chloride contamination levels.

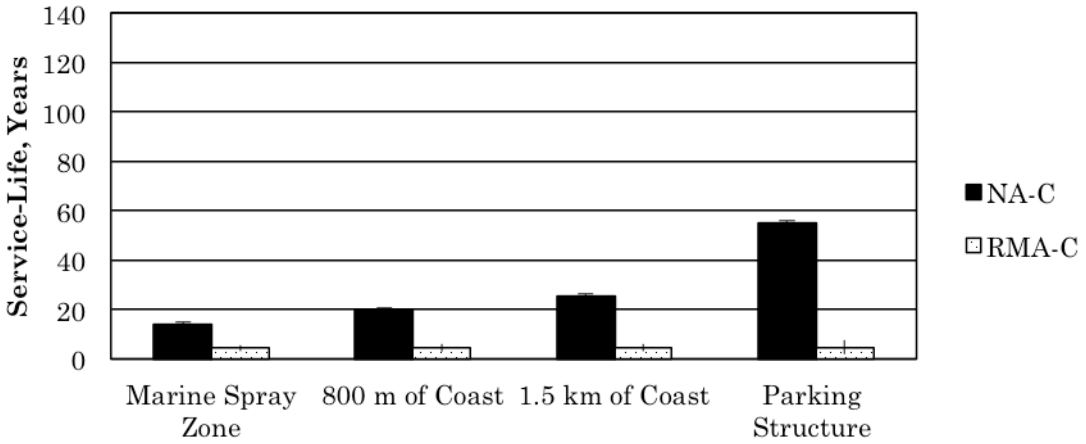

Figure 31– A side-by-side comparison of NA-C and RMA-C with a 100% replacement ratio in various environments. In this graph, RMA-C contains severe chloride contamination levels.

4.2.4 Service-Life Performance with SCM Additions

Figures 32-37 show the results discussed in the previous section next to the median service-life predictions for NA-C and RMA-C that were obtained by including Slag (SG). Similarly, Figures 38-43 show the results discussed in the previous section next to the median service-life predictions for NA-C and RMA-C that were obtained by including Ultra Fine Fly Ash (UFFA). The results clearly show that the inclusions of SCMs increase the service life of concrete. The only case where the service-life of RMA-C including SCMs did not exceed NA-C was with concrete made with recycled-aggregates that contained severe initial contamination and replacement ratios of 66% and 100%.

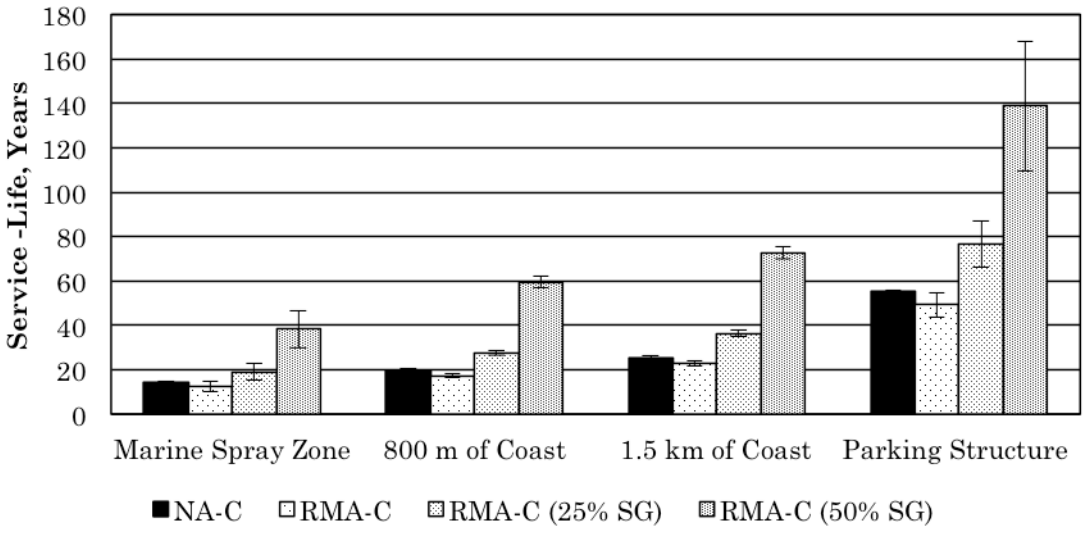

Figure 32 – A side-by-side comparison of NA-C and RMA-C with a 33% replacement ratio in various environments. In this graph, RMA-C containing mild chloride contamination levels with 25% and 50% cement replacement of Slag.

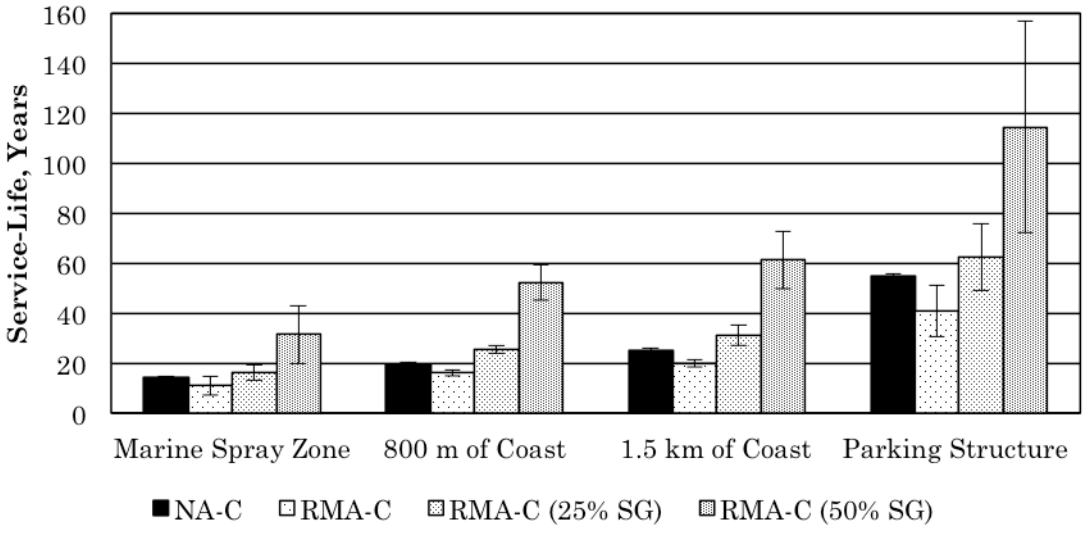

Figure 33 – A side-by-side comparison of NA-C and RMA-C with a 33% replacement ratio in various environments. In this graph, RMA-C containing severe chloride contamination levels with 25% and 50% cement replacement of Slag.

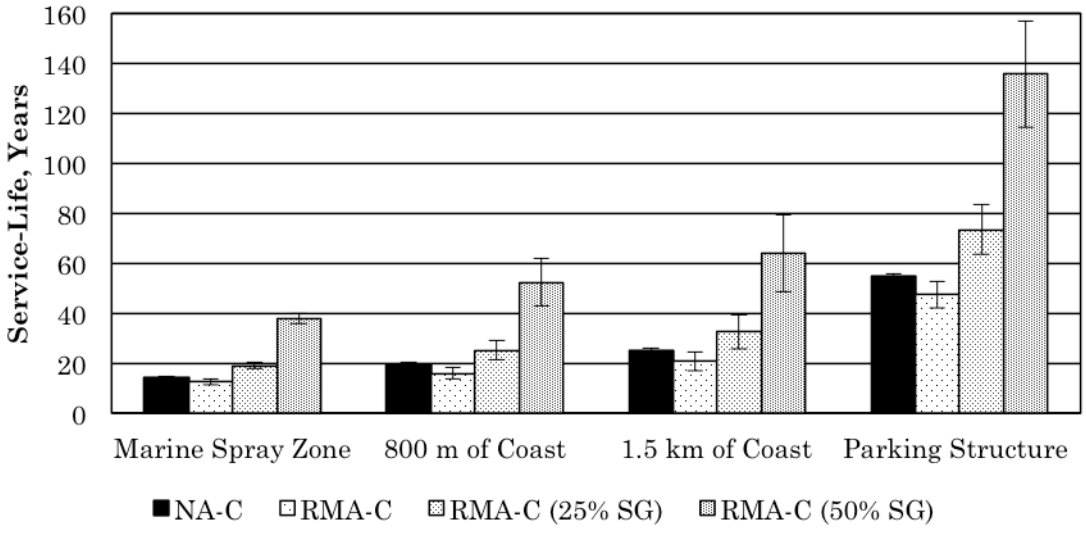

Figure 34– A side-by-side comparison of NA-C and RMA-C with a 66% replacement ratio in various environments. In this graph, RMA-C containing mild chloride contamination levels with 25% and 50% cement replacement of Slag.

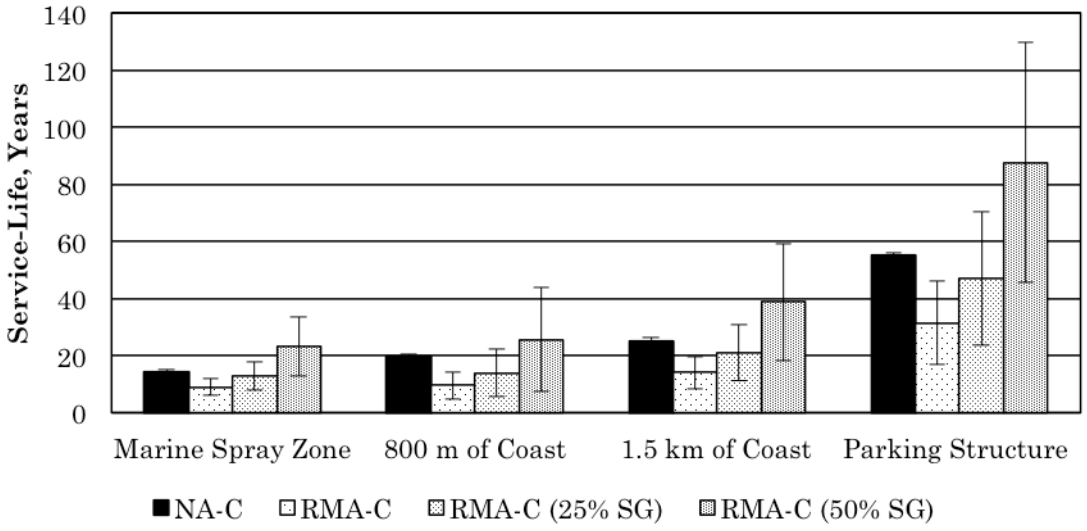

Figure 35 – A side-by-side comparison of NA-C and RMA-C with a 66% replacement ratio in various environments. In this graph, RMA-C containing severe chloride contamination levels with 25% and 50% cement replacement of Slag.

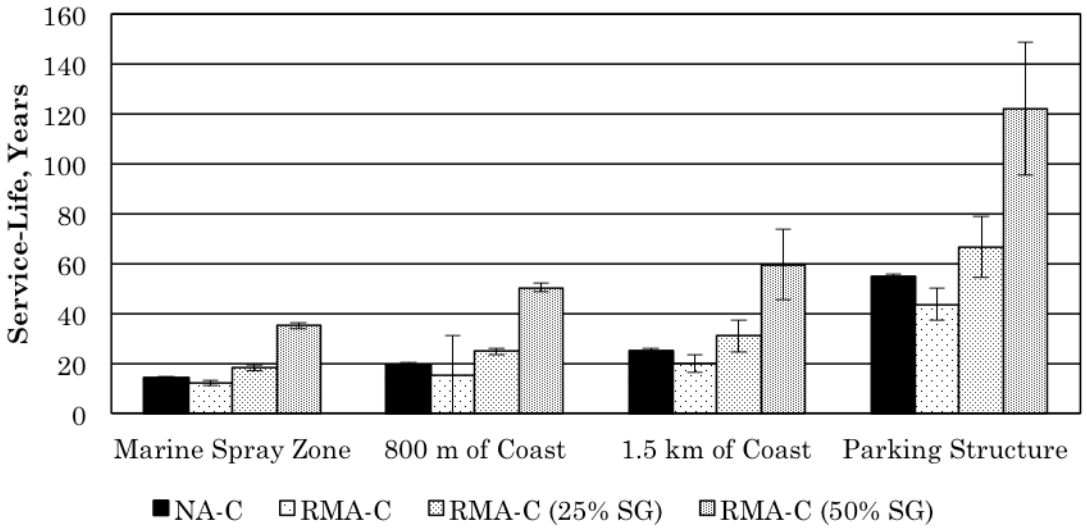

Figure 36 – A side-by-side comparison of NA-C and RMA-C with a 100% replacement ratio in various environments. In this graph, RMA-C containing mild chloride contamination levels with 25% and 50% cement replacement of Slag.

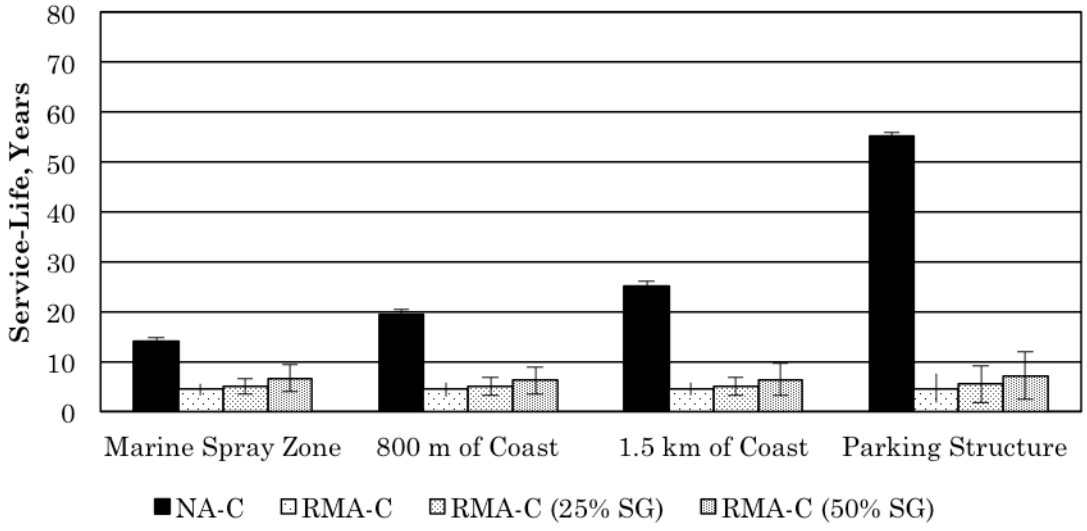

Figure 37– A side-by-side comparison of NA-C and RMA-C with a 100% replacement ratio in various environments. In this graph, RMA-C containing severe chloride contamination levels with 25% and 50% cement replacement of Slag.

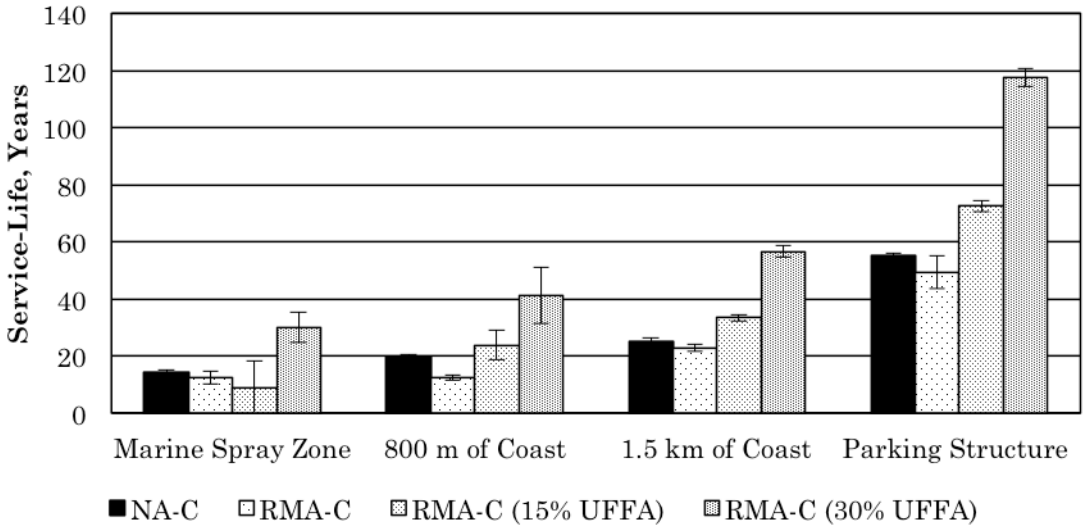

Figure 38– A side-by-side comparison of NA-C and RMA-C with a 33% replacement ratio in various environments. In this graph, RMA-C containing mild chloride contamination levels with 15% and 30% cement replacement of Ultra Fine Fly Ash (UFFA).

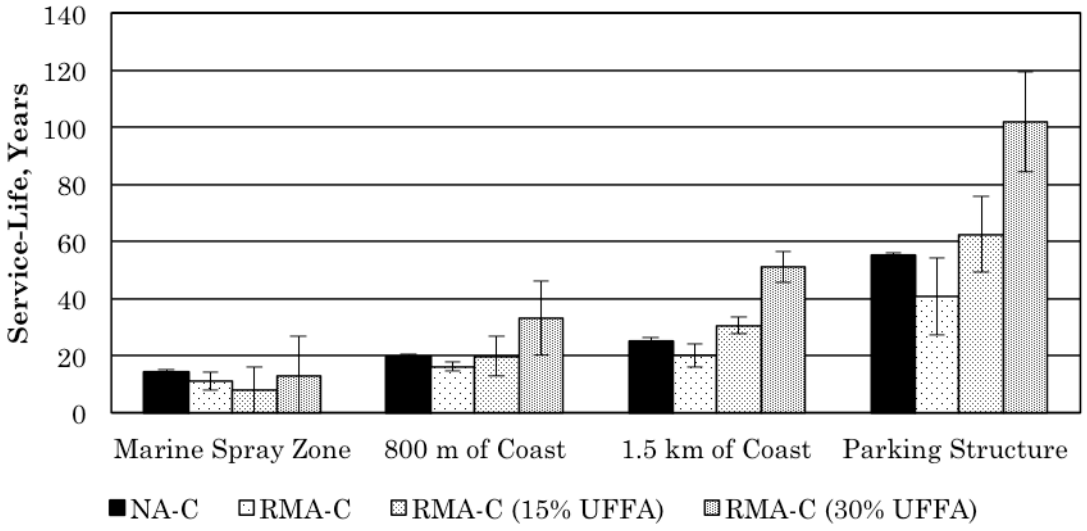

Figure 39 – A side-by-side comparison of NA-C and RMA-C with a 33% replacement ratio in various environments. In this graph, RMA-C containing severe chloride contamination levels with 25% and 50% cement replacement of Ultra Fine Fly Ash (UFFA).

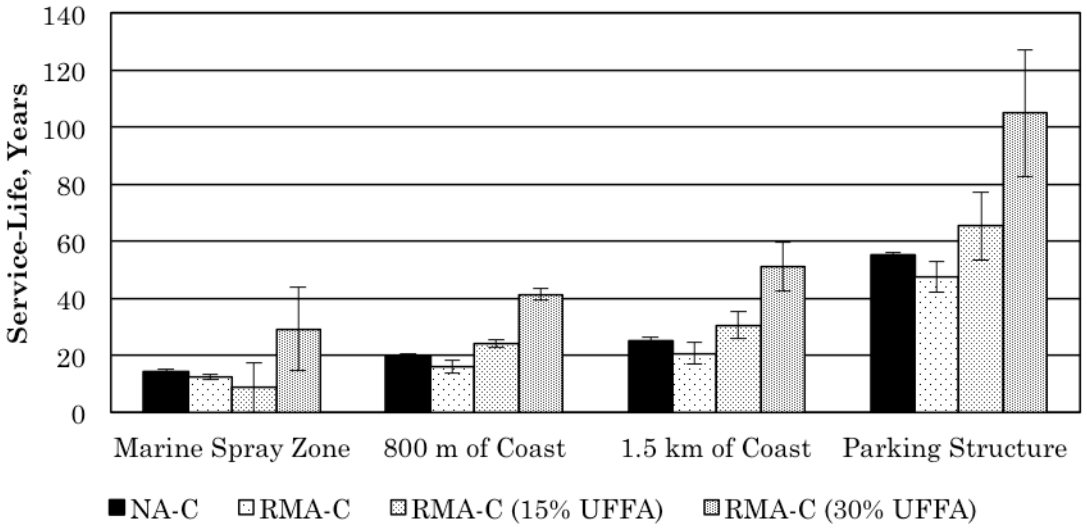

Figure 40 – A side-by-side comparison of NA-C and RMA-C with a 66% replacement ratio in various environments. In this graph, RMA-C containing mild chloride contamination levels with 15% and 30% cement replacement of Ultra Fine Fly Ash (UFFA).

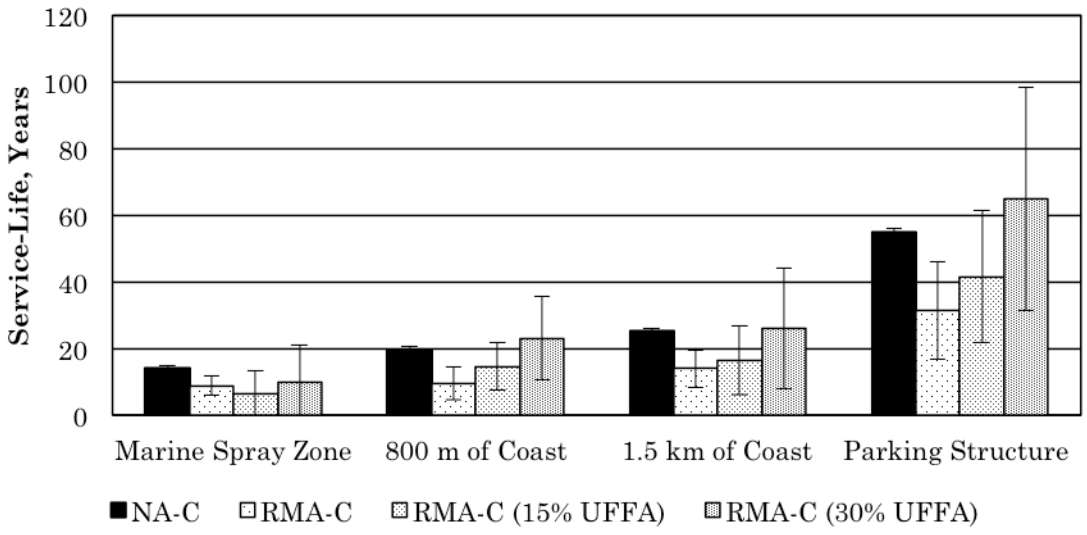

Figure 41 – A side-by-side comparison of NA-C and RMA-C with a 66% replacement ratio in various environments. In this graph, RMA-C containing severe chloride contamination levels with 15% and 30% cement replacement of Ultra Fine Fly Ash (UFFA).

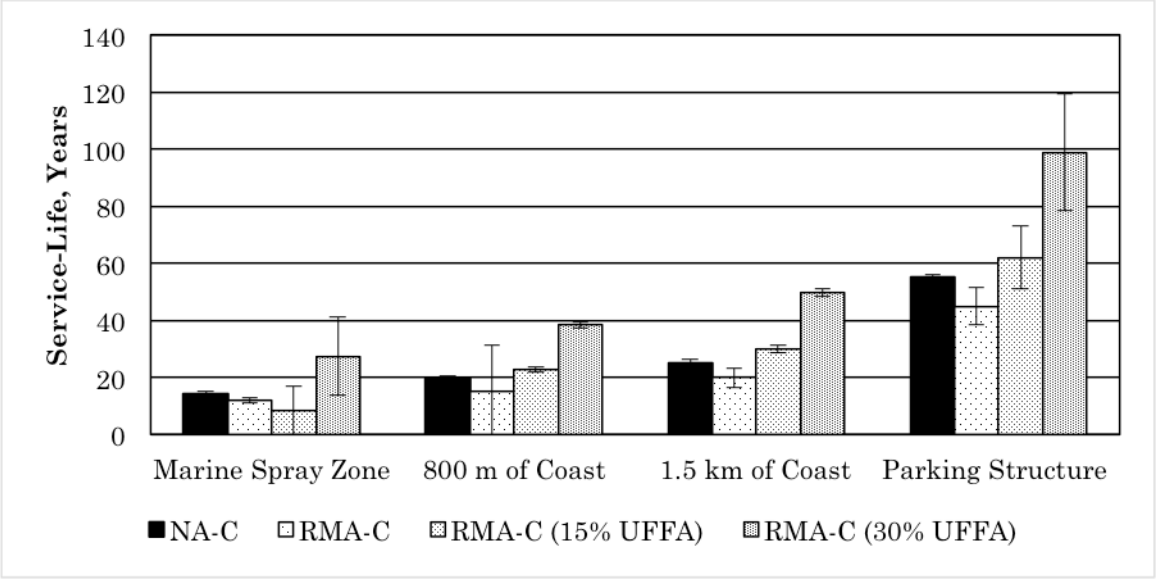

Figure 42 – A side-by-side comparison of NA-C and RMA-C with a 100% replacement ratio in various environments. In this graph, RMA-C containing mild chloride contamination levels with 15% and 30% cement replacement of Ultra Fine Fly Ash (UFFA).

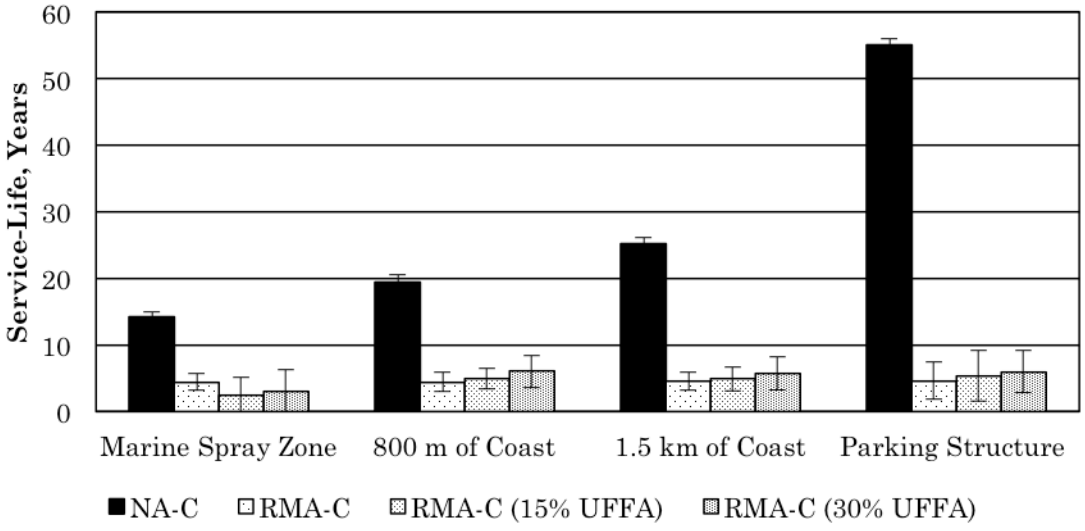

Figure 43 – A side-by-side comparison of NA-C and RMA-C with a 100% replacement ratio in various environments. In this graph, RMA-C containing severe chloride contamination levels with 15% and 30% cement replacement of Ultra Fine Fly Ash (UFFA).

4.2.5 Energy Analysis

The embodied energy was calculated using methods presented in section 3.5. Because the transportation was included as a general value, based on a distance of 8km or less given in the life cycle inventory, these numbers are not location-specific and are only differentiated by type of aggregate, the recycled-to-virgin aggregate replacement ratio, and the SCM replacement ratio of cement. In future work this approach could be improved up to include more accurate energy costs due to transportation. Figures 44 and 45 show the embodied energy of NA-C and RMA-C with SCM replacement ratios of slag and ultra-fine fly ash, respectively. These results show that replacing virgin-aggregates with recycled-aggregates increases the embodied energy needed to produce concrete when SCMs are not included. As expected, when UFFA and Slag are included the embodied energy decreases. Slag appears to create a more significant reduction in embodied energy than UFFA. Fig. 46 shows the percent difference of RMA-C with varying SCM cement replacement ratios and types from NA-C.

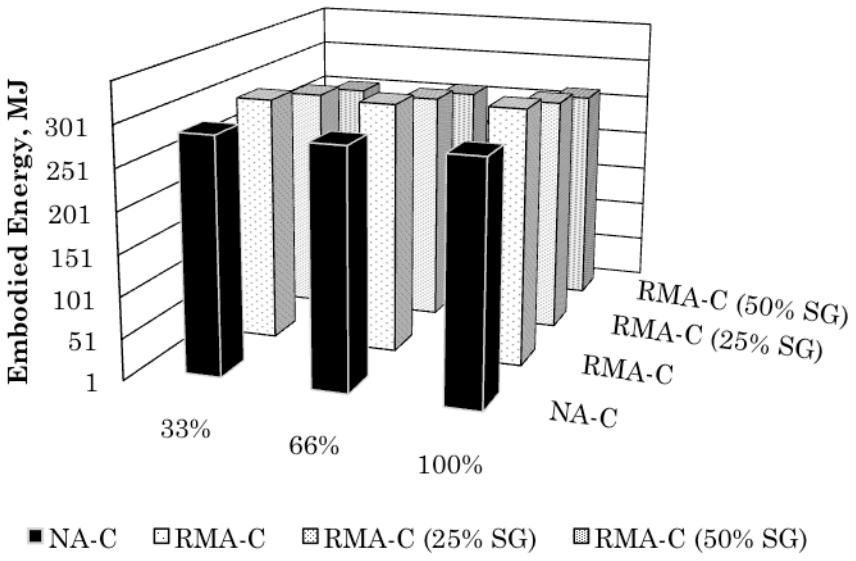

Figure 44 – A comparison of embodied energy (MJ) for RMA-C (including mixtures with Slag) with NA-C. Embodied energy for this study was not location dependent. Embodied energy was tabulated for aggregate replacement ratios of 33%, 66%, and 100%.

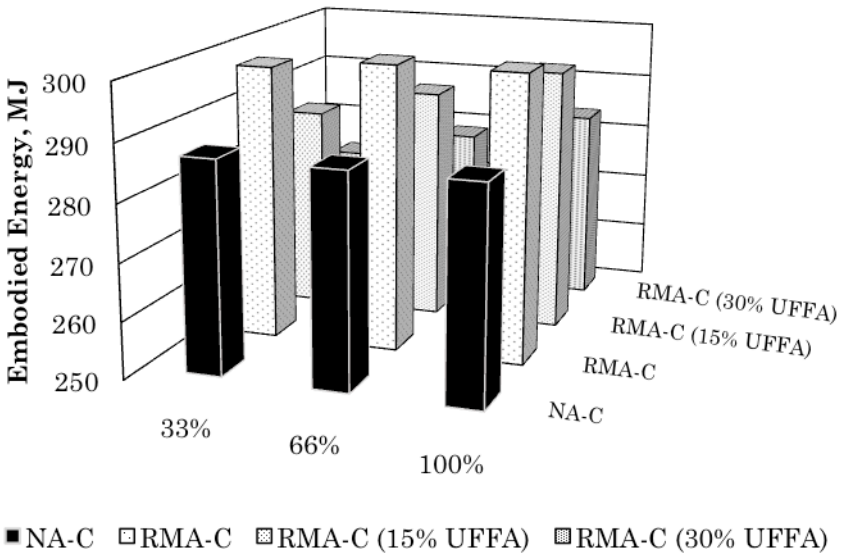

Figure 45 – A comparison of embodied energy (MJ) for RMA-C (including mixtures with Ultra Fine Fly Ash - UFFA) with NA-C. Embodied energy for this study was not location dependent. Embodied energy was tabulated for aggregate replacement ratios of 33%, 66%, and 100%.

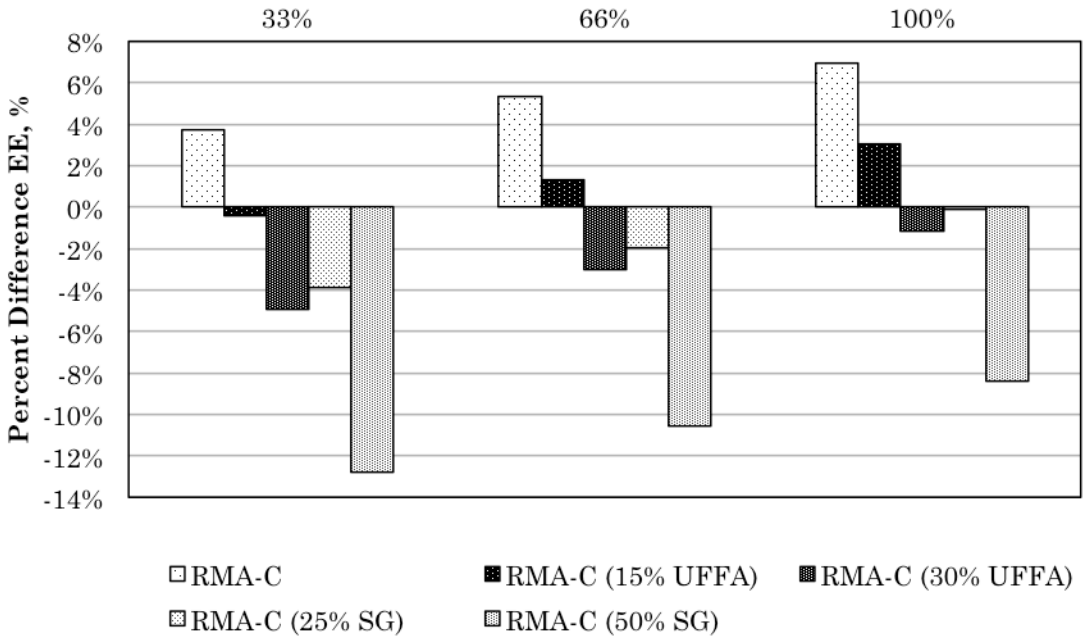

Figure 46 – An illustration of the percent difference of embodied energy for each RMA-C mixture including Slag and Ultra Fine Fly ash Mixtures from that of NA-C. Embodied energy was not dependent on location in this study.

4.2.6 Cost Analysis

The results of this portion of the study are based on the methods outline in section 3.5, where the cost of the functional unit is tabulated using the content (weight and volume) of each constituent material and its corresponding unit cost. The results of this study varied by location due to transportation costs, but were a point-to-point distance from a randomly selected location in each exposure environment to the closest source of recycled aggregates in the Los Angeles area. This random distance has no significance in this study, but was included in the model as an option to make service life and LCA simulations location-specific. Since this study does not

analyze location dependence, it was held constant for the sake of making comparisons between materials.

As expected, the results illustrate that the inclusion of recycled-aggregates decreases the total cost. Much greater cost savings are achieved with the inclusion of SCMs. A side-by side comparison of NA-C with each RMA-C mixture is illustrated in Fig. 47. The reduction due to the inclusion of SCMs is greater for slag than for ultra-fine fly ash. The percent differences of each RMA-C mixture from NA-C are illustrated in Fig. 48. In general, the cost of concrete decreases as recycled-aggregates and SCMs increases.

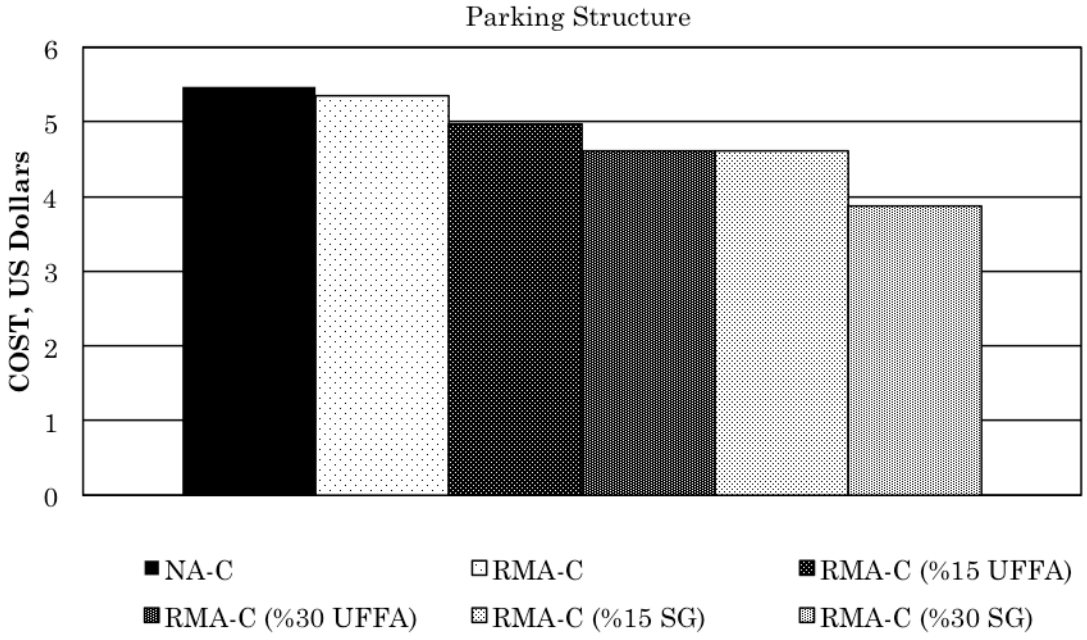

Figure 47 – A graph representing the cost (in US Dollars) for each mixture scenario for a parking structure located further than 1.5km from the coast.

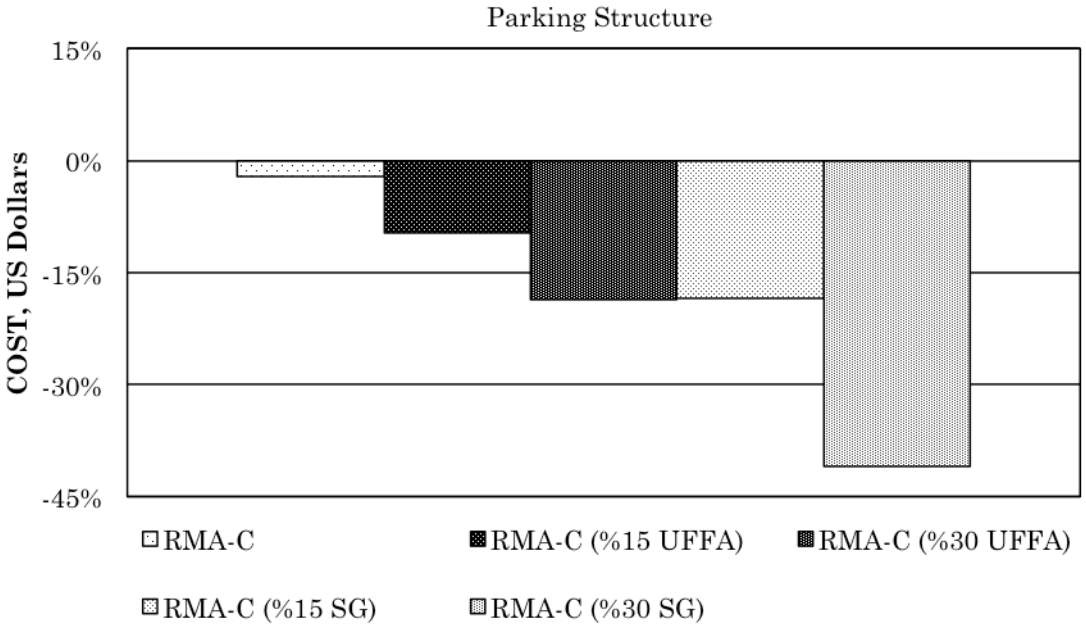

Figure 48 – A graph representing the percent difference of cost (in US Dollars) for each mixture scenario with respect to NA-C for a parking structure located further than 1.5km from the coast.

4.2.7 Incorporating Service Life and Life-Cycle Assessment

In this portion of the study, comparisons between concrete alternatives are made by comparing data collected from the energy and cost analyses. The energy and cost data were plotted against each other for each concrete mixture. Data were only plotted if the mixture resulted in an average minimum service life. For example, the graphs shown in Figures 49 and 50 show mixes that result in concrete with service lives greater than 25 and 50 years, respectively. The reason for plotting these two different graphs was to illustrate design options with could exceed a desired service life. If you have a lower desired service life, you will have more cost effective, energy efficient options.

Both figures demonstrate that all RMA-C mixtures are beneficial with respect to cost. The embodied energy of RMA-C, however, is higher than NA-C in some cases, and lower in others. The cases were RMA-C has higher embodied energy than NA-C is due to the recycled aggregate replacement ratio. The higher the replacement ratio of recycled aggregates to normal aggregates, the higher the embodied energy required to produce the concrete becomes. However, the embodied energy presented by high recycled aggregate content is countered with the inclusion of SCMs which provide energy reductions. For example, RMA-C with no SCMs requires more embodied energy to produce than NA-C regardless of replacement ratio. But when you compare RMA-C with the inclusion of 15% UFFA, RMA-C with a 33% replacement ratio of normal aggregate requires less embodied energy to produce. The RMA-C with the lowest cost has the lowest embodied energy. These figures illustrate the trade-offs between cost and embodied energy when comparing RMA-C to NA-C.

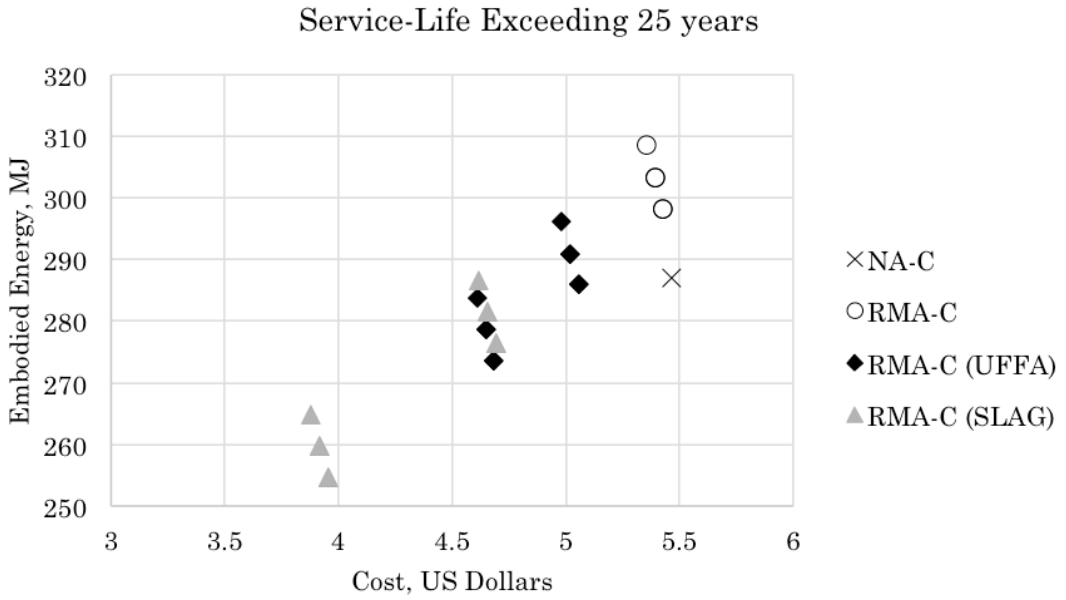

Figure 49 - Embodied energy vs. cost for service-life exceeding 25 years for NA-C and RMA-C. RMA-C data includes the inclusion of SCMs (UFFA – 15-30%, Slag 25-50%) and replacement ratios of virgin-aggregate concrete (33%, 66%, and 100%). Cover Depth = 0.07m.

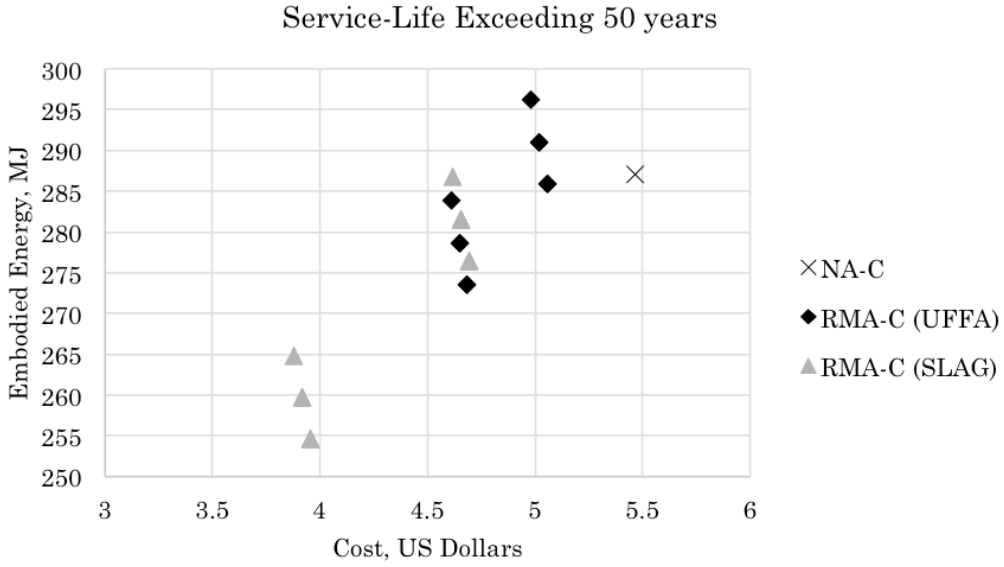

Figure 50 - Embodied energy vs. cost for service-life exceeding 50 years for NA-C and RMA-C. RMA-C data includes the inclusion of SCMs (UFFA – 15-30%, Slag 25-50%) and replacement ratios of virgin-aggregate concrete (33%, 66%, and 100%). Cover Depth = 0.07m.

CHAPTER V

CONCLUSIONS

In this study, two diffusion-based service-life models were developed by modifying existing analytical and numerical models to include the effects of recycled-aggregates and supplemental cementitious materials (SCMs). These models were used to make service-life comparisons of concrete containing virgin- and recycled-aggregates and SCMs. The effects of varying chloride boundary conditions, recycled-aggregate content, initial levels of chloride contamination present in the recycled-aggregate, and SCM content were investigated. A life-cycle assessment was conducted to take the constituents of the concrete used to achieve a certain service-life and measure life-cycle metrics in terms of embodied energy (MJ) and cost (US Dollars). This approach provided the basis for a framework to illustrate the trade-offs between material cost, service life performance, and environmental sustainability.

From this study, the following conclusions could be made:

- As expected, the service life of reinforced concrete decreases as the severity of the chloride environment increase;
- In general, an increase in the replacement ratio of virgin-aggregates with recycled-aggregates decreases the service life of reinforced concrete;
- The increased severity of chloride contamination levels in the recycled-aggregates decreases the service life of concrete;
- For aggregate replacement ratios of 33% and 66%, the severity of the chloride environment had a greater impact on service-life than the severity of initial chloride contamination levels;
- Both models developed in this study showed very poor service-life performance for concrete that contained 100% recycled-aggregate and aggregates with severe initial chloride contamination levels, especially if placed in severe chloride environments;
- All replacement ratios of aggregates that contain mild initial contamination that were placed in a mild chloride environment exceeded a service life of 40 years;
- The modified Crank-Nicolson model results showed that at lower recycled-aggregate replacement ratios (33%), service-life is comparable in all chloride environments;
- The inclusion of SCMs increased the service-life of RMA-C and exceeded NA-C for all scenarios other than a 100% replacement ratio of aggregates with

severe initial chloride contamination levels placed in severe chloride environments;

- UFFA may be more effective at extending the service-life of RMA-C than Slag;
- RMA-C without the inclusion of SCMs requires more embodied energy, but costs less than NA-C;
- The inclusion of Slag and UFFA in RMA-C decreases the required embodied energy to a lower value than that of NA-C;
- The inclusion of SCMs reduces the cost of reinforced concrete;
- Slag is more effective than ultra-fine fly ash at reducing the cost of concrete;
- Plotting embodied energy to cost can serve as a tool in determining environmental and economic trade-offs for concrete containing SCMs and recycled aggregates.

5.1 Recommendation for Future Work

5.1.1 Modifying Error Function Parameters

There are significant differences in the two models' prediction of service-life for NA-C. Since the Crank-Nicolson numerical approach takes into account non-steady state conditions that are neglected in Crank's simple error function analytical approach, parameters of the analytical approach could be modified to reflect more realistic approximations of service life by using the results from the numerical approac. Since the analytical model does not require as much computational power

as the numerical model, it would be advantageous to use the analytical model with modified parameters for service-life prediction.

5.1.2 Improvements of Life-Cycle Inventory

While the life cycle assessment inventory created for this study was sufficient for displaying a relationship between service-life and environmental impacts, improvements to this inventory could be made. Finding an inventory that includes the effects of silica fume and metakaolin in addition to fly ash and slag, would allow for an evaluation of all four SCMs, which the numerical model is capable of including in its service-life prediction. Compiling an inventory that has a more direct approach to address the incorporation of recycled-aggregates would also be advantageous.

5.1.3 Optimization & Location-Based Decision-Making

The modeling methodology presented in this study is, in fact, capable of determining service-life, embodied energy, and cost for concrete specimens at a specific latitude and longitude. The results have allowed for general conclusions to be made on the effects of distinct inputs. It is possible, however, to select a specific geographical point and run a multi-objective evolutionary algorithm, which provides a suite of potential solutions in an attempt to maximize and minimize specific performance objectives. This could serve as an extremely powerful tool for decision-makers who are trying to make decisions in regard to sustainable materials design by analyzing tradeoffs on cost, embodied energy, and service-life performance of "green" and conventional reinforced concrete.

REFERENCES

[1] Mehta, P., Monteiro, P., (2003). "Concrete: microstructure, properties, and materials," McGraw-Hill, NY

[2] WuPing, Yidong, X., (2011). "Life-cycle assessment of recycled-aggregate concrete containing fly ash," Mechanic Automation and Control Engineering (MACE), pp. 2287-2290.

[3] Knoeri, C., Sanye-Mengual, E., Althaus, H., (2013). "Comparative LCA of recycled and conventional concrete for structural applications," The international Journal of Life Cycle Assessment, 18(5), pp. 909-918.

[4] Estanqueiro, B. "Life cycle assessment of the use of recycled-aggregates in the production of concrete," Universidade Tecnica de Lisboa-UTL.

[5] Evangelista, L., Brito, J., "Environmental life cycle assessment of concrete made with fine recycled concrete aggregates," Universidade Tecnica de Lisboa-UTL.

[6] Riding, K. A., Thomas, M. D., Folliard, K. J. (2013). "Apparent Diffusivity Model for Concrete Containing Supplementary Cementitious Materials," *ACI Materials Journal*, 110(6): 705-713

[7] Debieb, F. Courard, L., Kenai, S., Degeimbre, R. (2010). "Mechanical and durability properties of concrete using contaminated recycled-aggregates," *Cem Concr Comp*, 32, pp. 421-26

[8] Crank, J., (1975). "The Mathematics of Diffusion,", 2nd edition, Clarendon Press.

[9] Life-365 Consortium III, (2014). "Life-365 Service life Prediction Model and Computer Program for Predicting the Service life and Life-Cycle Cost of Reinforced Concrete Exposed to Chlorides," Version 2.2.1.

[10] Xiao, J., Ying, J., Shen, L., (2011). "FEM Simulation of Chloride Diffusion in Modeled Recycled-aggregate Concrete," Construction and Building Materials, vol. 29, pp.12-23.

[11] Liu, J., Zing, F., Dong, B.Q, Ma, H.Y., Pan, D. (2014). "New equation for description of chloride ions diffusion in concrete under shallow immersion condition," *Materials Research Innovations*, 18.

[12] Meyer, C., (2009). "The greening of the concrete industry," Cem Concr Comp, 31(8), pp. 601-605

[13] Siddique, R., (2004). "Performance characteristics of high-volume Class F fly ash Concrete," Cem Conc Res, 34(3), pp. 487-493

[14] Fray, A., Bijen, J., Haan, Y., (1989). "The reaction of fly ash in concrete a critical examination." Cem Concr Res, 19(2), pp. 235-246.

[15] Mehta, P., Gjorv, O., (1982). "Properties of Portland cement concrete containing fly ash and silica-fume," Cem Conc Res, 12(5), pp. 587-595

[16] Sabir, B., Wild, S., Bai, J., (2001). "Metakaolin and calcined clays as pozzolans for concrete: a review," Cem Concr Comp, 23(6), pp 441-454.

[17] Ferrari, G., Miyamoto, M., Ferrari, A. (2014). "New Sustainable Technology for Recycling Returned Concrete," Construction and Building Materials, 67, pp. 353-9.

[18] Brito, J.D., Saikia, N. "*Recycled-aggregate in Concrete: Use of Industrial, Construction and Demolition Waste*," London: Springer, 2013. Print.

[19] Kou, S.C., Poon, C.S. (2006). "Compressive Strength, Pores Size Distribution and Chloride-Ion Penetration of Recycled-aggregate Concrete Incorporating Class-F Fly Ash," Journal of Wuhan University Technology – Materials Science Edition, vol. 21(4), pp. 130-6.

[20] Deal, T.A., (1997). "What It Costs To Recycle," C&D Debris Recycling, pp. 10-13.

[21] American Concrete Pavement Assosiation (ACPA), (2010). "Why recycle concrete pavements," Technical Research downloads, http://www.acpa.org. [Accessed 28 April 2015]

[22] IFC Incorporated, (1995). "Construction and Demolition Waste Landfills," U.S. Environmental Protection Agency, Office of Solid Waste, Report.

[23] USGS, (2000). Recycled-aggregates – Profitable Resource Conservation. Issue Brief no. FS-181-99. Web. 18 Apr. 2015.

[24] Malesev, M., Radonjanin, V., Marinkovic, S., (2010). "Recycled Concrete as Aggregate for Structural Concrete Production," *Sustainability*, vol. 2, pp. 1204-25.

[25] US Army Corps of Engineers (USACE), (2004). "Reuse of Concrete Materials from Building Demolition, Public Works Technical Bulletin 200-1-27.

[26] United States Department of Transpiration (USDOT), (2004), Federal Highway Administration, www.fhwa.dog.gov [Accessed 18 April 2015].

[27] Berndt, M. (2009). "Properties of Sustainable Concrete Containing Fly Ash, Slag and Recycled Concrete Aggregate," *Construction and Building Materials*, vol. 23, pp. 2606-2613

[28] Movassaghi, R. "Durability of Reinforced Concrete Incorporating Recycled Concrete as Aggregate (RCA)," *Waterloo: University of Waterloo Press* (2006).

[29] Villagran-Zaccardi, Y.A., Zega, C.J., & Di Maio, A.A. 'Chloride Penetration and Binding in Recycled Concrete,' *J Mater Civ Eng*, **20** (6) (2008) 449–55.

[30] National Ready Mixed Concrete Association (NRMCA), (2000). "Supplementary Cementitious Materials," Concrete in Practice 30.

[31] Portland Concrete Assosiation (PCA). "Fly Ash, Silica Fume, and Natural Pozzolans," Design and Control of Concrete Mixtures, EB001, Ch.3, pp. 57-72.

[32] SIMCO Technologies, (2015). "STADIUM® technology portfolio," www.simcotechnologies.com [accessed 10 April 2015]

[33] United States Department of Energy (US DOE), (2004). Energy Information Administration, http://www.eia.doe.gov [Accessed 15 April 2015]

[34] Hooton, R.D., Geiker, M.R., Bentz, E.C. (2002) "Effects of curing on chloride ingress and implication on service life," *ACI Mater J*, 99(2), pp. 201-6

[35] Srubar, W. (2015). "Stochastic Service-life modeling of chloride-induced corrosion in recycled-aggregate concrete," Cement and Concrete Compsites, Vol. 55, pp. 103-111.

[36] Vu, K., Stewart, M. (2000). "Structural reliability of concrete bridges including improved chloride-induced corrosion models", Structural Safety, 22(4), p. 313-333.

[37] Kirkpatrick, T., Weyers, R., Anderson-Cook, C., Sprinkel, M., Brown, M., (2002). "A model to predict the impact of specification changes on chloride-induced Corrosion Service Life of Virginia Bridge Decks," Report and Federally Funded Project.

[38] Zhang, J., Lounis, Z., (2006). "Sensitivity analysis of simplified diffusion-based corrosion initiation model of concrete structures exposed to chlorides," Cem Concr Res, 36(7), pp. 1312-1323.

[39] Lounis, Z. (2005). "Uncertainty modeling of chloride contamination and corrosion of concrete bridges," Applied research in uncertainty modeling and analysis, springer, US(2005), pp.497-511.

[40] McDonald, D., Pfeifer, D., Sherman, M., (1998). "Corrosion evaluation of epoxy-coated, metallic reinforcing bars in concrete," Report No. FHWA-RD-98-153. Washington DC.

[41] Tanaka, Y., Kawano, H., Watanabe, H., Nakajo, T., (2006). "Study on cover depth for prestressed concrete bridges in airborne-chloride environments," PCI J, 51 (2), pp. 42–53.

[42] Liu, Y. and Shi, X. (2012). "Stochastic Modeling of Service life of Concrete Structures in Chloride-Laden Environments." *J. Mater. Civ. Eng.*, 24(4), 381–390.

[43] Xiao, J., Li, W., Corr, D., Shah S., (2013). "Effects of interfacial transisiton zones on the stress-strain behavior of modeled recycled-aggregates concrete," Cem Conr Res, vol. 52, pp. 82-99.

[44] Broomfield, J., (2006). "Corrosion of steel in concrete: understanding, investigating and repair," ed. 7.

[45] Burakov, V., Kiris, V., Raikov, S., (2007). Optimization of conditions for spectral determination of chlorine content in cement-based materials," Translated from Zhurnal Prikladnoi Spektroskopii, Vol. 74(3), pp. 289–295

[46] Obla, K., (2008). "Specifying fly ash for use in concrete," Concrete InFocus, NRMCA, pp. 60-66.

[47] Ismael, N., Ghanim, M., (2014). "Properties of blended cement using metakaolin and hydrated lime," Advances in Cement Research, pp. 1-8

[48] Phurkhao, P., Kassir, M. (2005). "Note on chloride-induced corrosion of reinforced concrete bridge deck," Journal of Engineering Mechanics, vol. 131(1)

[49] Lui, T., Weyers, R., (1998). "Modeling the dynamic corrosion process in chloride contaminated concrete structures," Cement Concrete Research, 28(3), pp. 365-379.

[50] Bazant, Z., (1979). "Physical model for steel corrosion in concrete sea structure – theory," J Struct Div, vol. 105(6), pp. 168-175

[51] BPComposites LTD., www.bpcomposites.com, [accessed 01 May 2015]

[52] Li, C. (2003). "Life-Cycle Modeling of Corrosion-Affected Concrete Structures: Propagation." *J. Struct. Eng.*, 129(6), 753–761.

[53] Qing Li, C. (2004). "Reliability Based Service Life Prediction of Corrosion Affected Concrete Structures." *J. Struct. Eng.*, 130(10), 1570–1577.

[54] Care, S., Nguyen, Q., L'Hostis, V., Berthaud, Y., (2008). "Mechanical properties of the rust layer induced by impressed current method in reinforced mortar," Cem Conr Res, vol. 38(8), pp. 1079-1091.

[55] U.S. Geological Survey (U.S.G.S), (2015). "Mineral Commodity Summaries 2015," U.S. Geological Survey, p. 196, http://dx.doi.org/10.3133/70140094. [Accessed 15 April 2015].

[56] American Coal Ash Association (ACAA), (2014). "About Coal Ash," [Accessed 15 April 2015].

[57] Davis, M., McGinnis, M., (2015). "Use of Recycled concrete aggregates for improved sustainability of reinforced concrete building structures – economic considerations," Proceedings of the 2015 ASEE Gulf-Southwest Annual Conference, University of Texas San Antonio.

[58] US Environmental Protection Agency (USEPA), (2009). Office of Water, http://water.epa.gov. [Accessed 18 February 2015].

[59] Tuutti, K., (1982). Corrosion of steel in concrete," Report No. 4-82. Stockhold, Sweden: Swedish Cement and Concrete Research Institute.)

[60] EPD International, (2015). http://www.environdec.com. [Accessed 15 April, 2015].

[61] U.S. Climate Data, (2014). http://www.usclimatedata.com. [Accessed 25 October, 2014].

[62] Hammond, G., Jones, C., (2011). "Inventory of Carbon and Energy," Version 2.0.

APPENDIX

```
%Stochastic Service-Life Simulation of Reinforced Concrete
%
%Wil V. Srubar III, Ph.D.
%
%Todd L. Bergman, MS Candidate
%
%This computer code simulates the time-to-failure of concrete structures
%using a 1D analytical solution to the diffusion equation. Both
%conventional and recylced-aggregate concrete structures are considered.
%
clc
clear
%% Time to Corrosion Initiation Definitions

% X_m    = 0.070;               %Average Concrete Cover in meters
% X_s    = 0.005;               %Std Dev Concrete Cover in meters
s      = 35000;                 %Number of Monte Carlo Simulations
Ti     = zeros(1,s);            %Empty Matrix for Total Service Life
BC_m   = 1;                     %Average Chloride Boundary condition kg/m^2 3=severe,↙
1=mild
BC_s   = 0.2;                   %Std Dev Chloride Boundary condition kg/m^2 3=severe,↙
1=mild
f_m    = 0.7;                   %Average failure threshold in kg/m^2
f_s    = 0.05;                  %Std Dev failure threshold in kg/m^2
% D_m   = 4.5*10^-12;            %Average NA-C (Normal Aggregate Concrete) Diffusion↙
Coefficient in m^2/second
% D_s   = 1*10^-12;              %Std Dev NAC D in m^2/second
% D_m   = 8.5*10^-12;            %Average RCA-C (Recycled Coarse Aggregate Concrete) D↙
in m^2/second
% D_s   = 1.5*10^-12;            %Std Dev RCA D in m^2/second
D_m   = 12.5*10^-12;           %Average RMA (Recycled Mortar Aggregate Concrete) D in↙
m^2/second
D_s   = 2*10^-12;              %Std Dev RMA D in m^2/second

%% Tcrack Definitions

% ft_m     = 580;               %Average tensile strength of NAC concrete, psi
% ft_s    = 72.5;               %Std Dev tensile strength of NAC concrete, psi
% E_m      = 5076000;           %Average modulus of elasticity of NAC concrete, psi
% E_s      = 290000;            %Std Dev modulus of elasticity of NAC concrete, psi
ft_m     = 544;                 %Average tensile strength of RAC concrete, psi
ft_s    = 72.5;                 %Std Dev tensile strength of RAC concrete, psi
E_m      = 4350000;             %Average modulus of elasticity of RAC concrete, psi
E_s      = 435000;              %Std Dev modulus of elasticity of RAC concrete, psi
Phi      = 2;                   %Creep coefficient of concrete
v        = 0.18;                %Poisson's ratio
rho_r    = 225;                 %Density of rust, lb_m/ft^3
rho_s    = 490;                 %Density of steel, lb_m/ft^3
tp_m      = 0.0005;             %Average thickness of porous region between rebar and↙
concrete
tp_s     =0.00002;              %Std Dev thickness of porous region between rebar and↙
concrete
icorr_m  = 0.0015;              %Average corrosion rate, A/ft^2
icorr_s  = 0.0002;              %Std Dev corrosion rate, A/ft^2
alpha_l  = 0.523;               %Alpha minimum
alpha_h = 0.622;                %Alpha maximum
D_bar   = 0.625;                %Diameter of steel rebar, inches
```

```
%% Service-Life Simulation

for i = 1:s
%RANDOMLY GENERATE COVER GEOMETRY
% cover = abs(normrnd(X_m,X_s));
%FIXED COVER GEOMETRY
cover =.45;
%RANDOMLY GENERATE DIFFUSION COEFFICIENT, CONVERT TO m^2/year
D = abs(normrnd(D_m,D_s)*60*60*24*365);
%RANDOMLY GENERATE CHLORIDE BOUNDARY CONDITION
BC = abs(normrnd(BC_m,BC_s));
%RANDOMLY GENERATE CORROSION THRESHOLD FOR THE STEEL REBAR
F = abs(log(lognrnd(f_m,f_s)));

%%%%%Reclaimed COARSE** Aggregate Input Parameters%%%%%
% RC=1;                                       %Recycled Concrete Type RC=1(RCA) RC=2(RMA)
% c0_agg = 3;                                 %Recycled aggregate chloride content kg/m^2↙
3=severe, 1=mild
% AR_Ratio =0.66;                                %Aggregate Replacement Ratio
% agg = .01;                                  %Aggregate Diameter, meters
% Sigma  = 0.0005;                            %Thickness of old ITZ and mortar, meters↙
(50, 10, 20, 50, 100)
% num_agg = floor(cover/(2*(agg+2*Sigma)));   %Number of aggregates within cover
% xply = (0:num_agg-1);                       %Multiplier to obtain correct segment
% seg = cover/num_agg;                        %Size of segments for each aggregate,↙
meters
% z_lim = seg - (agg+3*Sigma/2);              %Allowable placement of aggregate within↙
each segment, meters

% % %%%%%Reclaimed MORTOR** Aggregate Input Parameters%%%%%
RC=2;                                       %Recycled Concrete Type RC=1(RCA) RC=2(RMA)
c0_agg = 3;                                 %Recycled aggregate chloride content kg/m^2↙
3=severe, 1=mild
AR_Ratio = 1;                              %Aggregate Replacement Ratio
Sigma  = 0.01;                              %Diameter of old mortar, meters (50, 10, 20, 50,↙
100)
num_agg = floor(cover/(2*(Sigma)));         %Number of aggregates within cover
xply = (0:num_agg-1);                       %Multiplier to obtain correct segment
seg = cover/num_agg;                        %Size of segments for each aggregate, meters
z_lim = seg - .5*Sigma;                     %Allowable placement of aggregate within each↙
segment, meters

%RANDOM GENERATION OF AGGREGATE PLACEMENT WITHIN EACH SEGMENT

for j=1:num_agg;
    if rand() <= AR_Ratio
        z1(j)=xply(j)*seg+rand(1)*z_lim;        %Distance to first ITZ, meters

        if RC==1;
            z2(j)=z1(j)+(agg+Sigma);            %Distance to second ITZ, meters
        else
            z2(j)=0;                            %Distance to second ITZ
        end
    else
        z1(j)=0;
        z2(j)=0;
    end
end
```

```
z3=reshape([z1' z2'].',[],1);
z3=z3';                                 %Change order to z1, z2, z3, z4, ...


%%RUN STOCHASTIC SIMULATION
%First, we set the initial concentration at rebar and time to 0
c = 0;
t = 0;
%SIMULATE TIME TO CORROSION INITIATION
%This while loop runs while the chloride concentration, c, at the steel
%rebar is less than that of the failure threshold AND while time is less
%than 200 years. If time to initiation exceeds 200 years, it is assumed
%that failure due to corrosion does not occur.
while c < F && t < 1000
    c = c0_agg*(sqrt(((2*Sigma)^2)/(4*D*t+(2*Sigma^2))))*...
        sum(exp(-((cover-z3).^2)/(4*D*t+(2*Sigma^2)))-exp(-((cover+z3).^2)/(4*D*t+↙
(2*Sigma^2))))...
        +BC*(1-erf(cover/sqrt(4*D*t)));
    t = t+1;
end
%%%REPORT TIME TO CORROSION INITIATION
%Once the concentration exceeds the threshold, the while loop will stop and
%report the corresponing time to initiation in years. This value is stored
%in the Time to Initiation Matrix, Ti.
Ti(i)=t;

%SIMULATE TIME TO CORROSION CRACKING
%RANDOMLY GENERATE MATERIAL AND PHYSCIAL PROPERTIES
ft = abs(normrnd(ft_m,ft_s));
E = abs(normrnd(E_m,E_s));
tp = abs(normrnd(tp_m,tp_s));
alpha = abs(alpha_l + (alpha_h-alpha_l).*rand);
icorr = abs(normrnd(icorr_m,icorr_s));

E_eff = E/(1+Phi);
a = (D_bar+2*tp)/2;
b = cover*100/2.54+a;
tcrit = cover*100/2.54*ft/E_eff*((a^2+b^2)/(b^2-a^2)+v);
Wporous = pi*rho_r*32.14*tp/12*(D_bar/12);
Wexpand = pi*rho_r*32.14*(D_bar/12+2*tp/12)*tcrit/12;

Wcrit = rho_s/(rho_s-alpha*rho_r)*(Wporous+Wexpand);
kp = (1/alpha)*pi*D_bar*icorr;
Tcrack = (Wcrit.^2)/(2*kp);

Tc(i) = Tcrack;
%Calculate total service lifetime by adding time to initiation and time to
%corrosion cracking.
Ts(i)=Ti(i)+Tc(i);
end

%% Iterate over Ts to get only values < 1000.
Z = size(Ts);
for i=1:s
        if Ts(i)>1000
        Ts(i) = 0;
        end
```

```
end
B = 0;
Ts = setdiff(Ts,B);

%% Goodness of Fit - Anderson Darling Test
k=lognfit(Ts);

dist=makedist('logn','mu',k(1),'sigma',k(2));
[hh,pp]=adtest(Ts,'Distribution',dist)

disp(k)

%% Generating Histagram
h = hist(Ts,ceil(max(Ts)));
h=h';
hold on;
%histfit(Ts,200,'lognormal');
```

```
clc
clear
%% Service-Life Parameters - for the development of time and temperature dependent↙
diffusion coefficient
s = 1;            %number of service life simulations
sl = 150;            %Max Service Life (years)
SL = sl*365;        %Expected Service life(days)
month=[31;28;31;30;31;30;31;31;30;31;30;31];                              %Days in each 12↙
Months of the Year Jan-Dec
Temp=[13.8;14.2;14.4;15.6;17.1;18.7;20.6;21.4;21.1;19.3;16.4;13.8];     %Corresponding↙
Temperatures for each month of the year Jan-Decin LA, CA
t=repmat(month,sl,1);                                                     %Rearangement of↙
time vector to span 200 years
t=cumsum(t,1);                                                            %Cumulative↙
Rearangment to account for continuing time
T=repmat(Temp+273.15,sl,1);                                               %Rearangment of↙
Temperature to span 200 years and coreespond with time

%% LOCATION MATRIX SETUP
latlim = [33 34.5]; map_latlim = [33.1 34.4]; %limiting coordinates to LA area
lonlim = [-119 -117.5]; map_lonlim = [-118.9 -117.6]; %limiting coordinates to LA area

[california, linelat, linelong, polylat, polylong] = Mapping(latlim, lonlim);

%% Looping service-life for each map coordinate within map limits
zone1 = [34.0371 -118.5392];        %EX. IN WATER
zone2 = [34.037023 -118.539342];    %EX. BEL-AIR BAY CLUB (WITHIN 50M OF COAST)
zone3 = [34.043258 -118.536419];    %EX. THE GETTY VILLA (WITHIN 800M OF COAST)
zone4 = [34.048381 -118.532223];    %EX. PEPPERDINE UNIVERSITY (WITHIN 1.5KM OF COAST)
zone5 = [34.052854 -118.493769];    %PARKING STRUCTURE FURTHER THAN 1.5KM
zones = [zone1; zone2; zone3; zone4; zone5];

location = zone5;
[distplant] = Distance(location);

% % Maximum Surface Chloride Concentration
% Define a chloride boundary condition that ramps up over a certain amount
% of time to a max concentration. Max concentration and time2max are
% location dependent.
[dist, Max_concentration, time2max, cc] = BoundaryCondition(sl, location, california);
disp(dist.min)
%% SCMs & ADMIXTURES
air = .02;    %desired air conent by volume
% Silica Fume, Ultra-Fine Fly Ash and Metakaolin must be applied separately
SCM = 0;    % 0=No SCMs 1=SF, 2=UFFA, 3=MK
SF = 0;     %Percent Silica Fume Replacement (%)
UFFA = 0;   %Percent Ultra-Fine Fly Ash (%)
MK = 0;     %Percent Metakaolin (%)
SG = 0;     %Percent Slag (%) ONLY AFFECTS decay coefficient (not Diffusion coefficient↙
directly)

[D_mod] = SCMS(SF, UFFA, MK, SCM); %Modification Factor due to SCMS

%% Calculating Apparent Diffusion Coefficient, D28, and Ultimate, Dult
w2c = 0.42;                                          %Water to Cement Ratio
m = 0.26+0.4*(UFFA/50+SG/70);                        %Time-dependent decay of diffusion↙
coefficient + role of FA and SG (FA 0-50%,SG 0-70%) [SF & MK assumed to have no effect]
D28 = (2.17*(10^-12)*exp(w2c/0.279))*2629743.83;    %Apparent Diffusion Coefficient at↙
```

```
time t=28days based on water to cement ratio (m^2/month) - This equation is taken from↙
Riding Paper (Not Life365)
% D28 = 1*10^(-12.06+2.40*w2c)*2629743.83;             %Apparent Diffusion Coefficient at↙
time t=28days based on water to cement ratio (m^2/month) - This equation is taken from↙
Life365
D28 = D28*D_mod;                                      %Modified Diffusion Coefficient at↙
time t=28days based on present SCM's
Drma_m = 12.5*10^-12;                                 %Average RMA Diffusion Coefficient↙
(Recycled Mortar Aggregate Concrete) in m^2/second

%% Random Aggregate Placement
% This section defines where aggregates are to be placed to account for
% intitial chloride contamination and corresponding diffusion coefficients
depth = 0.5;                              %Depth of specimen
slice = 1000;                             %Number of slices through cover depth. i=0 is↙
Boundary
c0_agg = 3;                               %Recycled aggregate chloride content kg/m^2↙
3=severe, 1=mild
AR_Ratio = 1;                             %Aggregate Replacement Ratio
sigma  = 0.01;                            %Diameter of old mortar, meters (10, 20, 50, 100)
db_t = convlength(0.375,'in','m');        %Diameter of Tension Reinforcement {input - in}
cover_t = 0.07;                           %top cover
db_c = convlength(0.375,'in','m');        %Diameter of Compression Reinforcement {input -↙
in}
cover_b = 0.07;                           %bottom cover

for b = 1:s
    [z, dx, stpt, dx_t, dx_b, num_agg, seg, xply, z_lim] = agg_placement(depth,slice,↙
AR_Ratio,sigma,db_t,cover_t,db_c,cover_b); %Calling agg_placement function

    zz = [z.t, z.core, z.b];        %Starting points (in terms of slices) for intital↙
concentrations

    %% Transient Diffusion Inputs & Parameters
    %Input Parameters
    f_m = 1.175;                      %Average failure threshold in kg/m^3
    dt = 1;
    c = zeros(slice+1,1);             %Total concentration @ time, t, and slice, i
    X = zeros(slice+1,1);             %Slices througout depth
    A = zeros(slice, slice+1);        %A matrix
    B = zeros(slice, slice+1);        %B matrix
    C = zeros(slice+1,1);             %Total concentration @ time, t+1, and slice, i
    UU = zeros(slice+1,numel(t));     %Matrix of concentrations at each time step
    r = zeros(numel(t),slice+1);
    Ti_t=zeros(1);
    Ti_c=zeros(1);

    for j=1:numel(zz)
        if zz(j)~= 0
            c(zz(j):zz(j)+(sigma/dx))=c0_agg;   %Defining Initial Contaminants throughout↙
the depth of the concrete slab
        end
    end
    initial = c;
    for zz = 1:slice+1
        X(zz)=(zz-1)*dx;    %Defining slices throughout depth
    end
    %% Calulating Time (Dt) & Temperature Dependent Diffusion Coefficient
```

```
    % D28_mat represents a matrix of D28s at each slice, which will vary
    % depending on whether new mortar or old mortar occupies it.
    % Dult_mat represents a matrix of Limiting Ultimate Diffusion Coefficients
    % that ensure that coressponding D28s don't decrease indefinitely.
    % Dt(m^2/month) - Apparent Diffusion coefficient at time t(days) & Slice
    % DT(m^2/month) - Apparent Diffusion Coefficient at time t with respect to
    % Temperature
    [D28_mat, Dult_mat, Dt, DT] = DiffusionCoefficient(Drma_m, c, c0_agg, slice, SL, D28,↙
t, m, T);

    %% Crank-Nicolson Method - A finite Difference Approach to Fick's Second Law
    % time-to-initiation is estimated deterministically using a one-dimensional
    % Crank-Nicolson finite difference approach, where the future levels of
    % chlorides in the concrete are a function of current chloride levels
    % The Following Assumtions are made:
    % - the material is hommogeneous (no surface effects)
    % - The surface concentration is constant at any given point in time
    % - The properties calculated at the start of each time step, remain
    %   constant throughout that time step
    % - Different from Life365 model, the diffusion coefficient does not remain
    %   uniform over the depth of the element
    % - Unlike Life365 diffusion process is active throughout the depth of the
    %   concrete slab.
    for i=1:numel(t)
        for k=1:slice+1
            r(i,k)=DT(i,k)*dt/(2*(dx^2));   % Calculating Dimensionless Courant  ↙
Friedrichs  Lewy (CFL) Number for Crank-Nicolson Method
        end
        n=slice+1;
        A=gallery('tridiag',n,-r(i),1+2*r(i),-r(i)); %Construct A Matrix
        A(1,1)=1; A(1,2:n)=0; A(n,n)=1; A(n,1:n-1)=0;

        B=gallery('tridiag',n,r(i),1-2*r(i),r(i));   %Construct B Matrix
        B(1,1)=1; B(1,2:n)=0; B(n,n)=1; B(n,1:n-1)=0;

        for j=1:slice+1
            if j == 1;
                c(j) = cc(i); c(slice+1) = cc(i); %redefining chloride concentrations for↙
current timestep
            end
        end

        %Solve For New Concentration
        C=A\B*c;
        %Arrange a matrix of x-dimensions and concentrations
        UU(:,i) = C;
        %Update New Boundary Conditions
        c = C;

        %% Logging Time to Corrosion Initiation for Top & Bottom Rebar
        if i == 1800
            Ti_t = t(i)/365;
            Ti_c = t(i)/365;
            break
        end
        if c(dx_t)>= f_m && Ti_t == 0 %if concentration at tension reinforcement exceeds↙
the threshold at the rebar - read time
            Ti_t = t(i)/365;
```

```
        elseif c(stpt.b)>= f_m && Ti_c == 0 %if concentration at compression reinforcment↙
exceeds the threshold at the rebar - read time
            Ti_c = t(i)/365;
        elseif c(dx_t)>= f_m && c(stpt.b)>= f_m %if concentration at C && Tension exceeds↙
the threshold at the rebar - BREAK
            break
        end
        Ti.t = Ti_t;
        Ti.c = Ti_c;
    end

    %% SIMULATE TIME TO CORROSION CRACKING
    [Tc] = Tcrack(db_c,db_t,cover_t,cover_b);

    %% Total Service-Life
    %Calculate total service lifetime by adding time to initiation and time to
    %corrosion cracking.
    Ts.t(b) = Ti.t+Tc.t;   %Service-Life for top portion of element (tension↙
reinforcment)
    Ts.c(b) = Ti.c+Tc.c;   %Service-Life for bottom portion of element (compression↙
reinforcment)
end

%     %% LCA: Embodied Engergy & Total Cost
%     [wt, volume, dens_conc, vol] = AVM(w2c, cover_t, sigma, air);
%
%     % ESTIMATION OF COMPRESSIVE STRENGTH BASED ON MIX DESIGN
%     f_c = 51290/(23.66^((w2c)+0.000378*(wt.cem)+.0279*air)); %Compressive Strength↙
kg/m^2
%
%     % EMBODIDED ENERGY BASED ON COMPRESSIVE STRENGTH AND SCMS
%     EE_kg = -0.0049*UFFA + 0.0052*SG + 0.00008*f_c +0.6235; % EE (KJ/kg)
%     if AR_Ratio == 0
%         EE = EE_kg/(dens_conc*vol); %EE without Recycled Aggregate
%     else
%         EE = EE_kg/(dens_conc*vol) + (0.14*AR_Ratio*(wt.CA+wt.FA)); %EE with Recycled↙
Aggregate
%     end
%
%
%     %TOTAL COST OF COVER REPLACEMENT
%     COST = (wt.cem)*(1-UFFA-SG)*0.0985 + (wt.cem)*(UFFA)*0.03 + (wt.cem)*(SG)*0.017↙
+...    %CEMENTITOUS MATERIALS
%         (wt.CA+wt.FA)*(1-AR_Ratio)*0.012 + (wt.CA+wt.FA)*(AR_Ratio)*0.01 +...   %↙
AGGREGATE COSTS
%         distplant*(wt.CA+wt.FA)*0.000182 +...                                    %↙
TRANSPORT COSTS
%         (volume.h20)*0.992342; %Total Cost of Concrete
%

%% HISTOGRAMS OF SERVICE LIFE
% figure(4)
% hist(Ts.t,25);
% hist(Ts.c,25);

%% MAPPING OF SERVICE-LIFE
% [int] = ServiceLifeMapping(coord, latlim, lonlim, linelat, linelong, polylat, polylong,↙
Ts);
```

```
% dlmwrite('Sim1_Ts.txt',[Ts.t,Ts.c]); dlmwrite('Sim1_EE.txt',EE); dlmwrite('Sim1_COST.↙
txt',[Ts.t,Ts.c])
% quit
```

```
function [z, dx, stpt, dx_t, dx_b, num_agg, seg, xply, z_lim] = agg_placement(depth,↙
slice,AR_Ratio,sigma,db_t,cover_t,db_c,cover_b)
dx = depth/slice;                                   %Thickness of slices (m)
dx_t = cover_t/dx;                                  %number of slices in top cover
dx_b = cover_b/dx;                                  %number of slices in bottom cover
core_dist = depth-(db_t+db_c)-(cover_t+cover_b);    %Core length
dx_core = core_dist/dx;                             %number of slices in core

num_agg.t = floor(cover_t/(2*sigma));               %number of aggregates in top cover
xply.t = (0:num_agg.t-1);                           %multiplier to reach segment for↙
aggregate placement
num_agg.core = floor(core_dist/(2*sigma));          %number of aggregates in core
xply.core = (0:num_agg.core-1);                     %multiplier to reach segment for↙
aggregate placement
num_agg.b = floor(cover_b/(2*sigma));               %number of aggregates in bottom cover
xply.b = (0:num_agg.b-1);                           %multiplier to reach segment for↙
aggregate placement

seg.t = floor(((cover_t/num_agg.t)+ 0.5*dx)/dx)*dx;
seg.core = floor(((core_dist/num_agg.core)+ 0.5*dx)/dx)*dx;
seg.b = floor(((cover_b/num_agg.b)+ 0.5*dx)/dx)*dx;

z_lim.t = seg.t - 1.5*sigma;    %1.5 sigma to prevent unrealistic failure
z_lim.core = seg.core - 1.5*sigma;
z_lim.b = seg.b - 1.5*sigma;

stpt.t = 0;
stpt.core = floor(((stpt.t + cover_t + db_t)+ 0.5*dx)/dx);
stpt.b = floor(((cover_t + db_t + core_dist + db_c)+ 0.5*dx)/dx);

z.t=zeros(1,num_agg.t);
z.core=zeros(1,num_agg.core);
z.b=zeros(1,num_agg.b);

for j=1:num_agg.t;
    if rand() <= AR_Ratio
        z.t(j)=stpt.t+floor(((xply.t(j)*seg.t+rand(1)*z_lim.t)+0.5*dx)/dx);        %↙
Distance to first ITZ, meters
    end
end

for j=1:num_agg.core;
    if rand() <= AR_Ratio
        z.core(j)=stpt.core+floor(((xply.core(j)*seg.core+rand(1)*z_lim.core)+0.5*dx)↙
/dx);        %Distance to first ITZ, meters
    end
end

for j=1:num_agg.b;
    if rand() <= AR_Ratio
        z.b(j)= stpt.b +floor(((xply.b(j)*seg.b+rand(1)*z_lim.b)+0.5*dx)/dx);        %↙
Distance to first ITZ, meters
    end
end

end
```

```
function [ wt, volume, dens_conc, vol] = AVM(w2c, cover_t, sigma, air)
%% ABSOLUTE VOLUME METHOD
% Simplified for Modeling. The concrete slump will be assumed to be 3" (0.07620m) which
% is appropriate for structural foundation walls (conservative).
depth  = 1;                          %Depth of Specimen
length = 1;                          %Length of specimen
vol = depth*length*cover_t;          %Volume of Specimen (cu m)
FM          = 2.5;                   %Fineness Modulus (2-3), is an empirical figure↙
obtained by adding the total percentage of the sample of an aggregate retained on each of↙
a specified series of sieves, and dividing the sum by 100
dens_h20    = 1000;                  %density of water, kg/m^3
dens_conc   = 2400;                  %density of concrete, kg/m^3
SG_h20      = 1;                     %
SG_cem      = 3.15;                  %Specific Gravities
SG_CA       = 2.68;                  %
SG_FA       = 2.64;                  %
SG_UFFA     = 2.5;                   %
SG_SG       = 1185/dens_h20;         %

% (1) WATER & AIR CONTENT

% FROM TABLE 7-6 APPROXIMATE MIXING WATER AND TARGET AIR CONTENT
% REQUIREMENTS FOR AGGREGATE SIZES
water_reduction = convmass(35,'lbm','kg');          %reduction of water due to crushed↙
fines
agg_size_matrix = [.375 .5 .75 1 1.5 2 3]*0.0254;   %Aggregate Diameter, m

NAE_matrix = [3 2.5 2 1.5 1 .5 .3]/100;             %Air Conent for Non-Air-Entrained↙
Concrete, %
NAE_water = [385 365 340 325 300 285 245];  %Mixing Water for Non-Air-Entrained Concrete,↙
kg per cu yd

AE_matrix = [8 7 6 5 4]/100;                        %Desired Air Conent for Air-Entrained↙
Concrete, %
AE_water = [340 325 305 295 275 265 225];  %Mixing Water for Air-Entrained Concrete, kg↙
per cu yd
AEA_matrix = [1 .9 .8 .7 .6];       %Manufacturer Recommended Dosage of AEA to achieve↙
desired air conent, fl oz per kg of cement

if air < .03
    wt.h20 = (interp1(agg_size_matrix,NAE_water, sigma) - (water_reduction))*0.↙
593276421*vol;   %Mixing Water w/ reduction due to crushed fines,kg
    air = interp1(NAE_water, NAE_matrix, (wt.h20/(0.593276421*vol)+(water_reduction)));↙
%approximate amount of entrapped air in non-air-entrained concrete, %
else
    wt.h20 = (interp1(agg_size_matrix,AE_water, sigma) - (water_reduction))*0.↙
593276421*vol; %Mixing Water w/ reduction due to crushed fines, kg
    AEA = interp1(AE_matrix, AEA_matrix, air);                          %fl oz per kg↙
cement - dosage of AEA to obtain desired air conent
end

% (2)CEMENT & AEA CONTENT
wt.cem = wt.h20/w2c;   %Cement content, kg

% (3) ESTIMATION OF COARSE AGGREGATE CONTENT
% FROM TABLE 7-5 VOLUME OF CAORSE AGGREGATE PER UNIT VOLUME OF VOLUME OF
% CONCRETE
FM_matrix = [2.4 2.6 2.8 3]';    %FM matrix used for interpolation values of course↙
```

```
aggregate per unit volume
CA_vol_matrix = [0.5 0.48 0.46 0.44; 0.59 0.57 0.55 0.53; 0.66 0.64 0.62 0.60;
                 0.71 0.69 0.67 0.65; 0.75 0.73 0.71 0.69; 0.78 0.76 0.74 0.72;
                 0.82 0.80 0.78 0.76]';   %Volume of dry-rodded coarse aggregate per unit↙
volume table

CA_unit_vol = interp1(FM_matrix, CA_vol_matrix, FM);
CA_unit_vol = interp1(agg_size_matrix, CA_unit_vol, sigma);   %Volume of coarse aggregate↙
per unit volume of concrete

wt.CA = CA_unit_vol*1601.84634*vol;                          %Coarse Aggregate, lb per↙
cover volume

% (4) ESTIMATION OF TEH WEIGHT OF FINE AGGREGATE BASED ON ABSOLUTE VOLUME -
% PLUS ALL OTHER CALCULATED VOLUMES.

volume.h20 = wt.h20/(1*dens_h20);                   %Volume of water
volume.cem = wt.cem/(SG_cem*dens_h20);              %Volume of cement
volume.CA  = wt.CA/(SG_CA*dens_h20);                %Volume of Coarse Aggregate
volume.air = air*vol;                               %Volume of Air
volume.knowntotal = volume.h20 + volume.cem +volume.CA + volume.air;
volume.FA = vol - volume.knowntotal;                %Volume of Fine Aggregate
wt.FA = volume.FA*SG_FA*dens_h20;                   %Weight of Fly Ash


end
```

```
function [dist, Max_concentration, time2max, cc] = BoundaryCondition(sl, location,↙
california)
%% Calculating Exposure Based on Distance to Coast

dist.coast = zeros(1,numel(california.Lat));

for i = 1:numel(california.Lat)
    dist.coast(i) = distance(location(1),location(2),california.Lat(i),california.Lon↙
(i)); %measures distance from specified location to every coastal coordinate within↙
mapping limits
end

[minval,ind]= min(dist.coast);  %Detects minimum value from dist.coast
dist.closest = [california.Lat(ind),california.Lon(ind)];
dist.min = deg2km(minval);  %Minimum distance to coast from specified location

concwt = 2350;                  %kg/m^3 Weight of reinforced concrete from Life365

if dist.min == 0;
    %Marine Splash Zone
    Max_concentration = concwt*.008;   %Maximum Surface Concentration kg/m^3
    time2max = 1;                 %Instantaneous Maxiumum Concentration (years)
elseif dist.min > 0 && dist.min <= .05;
    %Marine Spray Zone
    Max_concentration = concwt*.01;    %Maximum Surface Concentration kg/m^3
    time2max = .01/.001;                %Time to Maxiumum Concentration (years)
elseif dist.min > .05 && dist.min <= .8;
    %Within 800m of coast
    Max_concentration = concwt*.006;    %Maximum Surface Concentration kg/m^3
    time2max = .006/.0004;              %Time to Maxiumum Concentration (years)
elseif dist.min > .8 && dist.min <= 1.5;
    %Within 1.5km of coast
    Max_concentration = concwt*.006;    %Maximum Surface Concentration kg/m^3
    time2max = .006/.0002;              %Time to Maxiumum Concentration (years)
else
    %Further than 1.5km from coast
%     prompt = 'What type of structure is this? (Parking Structure, Urban Bridge, Rural↙
Bridge, Indoors)';
%     s1 = {'Parking Structure'; 'Urban Bridge'; 'Rural Bridge';'Indoors'};
%     str = input(prompt,'s');
%     tp = strcmp(str,s1);
%     if tp(1) == 1;  %Parking Structure
       Max_concentration = concwt*.008;    %Maximum Surface Concentration kg/m^3
       time2max = 200;             %Time to Maxiumum Concentration (years) - 200 as a↙
default value
%     elseif tp(2)== 1;   %Urban Bridge
%         Max_concentration = concwt*.0085;     %Maximum Surface Concentration kg/m^3
%         time2max = 200;      %Time to Maxiumum Concentration (years) - 200 as a default↙
value
%     elseif tp(3) == 1;  %Rural Bridge
%         Max_concentration = concwt*.007;  %Maximum Surface Concentration kg/m^3
%         time2max = 200;       %Time to Maxiumum Concentration (years) - 200 as a↙
default value
%     elseif tp(4) == 1;  %Indoors
%         Max_concentration = 0;              %Maximum Surface Concentration kg/m^3
%         time2max = 200;                     %Time to Maxiumum Concentration (years) -↙
200 as a default value
end
```

```
%     disp('Shortest Distance to Coast:'); disp(dist.min);
%     disp('Maximum Concentration:');disp(Max_concentration);
%     disp('Ramp-up Time:');disp(time2max);

    %% RAMP UP to Maximum Concentration
    if Max_concentration == 0
        y = 0;
    else
        y = linspace(0,Max_concentration,time2max*12);        %Build up to Max Surface↙
concentration
    end
    y = y.';                                                  %Transpose Build up matrix
    if sl <= time2max
        yy = repmat(Max_concentration, 1, 1);
    else
        yy = repmat(Max_concentration, abs((sl-time2max))*12, 1);         %Max Surface↙
concentration for rest of time steps
    end
    cc=[y; yy];                                              %Surface Concentration matrix

end
```

7/24/15 5:19 PM /Users/Todd/Down.../DiffusionCoefficient.m 1 of 1

```
function [D28_mat, Dult_mat, Dt, DT] = DiffusionCoefficient(Drma_m, c, c0_agg, slice, SL,↙
D28, t, m, T)
Dt = zeros(numel(t),slice+1);
DT = zeros(numel(t),slice+1);
D28_mat = zeros(slice+1,1);     %D28 at each slice - allows you to change the diffusion↙
coefficient at each slice.
Dult_mat = zeros(slice+1,1);    %Limiting Ultimate Diffusion Coefficient so that↙
diffusivity doesn't decrease indefinitely for each D28

%Input Parameters
R = 8.314462;       %Universal Gas Constant J/(mol K)
Tref = 293;         %Temperature Reference defined by life365 (K)
U = 35000;          %Activation Energy of Diffusion Process (J/mol)
t28 = 28;           %Days - 28days after pour

for z = 1:slice+1
    if c(z)== c0_agg;
        D28_mat(z)=(Drma_m*60*60*24*365);
    else
        D28_mat(z)= D28;
    end
    Dult_mat(z) = D28_mat(z)*(28/SL)^m;    %Limiting Ultimate Diffusion Coefficient so↙
that diffusivity doesn't decrease indefinitely for each D28
end

for i=1:numel(t)
    for k=1:slice+1
Dt(i,k) = D28_mat(k)*(t28/t(i)).^m + Dult_mat(k)*(1-(t28/t(i)).^m); %Apparent Diffusion↙
coefficient at time t(days) & Slice (m^2/month)
DT(i,k) = Dt(i,k)*exp((U/R)*((1/Tref)-(1/T(i))));                   %Apparent Diffusion↙
Coefficient at time t with respect to Temperature (m^2/month)
    end
end
end
```

7/24/15 5:19 PM /Users/Todd/Downloads/SimUPD.../Distance.m 1 of 1

```
function [distplant] = Distance( location)
%% Plant Locations and Coresspoming tolerance disance graphics
Plants = [33.801653 -117.989602;        % Ewels Materials 8200 Katella Avenue, Stanton,↙
CA 90680
    33.860972   -117.826867;        % Dan Copp Crushing Corp 1120 Richfield Road↙
Placentia, CA 92870
    33.698351   -117.820644;        % Ewles Materials 16081 Construction Circle West,↙
Irvine, CA 92606
    33.815365   -117.899878];       % Ampco Contracting 1328 Allec Street, Anaheim, CA↙
92805


tempdist = zeros(4,1);      %Distances between specified location and each plant
for i = 1:4
    tempdist = deg2km(distance(location(1),location(2),Plants(i,1),Plants(i,2)));
end
distplant = min(tempdist); %Distance to Closest Plant

end
```

```
function [california, linelat, linelong, polylat, polylong] = Mapping(latlim, lonlim)
%% Producing Coast Coordinates
states = geoshape(shaperead('usastatehi', 'UseGeoCoords', true));
stateName = 'California';
ca = states(strcmp(states.Name, stateName));
california = shaperead('usastatehi',...
    'UseGeoCoords', true,...
    'Selector',{@(name) strcmpi(name,'California'), 'Name'});

[linelat,linelong] = maptriml(california.Lat,california.Lon,latlim,lonlim);
[polylat,polylong] = maptrimp(california.Lat,california.Lon,latlim,lonlim);

%% Exposure Zones
% zone.one = km2deg(0.00001); %0km from coast
% zone.two = km2deg(0.05);    %0.05km from coast
% zone.three = km2deg(0.8);   %0.80km from coast
% zone.four = km2deg(1.5);    %1.5km from coast

% figure(1)
%% plotting map within limits
% axesm('MapProjection', 'miller', 'Frame', 'on',...
%     'FlatLimit', map_latlim, 'FlonLimit', map_lonlim)
% patchesm(polylat, polylong, 'y')
% plotm(linelat, linelong, 'black')
% %Buffers for exposure regoins
% [latone,lonone] = bufferm(polylat, polylong, zone.four, 'in');  %Buffer for Zone4
% geoshow(latone, lonone, 'DisplayType', 'polygon', 'FaceColor', 'm')
% [lattwo,lontwo] = bufferm(polylat, polylong, zone.three, 'in'); %Buffer for Zone3
% geoshow(lattwo, lontwo, 'DisplayType', 'polygon', 'FaceColor', 'b')
% [latthree,lonthree] = bufferm(polylat, polylong, zone.two, 'in',4); %Buffer for Zone2
% geoshow(latthree, lonthree, 'DisplayType', 'polygon', 'FaceColor', 'g')
% plotm(linelat, linelong,'g','LineWidth',.10) %allows for Buffer Zone2 to be visible
%
% for i=1:4
%     plotm(Plants(i,1),Plants(i,2),'ro','MarkerFaceColor','r')
%     plotm(scPlant(:,1,i),scPlant(:,2,i),'r')
%     hold on
% end
%
% plotm(LatLong(1), LatLong(2),'co','MarkerFaceColor','g','Marker','h','MarkerSize',10)
end
```

```
function[D_mod]=SCMS(SF, UFFA, MK, SCM)


D_SF = (0.206+0.794*exp(-SF/2.51));      %Modified Diffusion Coefficient Factor with the↙
inclusion of Silica Fume
D_UFFA = (0.170+0.829*exp(-UFFA/6.07));  %Modified Diffusion Coefficient Factor with the↙
inclusion of Fly Ash
D_MK = (0.191+0.809*exp(-MK/6.12));      %Modified Diffusion Coefficient Factor with the↙
inclusion of Metakaolin

if SCM == 1
    D_mod=D_SF;
elseif SCM == 2
    D_mod=D_UFFA;
elseif SCM == 3
    D_mod=D_MK;
else
    D_mod=1;
end
end
```

```
function [Tc] = Tcrack(db_c,db_t,cover_t,cover_b)

%SIMULATE TIME TO CORROSION CRACKING

%% Tcrack Definitions
% Parameters which effect the cracking model. These values are all material
% properties and are dependent on concrete mix, reinforcement type, and
% type of rust products being produced.
% fts.m     = 580;      fts.s    = 72.5;        %[Average; StdDev] tensile strength of↙
RAC concrete, psi
% Em.m     = 5076000;  Em.s     = 290000;       %[Average; StdDev] modulus of elasticity↙
of RAC concrete, psi
fts.m   = 544;      fts.s    = 72.5;        %[Average; StdDev] tensile strength of RAC↙
concrete, psi
Em.m     = 4350000;  Em.s     = 435000;      %[Average; StdDev] modulus of elasticity of↙
RAC concrete, psi
tpr.m       = 0.0005;   tpr.s    = 0.00002; %[Average; StdDev] thickness of porous region↙
between rebar and concrete
iCorr.m = 0.0015;   iCorr.s = 0.0002;       %[Average; StdDev] corrosion rate, A/ft^2
Phi     = 2;                                %Creep coefficient of concrete
v       = 0.18;                             %Poisson's ratio
rho_r   = 225;                              %Density of rust, lb_m/ft^3
rho_s   = 490;                              %Density of steel, lb_m/ft^3
alpha_l = 0.523;                            %Alpha minimum
alpha_h = 0.622;                            %Alpha maximum

Tcrack = zeros(2,1);
for w = 1:2;
    if w == 2;
        D_bar = convlength(db_c,'m','in');
        cover = convlength(cover_b,'m','in');
    else
        D_bar = convlength(db_t,'m','in');
        cover = convlength(cover_t,'m','in');
    end
    ft = abs(normrnd(fts.m,fts.s));
    E = abs(normrnd(Em.m,Em.s));
    tp = abs(normrnd(tpr.m,tpr.s));
    alpha = abs(alpha_l + (alpha_h-alpha_l).*rand);
    icorr = abs(normrnd(iCorr.m,iCorr.s));

    E_eff = E/(1+Phi);
    a = (D_bar+2*tp)/2;
    b = cover+a;
    tcrit = cover*ft/E_eff*((a^2+b^2)/(b^2-a^2)+v);
    Wporous = pi*rho_r*32.14*tp/12*(D_bar/12);
    Wexpand = pi*rho_r*32.14*(D_bar/12+2*tp/12)*tcrit/12;

    Wcrit = rho_s/(rho_s-alpha*rho_r)*(Wporous+Wexpand);
    kp = (1/alpha)*pi*D_bar*icorr;
    Tcrack(w) = (Wcrit.^2)/(2*kp);
end

Tc.t = Tcrack(1);
Tc.c = Tcrack(2);
```